RELIABILITY AND COST ANALYSIS OF POWER DISTRIBUTION SYSTEMS SUBJECTED TO TORNADO HAZARD

by

ABDULLAH MOUSA DARWISH BRAIK

Submitted in partial fulfillment of the requirements for the degree

of Master of Science

Thesis Advisor:

Dr. Yue Li

Department of Civil Engineering

CASE WESTERN RESERVE UNIVERSITY

January, 2019

CASE WESTERN RESERVE UNIVERSITY

SCHOOL OF GRADUATE STUDIES

We hereby approve the thesis/dissertation of

Abdullah Mousa Darwish Braik

. *Candidate for the degree of **Master of Science**

Committee Chair

Dr. Yue Li

Committee Member

Dr. Xiong Yu

Committee Member

Dr. Michael Pollino

Date of Defense

November 15, 2018

*We also certify that written approval has been obtained for any proprietary material contained therein.

Table of Contents

List of Tables

List of Figures

Reliability and Cost Analysis of Power Distribution Systems Subjected to Tornado Hazard

Abstract

by

ABDULLAH MOUSA DARWISH BRAIK

Tornadoes are hazards of low probability of occurrence and high consequences that cost the United States billions of dollars each year. Electric power distribution systems are susceptible to damage due to tornadoes with the utility poles being the most vulnerable components. Additionally, the reliability of power distribution systems can be affected by the deterioration of the strength of utility poles with age. Many utility companies nowadays are considering the use of steel and prestressed concrete poles instead of wood poles, which are the most widely used in the United States. Up to date, very few studies have been performed to study the behavior of power networks when subjected to tornadoes. This research proposes a framework to perform reliability analysis, cost analysis, and target hardening of power distribution systems subjected to tornado hazard. It also offers a framework to compare the reliability of wood, steel, and prestressed concrete utility poles subjected to tornadoes through fragility analysis considering the deterioration of the strength of the poles with age.

Acknowledgment

First, I would like to thank my thesis advisor Dr. Yue Li for his great advice, encouragement, and guidance throughout my program. I would also like to thank all my professors at Case Western Reserve University for their awesome classes and support during my program, especially my committee members Dr. Xiong "Bill" Yu and Dr. Michael Pollino for their valuable time and appreciated support and feedback. Additionally, I would like to thank Dr. Abdullahi Salman for his help and providing me with valuable resources that greatly helped me throughout my research. I would also like to thank all my fellow students at the civil engineering department for being good friends and colleagues, especially my research group members.

Moreover, I would like to express my deepest gratitude for Fulbright. Their scholarship gave me the chance to participate in this exchange program in which I benefited greatly in both the academic and cultural aspects.

Finally, and most importantly, I would like to thank my family for all their love, support, and encouragement. For my parents who raised me with love and supported me in every possible way, and for my sisters for their unwavering love and encouragement.

Preface

A paper with the title: "Risk-Based Reliability and Cost Analysis of Utility Poles Subjected to Tornado Hazard" has been submitted, based on Chapter 4 of this research thesis (Component Reliability: Reliability and Cost Analysis of Utility Poles Subjected to Tornado Hazard), to ASCE Journal of Aerospace Engineering. The work within the paper was developed and completed by the author of this research thesis. Moreover, Dr. Yue Li and Dr. Abdullahi Salman reviewed the paper and offered valuable suggestions.

1. Introduction

Tornadoes are columns of air in contact with cumulonimbus clouds and the earth surface rotating rapidly and violently (Elsner et al 2014). Although tornadoes could occur anywhere on earth, they are more common in the United States (Goliger et al 1998). Within the United States, the tornado alley (which is the region within the great plains in the central part of the United States that extends from northern Texas to the south of North Dakota) and Florida are the most tornado active regions (NOAA 2012). Despite being one of the most violent natural hazards, there is still a lack of research focusing on the impact of tornadoes on structures, which is mainly because of their low probability of occurrence (van de Lindt et al 2012a). However, after the occurrence of many strong tornadoes in the past few years (such as Tuscaloosa and Joplin in 2011 and Moore and El Reno in 2013) that resulted in billions of dollars in damage and loss of lives, it became clear that there is a need for more research in order to better understand the behavior of tornadoes and their interaction with structures, and to consider their loads in design codes (Masoomi et al 2016).

Tornadoes can cause considerable damage to electric power distribution systems (Campbell et al 2012; Goliger et al 1998; Hines 2008). For example, the F2 tornado that struck the city of Los Angeles, California (March 1983) caused significant damage to power distribution systems with most of the damage concentrated on wood utility poles. Many of the poles failed mostly because of flexural overstressing at ground level, resulting in high replacement cost in addition to the cost associated with many days of power and telephone services disconnection (Hart 1985). Similarly, the tornado that struck Joplin Missouri (May 2011) destroyed about 4,000 distribution poles and left about 40% of the population without electricity (NIST 2014). According to the Department of Energy (EIA 2018a), at least nine major power outages were caused by tornadoes between 2003 and 2013, with some outages affecting up to 200,000 customers and lasting for up to 7 days. Moreover, a utility pole can become a very dangerous tornado missile when snapped off the ground and thrown tens of feet in the air by a tornado, as many studies of the post tornado damage observed broken utility poles thrown long distances from their original locations (McDonald et al 1999). For example, the hundreds of tornadoes that struck many states in April 1974 resulted in many utility poles being snapped above the ground and thrown 4-7 m away, and one pole was even found to have travelled 50 m away from its original location (Mehta et al 1975). Although an object having a size and shape of a utility pole is unlikely to be carried by wind under normal conditions, the sudden release of the poles after its failure makes it possible for it to be carried by the tornado and thrown away (Malaeb 1980).

In the past, tornadoes were mainly studied for extremely critical infrastructure such as nuclear power plants and shelter rooms (e.g., Doan 1970; McDonald et al 1974). Recently, more researchers have been studying tornado interaction with other typical structures, mainly low-rise buildings (e.g., Alrasheedi et al 2011; Amini et al 2013; Haan et al 2009; Haan et al 2017; Kashani et al 2016; Masoomi et al 2016; Memari et al 2018; Roueche et al 2015; Selvem et al 2003; van de Lindt et al 2012b). Some researchers have also studied the effect of tornadoes on transmission and distribution line structures in order to better understand tornado interaction with the power system (Hamada et al 2010; Hamada et al 2011; Hamada et al 2014; Hamada et al 2015; Ibrahim et al 2017; Ishac et al 1994; Savory et al 2001; Shehata et al 2007). Unnikrishnan et al (2016) suggested a general framework to perform probabilistic assessment of power network subjected to tornadoes.

Due to the complexity of modeling the tornado-structure interaction with the power system structures, there is still a lack of papers studying this interaction through probabilistic analysis. Some researchers have recently performed probabilistic analysis on wood and steel poles subjected to hurricanes (Darestani et al 2016; Salman et al 2016; Shafieezadeh et al 2014), and other papers studied the behavior of the power distribution system when subjected to hurricanes through reliability analysis (Darestani et al 2017; Salman et al 2015). Still, up to date, reliability and cost analysis have not been performed on power distribution systems subjected to tornadoes.

2. Research Objectives and Framework

In this research, a framework for reliability analysis, cost analysis, and hardening of power distribution systems subjected to tornado hazard is proposed. In Chapter 3, background regarding the electric power network, different types of utility poles used in power distribution systems, tornado simulation, and tornado wind load estimation in design codes and probabilistic analysis is presented.

In Chapter 4, reliability and cost analysis are performed at component level where fragility curves are generated for utility poles, which are the most vulnerable components to strong wind hazards within the power distribution system. Fragility curves are generated, taking into consideration the deterioration of the strength of the poles with age, for different types of poles: wood, steel, and prestressed concrete. Cost analysis is performed through both life-cycle cost analysis and scenario-based analysis.

In Chapter 5, reliability and cost analysis are performed at system level, where the age-dependent fragility method proposed in Chapter 4 is used to perform reliability analysis, cost analysis, and target hardening of power distribution systems through scenario-based analysis. Finally, conclusions and suggested future work are presented in Chapter 6.

3. Background

3.1. Electric Power Network

The main function of the electric power network is to supply electricity to customers with the lowest cost and the highest reliability. When failure occurs within the system, the consequences could range from electricity not reaching a few customers to a blackout affecting entire cities. The failure of electric power systems cost the U.S. between 104 to 164 billion dollars each year (Lineweber et al 2001). Although the deterministic methods are useful to design the components and systems within the power network, they fail to consider the probabilistic behavior of the system and its vulnerability to loads and hazards that are impossible to predict and cannot be controlled (Chowdhury et al 2011; Li 2014).

In general, the electric power network consists of three systems: generation, transmission, and distribution. Although the three systems usually work dependently under a single utility, their reliability is usually analyzed separately, since otherwise the analysis would be very complicated, and the methods used for each system are different (Li 2014). This research focuses on the reliability of the electric power distribution system.

3.2. Wood, Steel, and Prestressed Concrete Utility Poles

Traditionally, wood poles have been the most commonly used in power distribution systems within the United States. Wood poles are typically treated, which can increase their life 20 to 40 times (Bolin et al 2011; Ryan et al 2014). The number of treated wood poles currently in use in the United States is between 120 and 200 million (Bolin et al 2011; Ryan et al 2014). Wood poles are commonly used due to their low initial cost and being natural insulators and easy to transport (Shafieezadeh et al 2014).

Despite having many advantages, wood poles suffer from some disadvantages, mainly concerning their durability and maintenance, in addition to many environmental concerns. As a result, in recent years, many utility companies have been shifting towards the use of other materials such as steel, prestressed concrete (PC), composites (e.g., fiber glass), etc. Among these materials, steel has been the most used in recent years (Mankowski et al 2002). Steel poles have many advantages such as lower maintenance cost, higher durability, being recyclable, being aesthetically appealing, having high strength-to-weight ratio, and the flexibility of their design and construction (Lacoursiere et al 1999).

PC poles have become more popular since being first introduced in the 1930s (Rodgers 1984). PC poles are now used in many applications such as electricity poles, flag poles, telephone poles, sign poles, and many other applications. The prestressing and precasting of poles not only reduce the amount of concrete and reinforcement needed to provide high strengths resulting in lighter and stronger poles but also produce a pole that is unlikely to crack under normal loading conditions. The spun-cast of poles under high speed results in very dense poles with very low permeability, which helps to protect the reinforcement from corrosion (Ahmed et al 2013).

Wood, steel, and PC poles are susceptible to strength deterioration over time. In wood poles, the biological factors such as fungi, insect, wood peckers, and marine borers are the main source for decay, as the effect of non-biological conditions such as ultra-violet light becomes significant only in the very long run and can be ignored for the lifespan of the wood poles. Among these, the fungi activity is by far the main source of decay. There are some wood decay models available in literature that can be used to estimate the degradation of the strength of poles over time. For example, Li et al (2005) created a model that was modified by Shafieezadeh et al (2014) where the degradation of the strength of wood poles over time was studied using field data of thousands of wood poles with ages varying from 1 to 79 years. In this model, both the conditional probability of decay and the percentage of decayed poles are calculated and used to estimate the time dependent strength of poles. Another wood decay model was developed by Wang et al (2008) based on a study of Australian wood species subjected to fungi decay. This study included 3 tests: in the first test, 77 species of untreated wood were tested for decay over 35 years in 5 different locations. The second test focused on the decay of the radiata pine sapwood treated by permethrin. In this test, specimens in 30 different locations were evaluated after 1, 2, and 2.5 years of installation. The third test studied the decay of 3 treated species of wood (radiata pine sapwood, Eucalyptus regnans heartwood, and Eucalyptus regnans sapwood) buried over 30 years. This model considered the effect of different wood species, treatment, and climate conditions (temperature and precipitation), and therefore, it is used in this research.

In steel poles, the corrosion (mainly underground corrosion) is the main cause of strength degradation. To reduce the effect of corrosion, steel poles are usually galvanized, as the galvanizing material (such as zinc) isolates steel from the external environment to protect it from corrosion, and because of it being anodic to steel, zinc can protect steel from corrosion cathodically in case the coating was damaged (Robinson 2005). The study performed by Romanoff (1957) was one of the earliest and most comprehensive to study the corrosion of steel buried in soil. Based on his research, Romanoff suggested a power model to estimate corrosion. He was followed by many other researchers that used the power model and suggested other parameters based on their studies. In this research, the model and parameters recently provided by Caleyo et al (2009) and Velázquez et al (2009) are used for the strength deterioration of the steel poles.

In PC poles, corrosion of reinforcement can considerably reduce the strength of the poles. Most of the studies in the past were performed on the corrosion of non-prestressed reinforced concrete structures (eg., Stewart et al 1998; Stewart et al 2007; Vu et al 2000). Recently, Darmawan et al (2007b) proposed a model to estimate the corrosion depth in prestressing wires in precast prestressed structures. This model is used in this study to estimate the strength deterioration in PC poles.

In this research, the reliability method for design of utility poles against natural hazards provided by ASCE-111 (Dagher 2006) is applied for wood, steel, and PC poles. More discussion about different types of poles, their design, and strength deterioration over time is presented in section 4.3.

3.3. Tornado Simulation

Both physical (laboratory) simulations and numerical (computer-based) simulations are used by researchers to study tornadoes and to better understand their nature and interaction with structures. Although physical simulation is relatively costly, it can still better capture the complex nature of the tornado vortices that is difficult to simulate numerically (Haan et al 2009). Ward (1972) was one of the first to create a physical tornado simulator and used it to explore the formation and dynamic characteristics of tornadoes. After that, he was followed by other researchers who tried to enhance the physical simulators and simulate full scale tornadoes (eg., Church et al 1979; Wan et al 1972).

Other researchers then modified the simulators to study the tornado interaction with structures (eg., Fouts et al 2002; Jischke et al 1983; Mishra et al 2008). Recently, some researchers (eg., Sarker et al 2006; Sengupta et al 2008; and Yang et al 2011) simulated the tornado wind force on tall rectanglular buildings, and Haan et al (2009) and Hu et al (2011) simulated the tornado wind force on gable roof buildings. Haan et al compared the pressure of tornado wind with that of straight-line wind and found that the load of the tornado wind can be larger when both have the same speed. The uplift tornado wind force on the main wind force resisting system was found to be 1.8-3.2 times that of the normal wind, while the uplift tornado wind force on the components and cladding was found to be 1.4-2.4 times that of the normal wind.

Although numerical simulation of tornadoes is still computationally expensive, it is becoming more feasible and efficient with the improvements in high speed computers. One of the first to simulate tornadoes numerically and show the variation of vortex structure was Harlow et al (1974) and was followed by other researchers who simulated the tornado vortex numerically (eg., Lewellen et al 1997; Lewellen et al 2000). Hangan et al (2008) used computational fluid dynamics (CFD) analysis to study the effect of swirl ratios on tornadoes.

Moreover, researchers have been performing numerical simulation to study the tornado-structure interaction. For example, Selvem et al (2003) and Sengupta et al (2008) used large eddy simulation to study the tornado force on rectangular buildings. Ishac et al (1994) and Savory et al (2001) studied the tornado force on transmission towers. Recently, some researchers (eg., Hamada et al 2010; Hamada et al 2011; Hamada et al 2014; Hamada et al 2015; Ibrahim et al 2017; and Shehata et al 2007) performed CFD analysis to study the tornado force on distribution and transmission lines structures. In these studies, tornado data obtained from actual measurements (Sarkar et al 2005) was used to generate profiles for different components of wind velocity (tangential, radial, and vertical) using the CFD method proposed by Hangan et al (2008). These tornado velocity profiles were then used to simulate the pressure on the elements of transmission lines. In this research, the results of these studies will be used to generate a simple method to estimate the tornado wind pressure on the conductors within the distribution lines.

3.4. Tornado Wind Load Estimation in Design Codes and Probabilistic Analysis

Although simulations give more realistic representation of tornadoes and help to improve our understanding of tornadoes and their interaction with structures, they are still too complicated to be used in structural design or in performing probabilistic analysis. Hence, there is a direction towards the use of the force equation derived for straight-line wind and modifying it to estimate the force of tornado winds. For example, ASCE-7 (2016) used the factors provided by Haan et al (2009) mentioned in the previous section and suggested methods to modify the normal wind force equation to estimate that of tornadoes. Moreover, those factors were used by other researchers to perform probabilistic and reliability analysis of buildings subjected to tornado wind hazard (eg., Masoomi et al 2016; Memari et al 2018; van de Lindt et al 2012b). Moreover, ASCE-74 (Wong et 2010) also allows a method to modify the straight-line wind force equation to estimate the tornado wind load on transmission and distribution line structures. This method will be discussed in detail in section 4.2.

4. Component Reliability: Reliability and Cost Analysis of Utility Poles Subjected to Tornado Hazard

4.1. Introduction

In this chapter, a framework for reliability analysis of utility poles subjected to tornado hazard taking into consideration the deterioration of strength with age is introduced. Three types of poles are considered in this study: Wood, steel, and prestressed concrete (PC) poles. Also, three cities with different tornado occurrence probabilities are considered in this study: Norman-OK, Xenia-OH, and Tampa-FL. Life-cycle cost analysis and scenario-based cost analysis are also performed based on the reliability analysis.

Section 4.2 presents a method for estimating the tornado wind load on utility poles. Then, wood, steel, and PC poles are designed, and their strength deterioration models are developed in Section 4.3. Having generated both the tornado load demand and the strength capacity of the poles, a framework to perform fragility analysis on utility poles subjected to tornado hazard and strength deterioration over time is proposed in Section 4.4. The fragility curves are then used to perform cost analysis through both life cycle cost analysis and scenario-based cost analysis in Section 4.5. A flowchart of the proposed framework is shown in Figure 1.

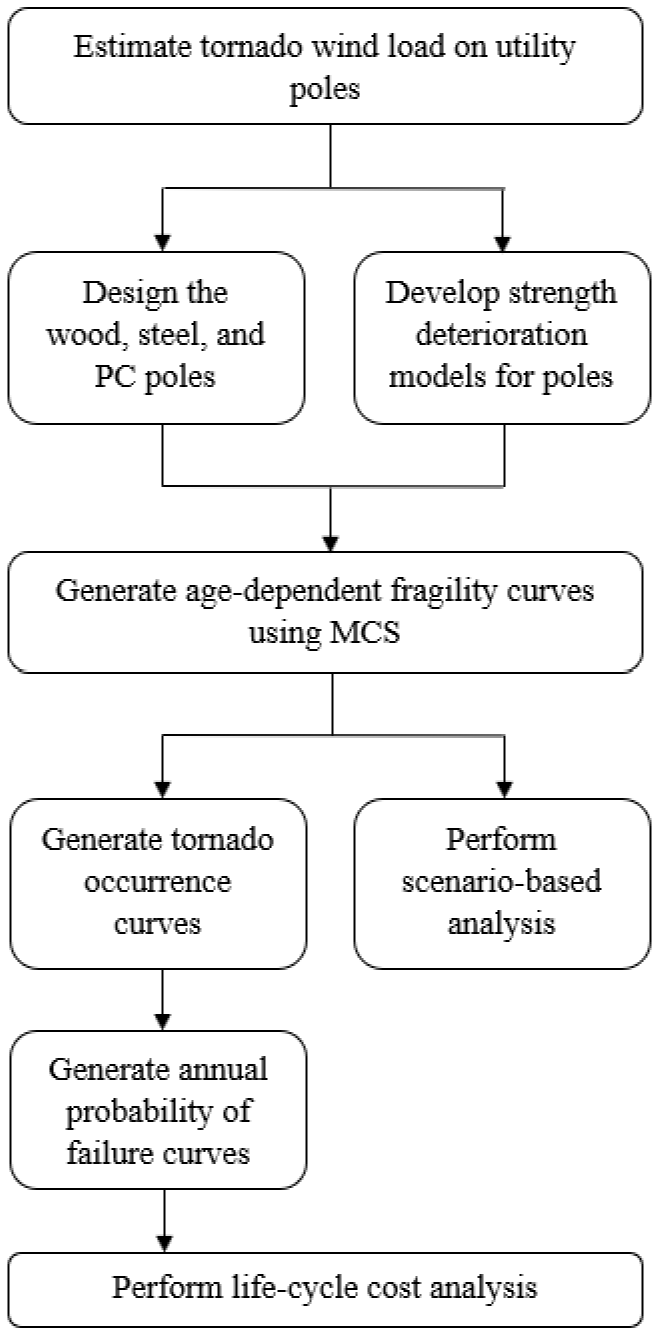

Figure 1: Flowchart of component reliability framework

4.2. Tornado Applied Load

4.2.1. Tornado Intensity, Wind Speed, and Path Width

In order to classify tornadoes, several scales were proposed, mainly the Fujita scale (F scale), Enhanced Fujita scale (EF scale), and the T-scale (Meaden et al 2007). The EF scale, which is used in the United States since it replaced the F scale, classifies tornadoes into 6 scales based on the resulting damage (WSEC 2006). Damage indicators are used to classify tornadoes because there is still a lack of data obtained from actual measurements of tornadoes (Edwards et al 2013). Although the tornado wind is a non-stationary wind and differs in nature from synoptic and straight-line winds, the EF scale relates each tornado scale to a lower and upper bound of 3-sec average gust wind speeds. This is based on the mean of the predictions made by experts for the equivalent 3-sec gust wind speed that would cause the damage (WSEC 2006). Relating wind speed to damage as mentioned above has a lot of shortcoming, mainly because it doesn’t take into account the varying speed and direction of the tornado (Wurman et al 2013). However, it is still up to date the method being used due to the lack of data as mentioned previously.

Recently, data of nearly 40,000 tornadoes recorded in the United States in the period between 1973-2011 were used to estimate the length and width of each EF scale category and modeled as random variables (Standahor-Alfana et al 2014). Masoomi et al (2018) suggested fitting the data into Weibull distribution functions, and determined the Weibull parameters for the lengths and widths of all the EF categories. The wind speed related to each F scale and EF scale category and the mean of the tornado total width obtained from Masoomi et al are shown in Table 1 (Edwards et al 2013; Masoomi et al 2018).

Table 1: F scale and EF scale wind speed and tornado path width

F category	3-sec gust wind speed (m/s)	EF category	3-sec gust wind speed (m/s)	Tornado mean width (m)
F0	20–35	EF0	29–38	40
F1	35–52	EF1	38–49	96
F2	53–72	EF2	50–60	197
F3	72–93	EF3	61–74	419
F4	94–117	EF4	74–89	669
F5	117–142	EF5	>89	837

The tornado wind speed at which utility poles are expected to fail is about 53 m/s (McDonald et al 2006), which falls in the middle of the EF2 range. However, utility poles have been observed to fail at tornado wind speeds as low as 39 m/s, which is at the lower bound of the EF1 range (Wurman et al

2013). More than 95% of tornadoes have a rating of F3 or less, and more than 85% of tornadoes have a rating of F2 or less (Fujita 1987). These tornadoes not only have a considerable probability of occurrence but also fall within the capacity of most structures including utility poles. Hence, it could be feasible to design against EF2 tornadoes, and even against EF3 tornadoes if better performance is desired in tornado-active regions.

4.2.2. Tornado Wind Load on Utility Poles

ASCE-111 (Dagher 2006) and ASCE-74 (Wong et al 2010) recommend the use of Equation (1) to determine the wind force on transmission and distribution line structures:

$$F_p = QK_zK_{zt}GC_fAV^2 \tag{1}$$

Where F_p (N) is the tornado wind load acting on the centroid of the component; Q is the air density factor. In general, it depends on the temperature, atmospheric pressure, and humidity, but for simplicity, it can be set equal to 0.613 (Wong et al 2010); k_z is the velocity pressure exposure coefficient; k_{zt} is the topographic factor; G is the gust response factor; C_f is the force coefficient; A (m^2) is the area projected to tornado wind pressure; and V (m/s) is the tornado wind velocity.

Equation (1) was derived for the pressure of normal straight-line winds, but ASCE-74 allows a simple method that can be used to modify this equation to estimate the tornado wind load. According to ASCE-74, since tornado wind is gust wind, both k_z, and G are set equal to 1.0. k_{zt} is set equal to 1.0 in this study to neglect the topographic effect. The tornado wind speed, V, used in the equation is the 3-sec gust wind speed of the tornado related to the EF scale.

C_f depends on the shape of the element and can be obtained from ASCE-74 for different shapes. For circular cylindrical utility poles, C_f is equal to 0.9. It is modeled in this study as a normally distributed random variable with a coefficient of variation of 0.12 (Ellingwood et al 1999). Although ASCE-74 allows this method for tornadoes of moderate intensities of EF2 and less, it will be shown from the fragility curves generated in this research that the fragility reaches high values at the end of the EF2 scale, sometimes even approaching 1.0. Moreover, most tornadoes in the United States are of moderate and low intensities (Wong et al 2010). Hence, this method is used in this research to estimate the tornado force on utility poles for all EF intensities.

4.2.3. Tornado Wind Load on Conductors

ASCE-74 allows neglecting the tornado wind load on conductors (wires) of transmission lines of long spans, since they are usually longer than the width of moderate tornadoes. However, the average span of distribution lines ranges from 30-46 m in suburban areas, which is smaller than the average width of even the EF1 tornado as shown in Table 1 , to 91-122 m in rural areas, which is still much smaller than the average width of EF2 tornadoes (Short 2014). Hence, it is important to consider the tornado force on conductors. In this research, a span of 46 m is considered for demonstration (Short 2014), but the presented framework can be used for any value within the above range, although the results could be conservative for longer spans as will be explained below.

Some researchers have recently been performing computational fluid dynamic (CFD) simulations to model the tornado pressure on transmission and distribution lines structures (eg., Hamada et al 2010; Hamada et al 2011; Hamada et al 2014; Hamada et al 2015; Ibrahim et al 2017; Shehata et al 2007). Although such simulations could give more realistic modelling of tornadoes and help improve our understanding of tornadoes and their interaction with structures, they are still too complicated to be used in structural design or in performing probabilistic analysis. Hence, in this study, a simpler method is proposed to estimate all components of wind force acting on the conductors.

Hamada et al (2010) and Hamada et al (2015) used the method suggested by Hangan et al (2008) and the tornado field measurement provided by Sarkar et al (2005) to generate a velocity profile in all three directions (tangential, radial, and vertical) over the height and radius of an F2 tornado. The maximum tangential velocity at a height of 11.1 m (which is the height of conductors in this study) is 72 m/s. The radial velocity associated with this tangential velocity is 34 m/s, and the vertical velocity is 6.5 m/s. The F2 velocity range is 53-72 m/s as shown in Table 1 , and hence, by dividing each velocity component over this range we get a factor of 1-1.36 for the tangential component, 0.47-0.64 for the radial component, and 0.09-0.12 for the vertical component. This factor is multiplied by the velocity in Equation (1) to estimate the three components of the tornado force on the conductors. The area of the conductors is usually several times larger than that of the cross-arm (Short 2014), and hence, the worst scenario is assumed to occur when the resultant of the tangential and radial components is perpendicular to the conductors. Hence, the tornado force on the cross-arm is not considered in this research. A section showing the poles, conductors, and cross-arms in the distribution line is shown in Figure 2. Moreover, the factor of the vertical velocity component is much less than that of the other two components, and since it will be squared in the wind force equation, it is neglected in this study. Hence, the maximum resultant force on the conductors can be estimated by Equation (2):

$$F = QK_zK_{zt}GC_fA(f_T^2 + f_R^2)V^2 \tag{2}$$

Where F (N) is the tornado wind load acting on the conductors; Q, K_z, K_{zt} and G are same as those used for utility poles; the force coefficient, C_f, for conductors is 1.0 as recommended by ASCE-111. It is modeled in this study as a normally distributed random variable with a coefficient of variation of 0.12 (Ellingwood et al 1999); A (m^2) is the area of the conductors, which equals the diameter of the conductor multiplied by the effective span length of the conductors; the 3-sec gust wind speed, V, of the tornado related to the EF scale; f_T is a uniformly distributed random variable between 1.0 and 1.36, representing the tangential component of the velocity; and f_R is a uniformly distributed random variable between 0.47 and 0.64, representing the radial component of the velocity.

Although the factors of the tangential and radial components were derived using F2 tornado velocity profile, because of lack of velocity profiles for F1 and F3 tornadoes, they are used in this study for all intensities. The effective span of the conductors subjected to tornado wind is assumed to have a maximum of half the tornado mean width shown in Table 1 . This is still conservative, since not all the span will be subjected to velocity associated with the EF intensity. For example, for an EF2 tornado, approximately 47.5% of the width (94 m using the mean width of EF2) is subjected to EF2 tornado velocities, and the remaining width is subjected to EF1 and EF0 velocities (Standohar-Alfano et al 2014). Hence, this method gives more accurate results for smaller spans.

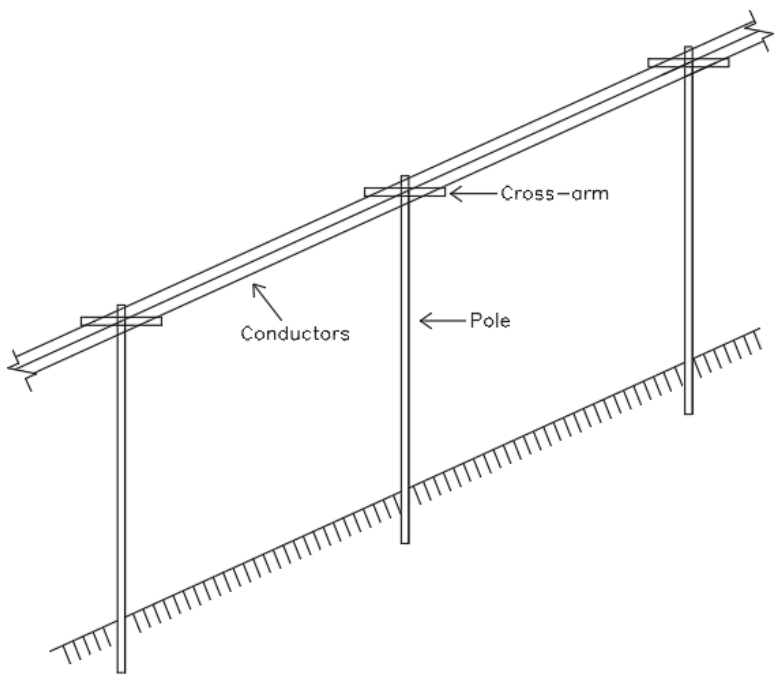

Figure 2: Distribution line typical section

4.2.4. Tornado Demand Moment

The bending moment acting on the pole at ground level can be determined by modeling the pole as a cantilever beam. The flexural stress at the ground level is usually critical even though the poles are tapered (Dagher 2006). Hence, the tornado demand moment can be calculated by Equation (3) (Dagher 2006):

$$M_s = F_p h_p + F_c h_c \tag{3}$$

Where M_s is the tornado demand moment on the utility pole at the ground level; F_p is the tornado wind force on the pole; h_p is the moment arm, equals the distance between the ground and the centroid of the pole; F_c is the tornado wind force on the conductors; and h_c is the height of the conductors above the ground level.

4.3. Design and Strength Deterioration of Utility Poles

To perform fragility analysis, the poles are designed for their dimensions and strengths. The capacities and dimensions are all associated with uncertainties and their values can be characterized using probability density functions (Dagher 2006). The dimensions and strengths of utility poles are designed such that all three types of wood, steel, and PC poles will have similar applied loads and initial strengths to allow comparison. Moreover, as this study considers the deterioration of the strength of poles with age, it is important to model the degradation of the capacity of wood, steel, and PC poles over time.

4.3.1. Design of Wood Poles

The capacity of wood poles depends on their species and grades (ANSI-O5.1. 2002). The southern pine is the most widely used wood specie in the U.S. (Wolfe et al 1997). Hence, the wood pole used in this study is southern pine wood pole. Within the southern pine wood poles, class 4 has been the most common (Foedinger 2003) and is used in this study, although some recent researchers suggest that other classes such as class 3 could be more common nowadays (Shafieezadeh et al 2014).

The strength of the wood pole follows a lognormal distribution with a mean strength of 55.2 MPa (ANSI-O5.1. 2002). Shafieezadeh et al (2014) calculated the coefficient of variation of the capacity of wood poles and plotted the results as a function of time. The coefficient of variation for a new wood pole is equal to 0.17, then increases with age to reach 0.4 for a 60 years old pole. The strength and dimensions of wood utility poles are summarized in Table 4 along side other random variables used in this study.

The moment capacity of the wood pole at ground level can be calculated using Equation (4):

$$M_{R-w} = f_w \frac{\pi}{32} D_{g-w}^3 \tag{4}$$

Where M_{R-w} is the moment capacity of the wood pole at ground level; f_w is the strength of wood; and D_{g-w} is the wood pole diameter at ground level.

4.3.2. Strength Deterioration of Wood Poles

Wood poles are susceptible to strength deterioration over time due to the activity of fungi, insects, wood peckers and marine borers. Decay fungi are considered by far the most important source of decay for wood poles in the United States. Decay of wood poles can occur both above and below ground. However, in treated southern pine poles (which is the most used in the U.S. nowadays), most of the decay usually happens below the ground (Morrell 2012). Depending on the durability and thickness of sapwood and heartwood, decay in wood poles can be either internal or external. The southern pine wood has a thick sapwood external layer and thus its decay is usually external (Shafieezadeh et al 2014). External decay can considerably affect the strength of the poles, since most of the strength is in the outer 50-75 mm (Morrell 2012).

In 2008, Wang et al developed a wood decay model based on a study of Australian wood species subjected to fungi decay and suggested a bilinear equation defined by the decay rate and time lag. The decay depth is expressed by Equation (5) (Wang et al 2008):

$$d = (t - t_{lag})r, \qquad t > t_{lag} \tag{5}$$

Where d (mm) is the decay depth, and it is assumed here to cause a uniform loss in cross-section area; t (years) is the time after installation; t_{lag} (years) is the time lag, which is the time after which the decay initiates; and r (mm/year) is the decay rate. The time lag can be calculated by Equation (6):

$$t_{lag} = 5.5r^{-0.95} \tag{6}$$

While the decay rate can be calculated by Equation (7):

$$r = k_{wood}k_{climate} \tag{7}$$

Where k_{wood} is the wood parameter, and is equal to 5.44 for southern pine sapwood, while $k_{climate}$ is the climate parameter, calculated by Equation (8), Equation (9), and Equation (10):

$$k_{climate} = f(R_{mean})^{0.3}g(T_{mean})^{0.2} \tag{8}$$

$$f(R_{mean}) = \begin{cases} 0 & if\ R_{mean} \leq 250mm\ or\ N_{dm} > 6 \\ 10\left[1 - e^{-0.001(R_{mean}-250)}\right]\left(1 - \frac{N_{dm}}{6}\right) & if\ R_{mean} > 250mm\ and\ 0 \leq\ N_{dm} \leq 6 \end{cases} \tag{9}$$

$$g(T_{mean}) = \begin{cases} 0 & if\ T_{mean} \leq 5^oC \\ -1 + 0.2T_{mean} & if 20^oC \geq T_{mean} > 5^oC \\ -25 + 1.4T_{mean} & if\ T_{mean} > 20^oC \end{cases} \tag{10}$$

Where R_{mean} (mm) is the mean annual rainfall, N_{dm} is the number of dry months in a year (the dry month in this study is any month with a precipitation less than 5 mm), and T_{mean} (°C) is the mean annual temperature. The above decay rate is for untreated wood, and can be modified to consider treatment by Equation (11) (note that for treated poles, r_{tr} replaces r in Equation (5) and Equation (6)):

$$r_{tr} = \frac{r}{1 + BC_{CCA-equiv}} \tag{11}$$

Where B is equal to 45 for southern pine wood; and $C_{CCA-equiv}$ is the CCA equivalent of the retention of the preservative wood treatment. Assuming a creosote treatment of the sapwood only, $C_{CCA-equiv}$ can be obtained by Equation (12):

$$C_{CCA-equiv} = 0.0007D_{tr} \tag{12}$$

Where D_{tr} is the air-dry density of timber, assumed 617 kg/m^3 in this study. The values of $R_{mean}, T_{mean}, and\ \ N_{dm}$ for the cities considered in this study are summarized in Table 2 (U.S. Climate data 2018).

Table 2: R_{mean}, T_{mean}, and N_{dm}

City	R_{mean} (mm)	T_{mean} (°C)	N_{dm}
Norman, OK	987	15.58	0
Xenia, OH	1065	11.86	0
Tampa, FL	1176	22.97	0

4.3.3. Design of Steel Poles

The steel used in distribution poles is usually ASTM-A572 Grade 65, as this high strength low alloy steel has higher corrosion resistance compared to carbon steel, and it satisfies the minimum yielding strength requirement of 450 MPa as required by ASTM-A572 (ASTM 2007) for galvanized steel utility poles. The strength is modeled as a lognormal distributed random variable with a coefficient of variation of 0.15 (Dagher et al 2006). According to the ASCE-72 (1990) guidelines, the strength of utility poles is generally governed by bending or local buckling depending on the ratio of outer diameter to the wall thickness (D_{g-s}/t_s). If $D_{g-s}/t_S < 6000/f_{ys}\ (ksi)$, then the strength of the pole can be considered as its yielding strength, while if $12000/f_{ys}\ (ksi) > D_{g-s}/t_s > 6000/f_{ys}\ (ksi)$, then the strength of the steel pole will be controlled by local buckling. Hence, the moment capacity of the steel pole at ground level can be determined using Equation (13):

$$M_{R-s} = \begin{cases} f_{ys}\dfrac{\pi}{32}\dfrac{D_{g-s}^4 - \left(D_{g-s} - 2t_s\right)^4}{D_{g-s}} & , \dfrac{D_o}{t} < \dfrac{6000}{f_{ys}} \\ \left(0.7f_{ys} + \dfrac{1800}{\frac{D_o}{t}}\right)\dfrac{\pi}{32}\dfrac{D_{g-s}^4 - \left(D_{g-s} - 2t_s\right)^4}{D_{g-s}} & , \dfrac{12000}{f_{ys}} > \dfrac{D_o}{t} > \dfrac{6000}{f_{ys}} \end{cases} \quad (13)$$

Where M_{R-s} (kip-inch) is the moment capacity of the steel pole at ground level; f_{ys} (ksi) is the yielding strength of steel; D_{g-s} (inch) is the steel pole diameter at ground level; and t_s (inch) is the wall thickness of the steel pole.

Steel poles are usually tapered with similar dimensions to those of wood poles of the same length and class (Bolin et al 2011). In this study, the steel pole is designed to have the same outer diameter and initial moment capacity of that of the wood pole previously discussed, and hence, the steel pole is a hollow tube with a thickness of 0.0046 m that makes its initial ground flexural strength equal to that of the wood pole. Yielding strength controls since $D_{g-s}/t_s < 6000/f_{ys}$. The strength and dimensions of the steel utility poles are summarized in Table 4 along side other normal variables used in this study.

4.3.4. Strength Deterioration of Steel Poles

The main cause of deterioration of steel strength over time is corrosion. To reduce the effect of corrosion, steel utility poles are usually galvanized, with zinc being the most widely used galvanizing material (Zamanzadeh et al 2007). In general, thick zinc coating (around 76 μm) protects the steel from corrosion until it is exhausted, and after that, it helps reduce the rate of steel corrosion (Robinson 2005). Although corrosion to steel poles can occur both above and below the ground level, the underground corrosion usually occurs at a higher rate (Revie et al 2008). Therefore, underground corrosion is assumed to control the steel strength reduction in this study. The rate of underground corrosion mainly depends on soil conditions. Other factors such as the type of steel were found to have little effect (Mughabghab et al 1989; Romanoff 1957; Velázquez et al 2009).

It is first important to estimate the life of the zinc coating, as it can be assumed that the steel pole is protected against corrosion as long as the zinc is still in place. ASTM-A123 (ASTM 2013) requires a minimum thickness of zinc coating of 76 μm. The life of the zinc coating depends on the soil conditions such as the amount of chloride in the soil, the PH of the soil, and the moisture content. The American Galvanization Association (AGA) provides charts that can estimate the loss of thickness of zinc coating with time for different soil conditions (AGA 2011a; AGA 2011b). From those charts, the estimated life of the zinc coating is between 20 and 30 years.

Caleyo et al (2009) performed probabilistic analysis to estimate the time evolution of corrosion of buried pipes taking into consideration different soil factors including the PH of the soil, the density of the soil, the water content, the amount of chloride, and other factors. Their work was based on data obtained over a three-year period from 250 different excavated pipeline sites. After performing probability analysis, they suggested the following model (Equation (14)) for the corrosion depth over time:

$$d = k(t - t_o)^n, \qquad \mathrm{t} > \mathrm{t_o} \tag{14}$$

where d is the depth of corrosion (in), and it is conservatively assumed here to cause a uniform loss of thickness within the steel pole cross-section; k and n are regression parameters that were estimated by the researchers using probabilistic analysis; t is the total bury time (years); and t_o is the time required for the corrosion to initiate (years). Although Caleyo et al (2009) suggests some values for t_o for different types of soils, in this study, t_o is assumed to be the lifespan of the zinc coating, and modeled as a uniformly distributed random variable between 20 and 30 years. Caleyo et al (2009) and

Velázquez et al (2009) give values of k and n for different types of soil, mainly clay, clay loam, sandy clay loam, and a combination of the previous soil types. In general, each city can have different types of soil and hence, knowing the exact location of the pole installation within the city is important to use this model more accurately. In this study, the poles installed in both Norman, OK and Tampa, FL are assumed to be buried in a sandy clay loamy soil, while the soil type in Xenia, OH is assumed to be clay loam. Note that the previous types are only types that can exist in those cities and used here for demonstration but cannot be used in general to represent an entire city. For types of soil different than those provided in the above studies, the procedure they suggested can be used as a framework to generate the corrosion parameters after performing tests on the soil. The values of k and n for the cities considered in this study are shown in Table 3 (Caleyo et al 2009; Velázquez et al 2009).

Table 3: Steel corrosion regression parameters

City	k	n
Norman, OK	0.144	0.734
Xenia, OH	0.163	0.793
Tampa, FL	0.144	0.734

4.3.5. Design of PC Poles

In general, there is no direct equivalence between wood poles and PC poles other than the load carrying capacity, although utilities standard can be partly based on the ANSI specifications (Oliphant et al 2012). Utilities generally design the pole when a specific height, configuration, and load are required, and this can differ between different companies. In this study, to allow comparison, the poles are designed, in addition to having the same height and capacity, to also have the same outer diameter to that of the wood and steel poles, so that both the applied moment and the capacity moment will be equal for new poles of different materials. PC poles in general are designed against several limit states including flexural strength, cracking strength, shear and torsional strength, column (buckling) strength, and deflection (Oliphant et al 2012). The cracking strength of concrete is important to make sure that the pole doesn't crack under service loads which might lead to the prestressing steel being exposed to corrosion factors. However, as the behavior of the pole here is studied against tornadoes which are extreme wind hazards, this limit state is not considered, and for the same reason, deflection limit state is also not considered. The shear and torsion strength limit state rarely controls, and is only critical for short poles with short embedment (Oliphant et al 2012).

Hence, the flexural bending is the only limit state considered here. As with the case of wood and steel poles, PC poles usually fail from flexural bending at ground level, and hence it is the controlling limit state in this study (Dagher et al 2006).

The PC pole used in this study is prestressed with 12 seven wires 11.1 mm ASTM-A416 high-strength steel strands with an ultimate breaking strength of 1860 MPa and a strand steel area of 74.2 mm^2 (ASTM 2005), surrounded by high strength concrete of 76 MPa compressive strength. Both the strength of reinforcement and concrete are modeled as lognormally distributed random variables with a coefficient of variation of 0.15 (Dagher et al 2006). The resisting moment of the PC pole at ground level M_{R-PC} can be calculated by Equation (15) and using Figure 3 (Oliphant et al 2012):

$$M_{R-PC} = \sum_{i=1}^{n} e_i A_{ps-i} f_{ps} + 0.85 f_c' A_c'(1-k)c \tag{15}$$

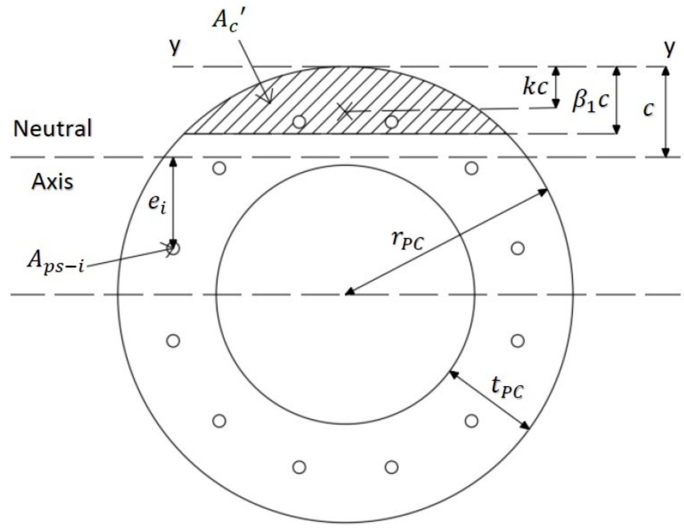

Figure 3: Prestressed concrete pole section

Where n is the number of prestressed strands; A_{ps-i} is the area of prestressed strand; f_{ps} is the yield stress of the prestressed strand minus the losses (assumed 20% in this study), and its sign depends on the location of strand above or below the neutral axis; ${f_c}'$ is the compressive strength of the concrete; ${A_c}'$ is the effective area of the concrete, and equals the area from the top of the concrete until a distance equals $\beta_1 c$, where c is the location of the neutral axis measured from the top of the pole (line y-y in Figure 3), $\beta_1 = \min(0.85, \max(0.65, 0.85 - 0.008[f_c' - 30]))$, kc is the location of the centroid of the effective area of concrete measured from the top of the pole; e_i is the distance between the centroid of the strand and the neutral axis. Also, r_{PC} and t_{PC} in Figure 3 are the outer radius and the thickness of the PC pole section respectively. The strength and dimensions of the concrete utility pole are summarized in Table 4 along side other random variables used in this study.

4.3.6. Strength Deterioration of PC Poles

In non-prestressing reinforcement, corrosion is not a major concern in general when it comes to the loss of strength, unless it is subjected to a very severe corrosive environment. Under normal conditions, aesthetic and serviceability issues arise long before pitting corrosion in the reinforcement starts to affect the size of the bars (Hope et al 2001). However, corrosion in prestressing reinforcement is a major concern and can considerably affect the design life of structures. This is mainly because the prestressing reinforcement bars are usually stressed to nearly two-thirds of their ultimate strength. Hence, pitting corrosion can lead to localized stresses and fracture. Also, prestressing reinforcement is several times stronger than non-prestressing reinforcement, and any loss in its area will considerably affect the overall strength of the structure (Hope et al 2001). Still, unlike non-prestressed reinforcement, corrosion of prestressed reinforcement is not well documented (Darmawan et al 2007a; Mangual et al 2012).

The corrosion of pre-tensioned reinforcement depends mainly on the quality of concrete, the concrete cover, the steel reinforcement, corrosivity of the environment, and quality control in the manufacturing process (Hope et al 2001). Both carbonation and chlorine contamination can cause the corrosion of reinforcement, but research shows that chloride penetration is usually the major cause of corrosion, especially in regions where humidity is high (Thoft-Christensen et al 1996). This study considers localized (pitting) corrosion as the most critical in strength deterioration. This is because although pitting corrosion occurs in a localized length of the prestressing reinforcement, it can be several times deeper than the average (uniform) corrosion in the steel (Gonzalez et al 1995).

Although there is a need for more research to better understand the mechanism of pitting corrosion in prestressed concrete, the use of extreme value theory gives reasonable approximations. Darmawan et al (2007b) developed a probabilistic model for pitting corrosion of prestressing strands in pretensioned prestressed structures as a function of the length of the strands susceptible to chloride contamination, the rate of the corrosion, and the time after the corrosion initiation. The pitting corrosion depth (a) in mm is modeled by the following Gumbel distribution shown in Equation (16):

$$f_a(t, i_{corr}, L) = \frac{\propto}{\lambda^{0.54}} e^{-\propto\left(\frac{a}{\lambda^{0.54}}-\mu\right)} e^{-e^{-\propto\left(\frac{a}{\lambda^{0.54}}-\mu\right)}}, \qquad t > T_i \qquad (16)$$

Where $\propto, \lambda, and\ \mu$ are Gumbel parameter; L (mm) is the length of the pole; t (years) is the time after the pole is installed; T_i (years) is the time for the corrosion to initiate; i_{corr} $(\mu A/cm^2)$ is the corrosion rate of steel. The

Gumbel parameters are calculated using Equation (17), Equation (18), Equation (19), and Equation (20):

$$\lambda = \frac{D_{wire}^2 - \left[D_{wire} - 0.0232 i_{corr}\left(1 + \frac{k}{\theta+1}\left[(t-T_i)^{\theta+1} - 1\right]\right)\right]^2}{D_{wire}^2 - \left[D_{wire} - 0.0232 i_{corr}\left(1 + \frac{k}{\theta+1}\left[T_o^{\theta+1} - 1\right]\right)\right]^2} \quad (17)$$

$$T_o = \exp\left[\frac{1}{\theta+1}\ln\left(\frac{(\theta+1)\left(i_{corr-exp}T_{o-exp}\right) + (k-\theta-1)i_{corr}}{k i_{corr}}\right)\right] \quad (18)$$

$$\mu = \mu_{o-exp} + \frac{1}{\alpha_{o-exp}}\ln\left(\frac{L}{L_{o-exp}}\right) \quad (19)$$

$$\propto = \alpha_{o-exp} \quad (20)$$

Where D_{wire} (mm) is the initial diameter of the prestressing wire; k and θ are the empirical factors of the corrosion rate, and equal to 0.85 and -0.29 respectively; $i_{corr-exp}$=186 μA/cm^2; T_{o-exp}=0.03836 years; α_{o-exp}=8.1. The corrosion rate of steel i_{corr} can be estimated using Equation (21) (assuming a relative humidity of 80%) (Darmawan et al 2007b; Vu et al 2000):

$$i_{corr} = 27(1 - wc)^{-1.64}/C \quad (21)$$

where C (mm) is the concrete cover, and wc is the water-cement ratio, which can be estimated by Bolomey's formula using Equation (22) (Vu et al 2000):

$$wc = \frac{27}{f_c' + 13.5} \tag{22}$$

Where f_c' is the concrete compression strength (MPa).

T_i can be calculated by Fick's second law of diffusion using Equation (23) (Darmawan et al 2007b; Thoft-Christensen et al 1996; Vu et al 2000):

$$T_i = \frac{C^2}{4D_c}\left[\mathrm{erf}^{-1}\left(\frac{C_o - C_{cr}}{C_o}\right)\right]^{-2} \tag{23}$$

Where D_C is the chloride diffusion coefficient (cm^2/year); C_o is the equilibrium surface chloride content, and within the united states, it has a mean of 3.5 kg/m^3 and a coefficient of variation of 0.5, and modeled here as a lognormal distributed random variable (Stewart et al 1998); C_{cr} is the critical surface chloride content at which corrosion initiates, and as it ranges between $0.6 - 1.2$ kg/m^3 (Stewart et al 1998), it is modeled as a uniformly distributed random variable between these two values in this study; and erf is the error function. The chloride diffusion coefficient can be approximated by the Equation (24) (Bentz et al 2014; Stewart et al 1998), with a coefficient of variation of 0.75 modeled as a lognormal distributed random variable (Gonzalez et al 1995):

$$D_C = (3.154x10^7)(10^{-10+4.66wc}) \tag{24}$$

Finally, the loss of the prestressing strands area can be approximated by the model provided by Val et al (1997) (see Figure 4). Pitting is assumed to occur in the outer surfaces of the 6 outer strands, and the 7th strand in the middle is assumed protected from corrosion (Darmawan et al 2007b). The area of the wire $A(t)_{wire}$ as a function of time is approximated using Equation (25), Equation (26), Equation (27), Equation (28), Equation (29), and Equation (30):

$$A(t)_{wire} = \begin{cases} \frac{\pi}{4} D_{wire}^2 - A_1 - A_2 & if\ \frac{D_{wire}}{\sqrt{2}} \geq a \\ A_1 - A_2 & if\ \frac{D_{wire}}{\sqrt{2}} < a \leq D_{wire} \\ 0 & if\ a > D_{wire} \end{cases} \tag{25}$$

$$A_1 = 0.5 \left[\theta_1 \left(\frac{D_{wire}}{2} \right)^2 - b \left| \frac{D_{wire}}{2} - \frac{a^2}{D_{wire}} \right| \right] \tag{26}$$

$$A_2 = 0.5 \left[\theta_2 a^2 - b \frac{a^2}{D_{wire}} \right] \tag{27}$$

$$\theta_1 = 2 \arcsin \left(\frac{b}{D_{wire}} \right) \tag{28}$$

$$\theta_2 = 2 \arcsin \left(\frac{b}{2a} \right) \tag{29}$$

$$b = 2a \sqrt{1 - \left(\frac{a}{D_{wire}} \right)^2} \tag{30}$$

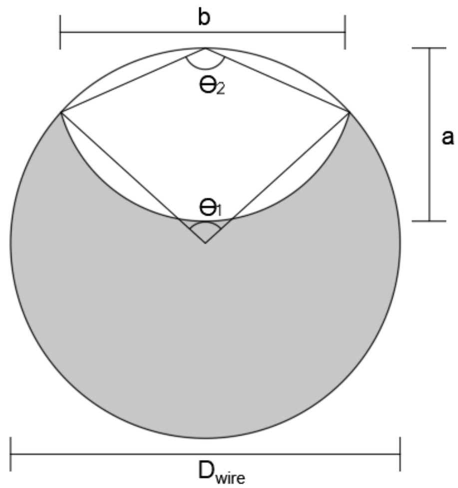

Figure 4: Pitting configuration

4.3.7. Conductors

This study focuses on the failure of utility poles at ground level, as it is the most important failure of poles when subjected to high-intensity winds, and hence, the conductors are considered only to transfer the tornado wind load to the poles. Each pole is assumed to be attached to three aluminum conductors reinforced with steel 0.6 m below the top of the pole, spanning 46 m (Short 2014). The diameter of the conductors has a mean of 18.3 mm (Short 2014). The dimensions of the conductors used in this study are summarized in Table 4.

4.4. Fragility Analysis

4.4.1. Fragility Curves

Fragility functions give the conditional probability that a structure (or a part of it) will meet or exceed a specific level of damage or limit state (that could be failure), given a specific value of hazard intensity. The fragility function can be expressed by Equation (31):

$$F_R(V) = P\left[\left(M_R(V) - M_S(V)\right) < 0 \middle| V = \mathrm{v}\right] \tag{31}$$

where V is the 3-sec tornado gust wind speed, M_R is the moment capacity of the utility pole calculated using Equation (4) for wood pole, Equation (13) for steel poles, or Equation (15) for PC poles; and M_S is the moment demand of the tornado load acting on the utility pole calculated using Equation (3). The fragility function $F_R(V)$ can best be expressed by a lognormal cumulative distribution function using Equation (32) (Masoomi et al 2016; Ellingwood et al 2004):

$$F_R(\mathrm{v}) = \Phi(\ln(\mathrm{v}/m_R)/\xi_R) \tag{32}$$

where Φ is the standard normal cumulative distribution function, and m_R and ξ_R are the logarithmic median and standard deviation of the capacity R, respectively. To determine the probability of the capacity being exceeded by the demand, a Monte Carlo Simulation (MCS) is performed in this study with 10^5 values generated for each random variable. The random variables used in this study are summarized in Table 4. The probability of failure is then calculated as the ratio of the number of failed poles to the total number of poles.

Table 4: Summary of the random variables used in the MCS

	Mean	C.O.V	Distribution
C_{f-pole}	1.0	0.12	Normal
$C_{f-conductor}$	1.0	0.12	Normal
Strength of wood pole (MPa)	55.2	Varies with age	Lognormal
Height of wood pole above ground (m)	11.7	0.04	Normal
Diameter of wood pole at ground level (m)	0.28	0.04	Normal
Diameter at top of wood pole (m)	0.17	0.04	Normal
Strength of steel pole (MPa)	450	0.15	Lognormal
Height of steel pole above ground (m)	11.7	0.025	Normal
Outer Diameter of steel pole at ground level (m)	0.28	0.025	Normal
Outer Diameter at top of steel pole (m)	0.17	0.025	Normal
Thickness of steel pole (m)	0.0046	0.025	Normal
f_s of prestressed concrete pole (MPa)	1860	0.15	Lognormal
f_c' of prestressed concrete pole (MPa)	76	0.15	Lognormal
Area of 7-wire strand in prestressed concrete pole (mm^2)	74.2	0.035	Normal
Height of prestressed concrete pole above ground (m)	11.7	0.025	Normal
Diameter of prestressed concrete pole at ground level (m)	0.28	0.025	Normal
Outer diameter at top of prestressed concrete pole (m)	0.17	0.025	Normal
Concrete thickness in prestressed concrete pole (m)	0.089	0.025	Normal
Diameter of conductor (m)	0.0183	0.03	Normal
Length of conductor (m)	46	0.06	Normal

Fragility curves for new wood, steel, and PC poles under tornado hazard are shown in Figure 5. It can be seen from the figure that the fragility curves for new poles are similar for all materials, as they are designed to have similar initial strength. This will facilitate comparison of long-term performance and lifecycle cost. Figure 6 shows the fragility curves for a new wood pole under both tornado and hurricane wind. The fragility curve under hurricane wind is developed using the procedure proposed by Salman et al (2016). It is seen from the figure that the fragility under tornado wind is much higher than that under hurricane wind of the same speed.

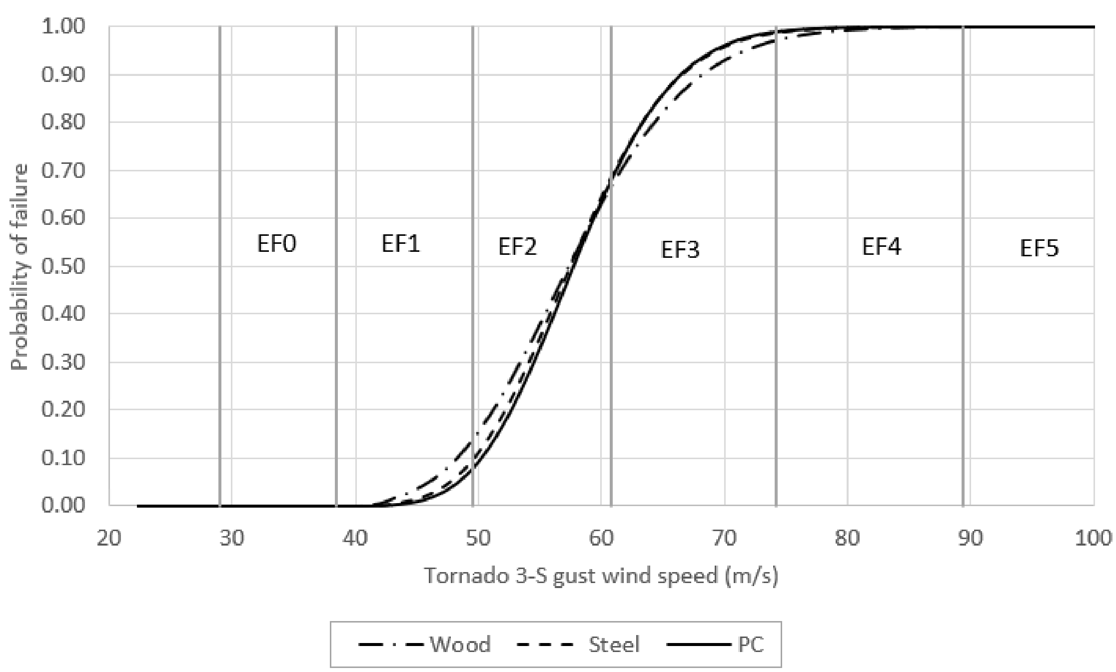

Figure 5: Fragility curves for new poles

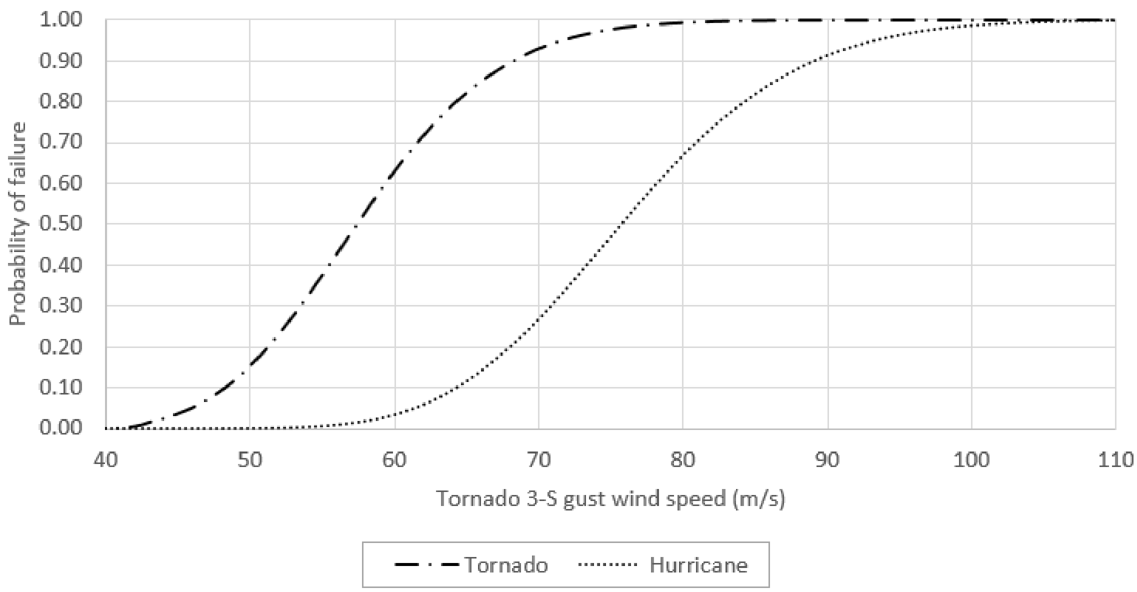

Figure 6: Fragility curves for a new wood pole subjected to tornado and hurricane winds

4.4.2. Age-Dependent Fragility Analysis

The strength deterioration models for wood, steel, and PC utility poles discussed in the previous sections can be taken into consideration in the fragility analysis by setting the capacity M_R as a function of time. Figure 7 shows the deterioration of the resisting moment of the wood, steel, and PC poles over time for the cities considered in this study, plotted as a percentage of the initial resisting moment. The fragility curves of the poles at different ages for the cities considered in this study are shown in Figure 8, Figure 9, and Figure 10.

At 20 years, the fragility of wood poles has increased compared to new poles while those of the steel and the PC poles almost remain the same. This is because corrosion in both steel and PC poles has not initiated yet. At 40 years and beyond, all the fragilities have increased, and the deterioration is highly affected by the location for wood and steel poles. The deterioration of PC poles occurs gradually after initiation since the corrosion initiation time was modeled as a random variable. The new poles, in general, are slightly vulnerable to EF1 tornadoes, moderately vulnerable to EF2 tornadoes, and highly vulnerable to EF3 and stronger tornadoes. However, over time, the fragility curves start shifting to the left causing the poles to become more vulnerable to weaker tornadoes. Considering the considerable probability of occurrence of those tornadoes, this supports the codes direction towards designing against EF2 tornadoes, and even against EF3 tornadoes in tornado-active region.

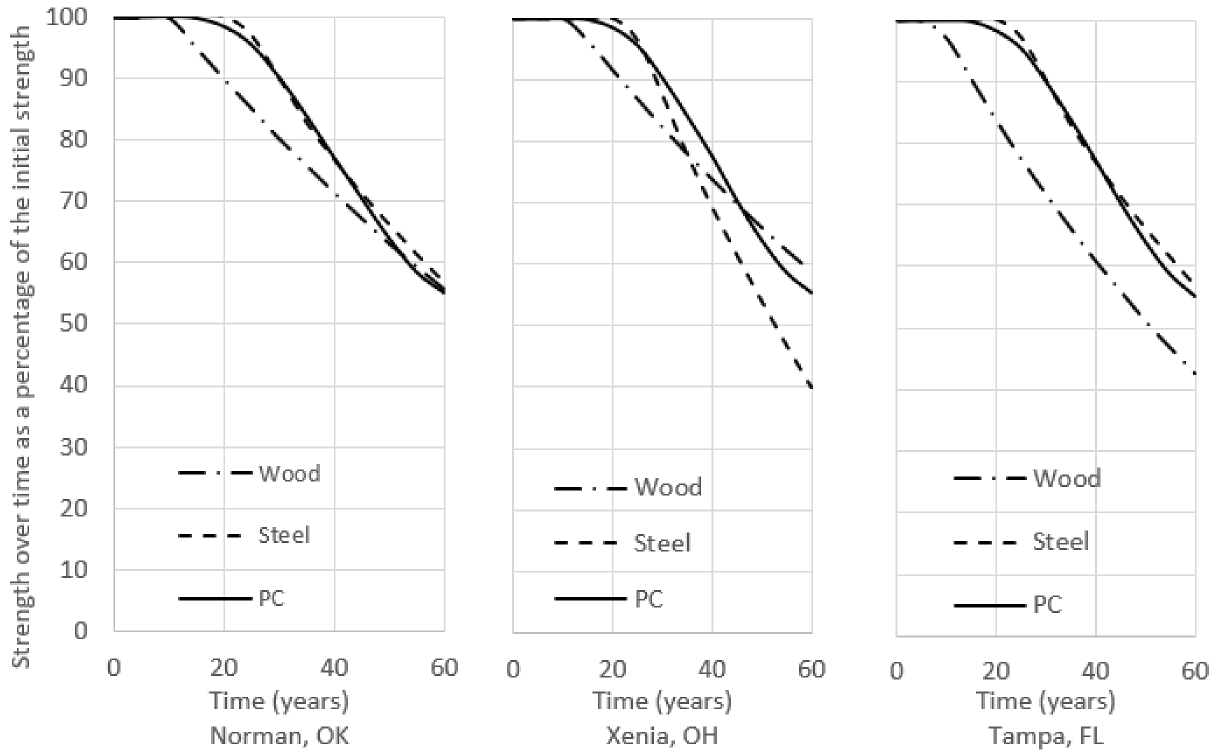

Figure 7: Deterioration of resisting moment over time

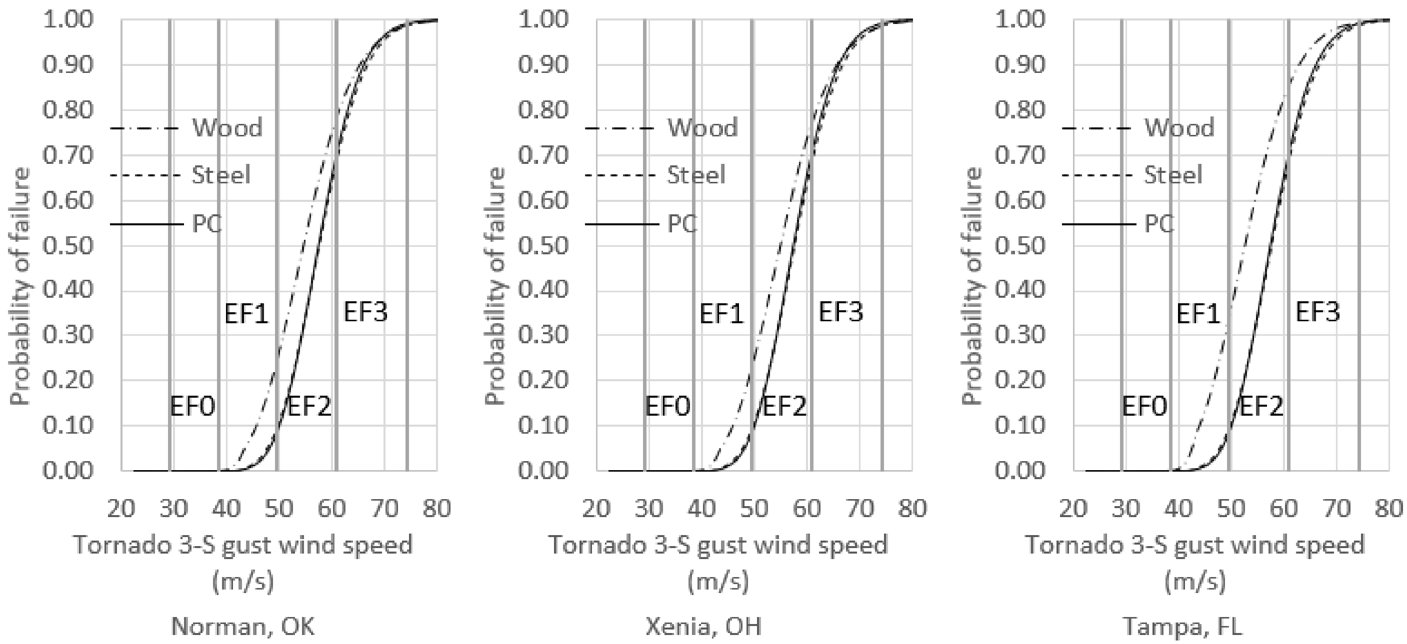

Figure 8: Fragility curves at 20 years

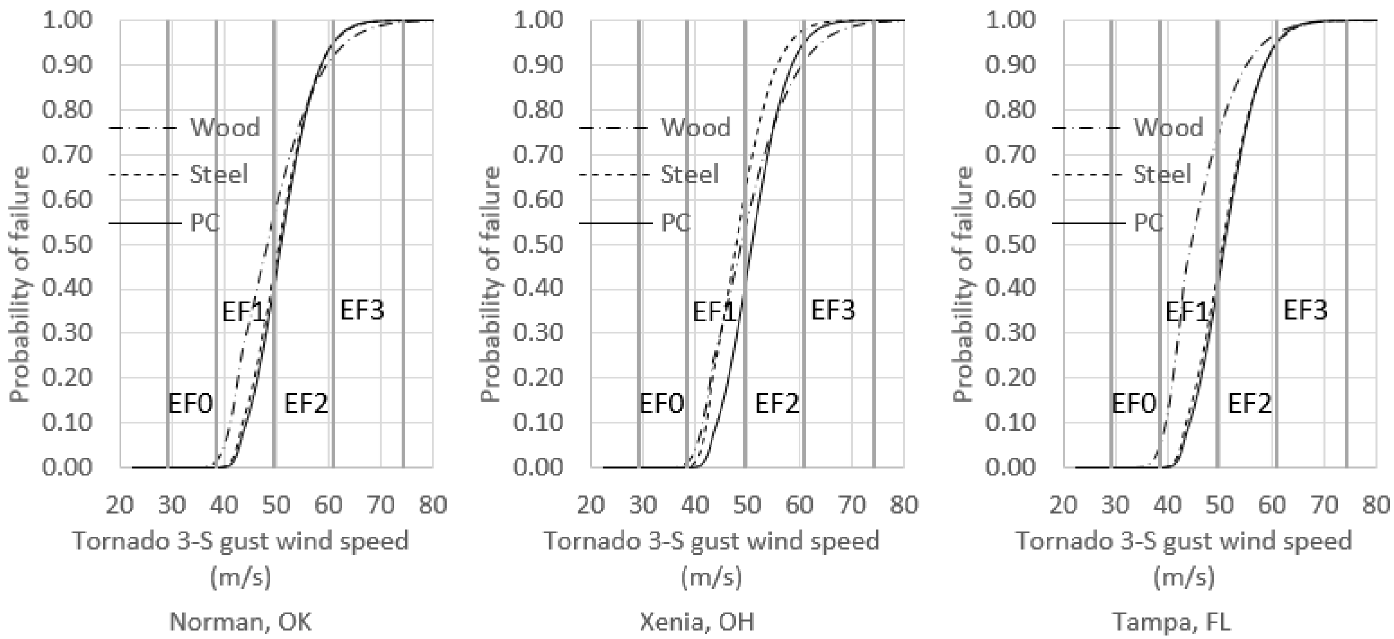

Figure 9: Fragility curves at 40 years

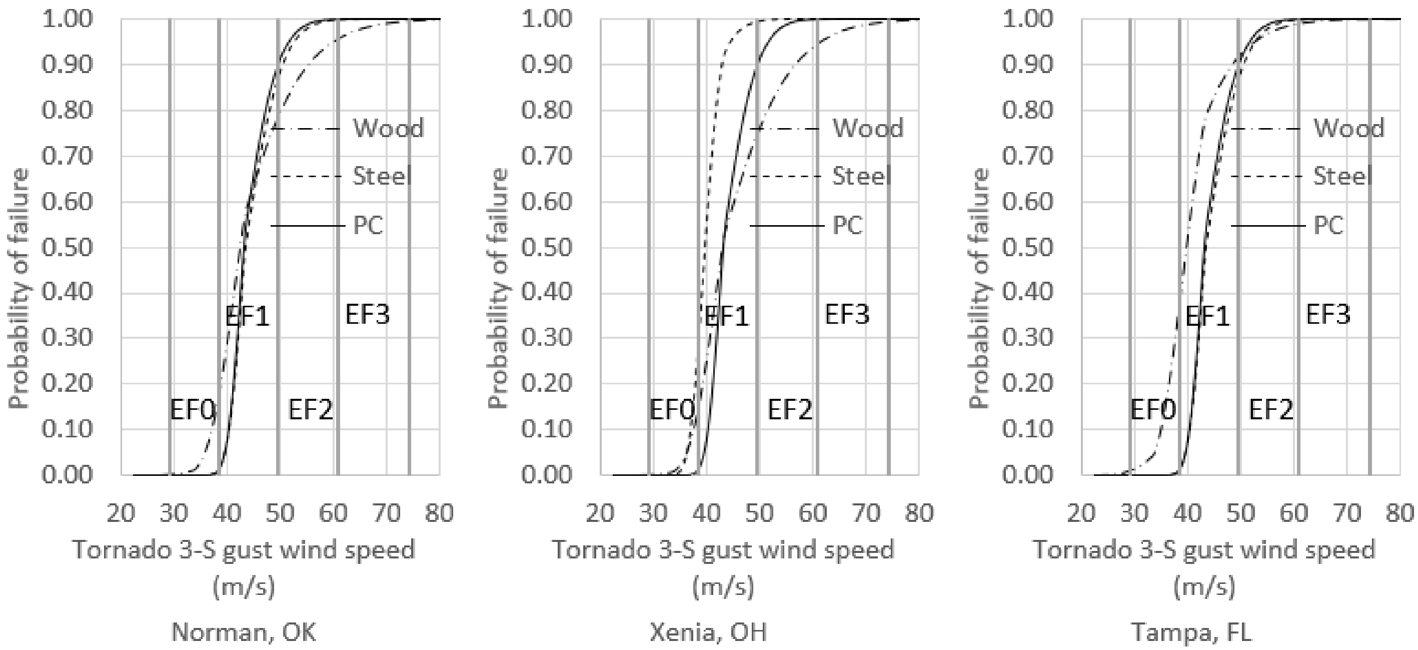

Figure 10: Fragility curves at 60 years

4.5. Cost Analysis

Cost analysis to study the impact of natural hazards on structures and infrastructure can be carried out in two ways: scenario-based cost analysis and lifecycle cost analysis. In a scenario-based analysis, the impact of a specific hazard intensity level is considered (e.g., a historic or a hypothetical tornado). However, the probability of occurrence of the specific hazard level is not considered. Lifecycle analysis, on the other hand, is a risk-based analysis, i.e., all possible hazard intensity levels and their probability of occurrence are considered over the entire life of the structure or infrastructure. Although life-cycle cost analysis is an important method to study hazards interaction with infrastructure systems in general through probabilistic analysis, a scenario-based analysis could better indicate the impact of tornadoes on utility poles. This is because tornadoes are extreme hazards with a very low probability of occurrence. Moreover, life-cycle cost analysis requires more data when compared to scenario-based analysis in order to produce accurate results that can be helpful in decision making. In this study, both scenario-based and lifecycle cost analysis are demonstrated.

4.5.1. Life-Cycle Cost Analysis

4.5.1.1. Tornado Occurrence Curves

To calculate the annual probability that the utility poles would fail under tornado hazard load, it is first necessary to obtain the mean annual probability of the tornado wind speed meeting or exceeding every velocity value within the range being studied for all locations included in this study. Standohar-Alfano et al (2014) used the data they obtained from tornadoes in the United States in the period between 1973 and 2011 to develop empirically based tornado hazard maps that give the mean probability of occurrence of tornadoes from all EF scales for various locations in the United States. For each location considered in this study, the mean probability of meeting or exceeding each EF scale is obtained from those hazard maps and is associated with the lower bound velocity for the scale. A second order exponential function of the following form shown in Equation (33) is a good fit for the cumulative distribution function of the tornado velocity v (Masoomi et al 2016):

$$F_{\mathrm{v}}(\mathrm{v}) = e^{\left(d_1 e^{d_2 \ln \mathrm{v}} + d_3 e^{d_4 \ln \mathrm{v}}\right)} \tag{33}$$

The probability density function can be found using Equation (34):

$$f_{\mathrm{v}}(\mathrm{v}) = \frac{d}{dv}\left(1 - F_{\mathrm{v}}(\mathrm{v})\right) \tag{34}$$

where d_1, d_2, d_3, and d_4 are parameters obtained by curve fitting of the second order exponential function in Equation (33), where v is in mph. The parameters for the cities used in this study are shown in Table 5. The curves for the mean annual probabilities of meeting or exceeding the tornado velocity values ($F_{\mathrm{v}}(\mathrm{v})$) are plotted in Figure 11. $F_{\mathrm{v}}(\mathrm{v})$ can be used as a cumulative distribution function (CDF) for wind speeds of 22 m/s and above (Masoomi et al 2016), which is within the range of typical tornado wind speed in the United States.

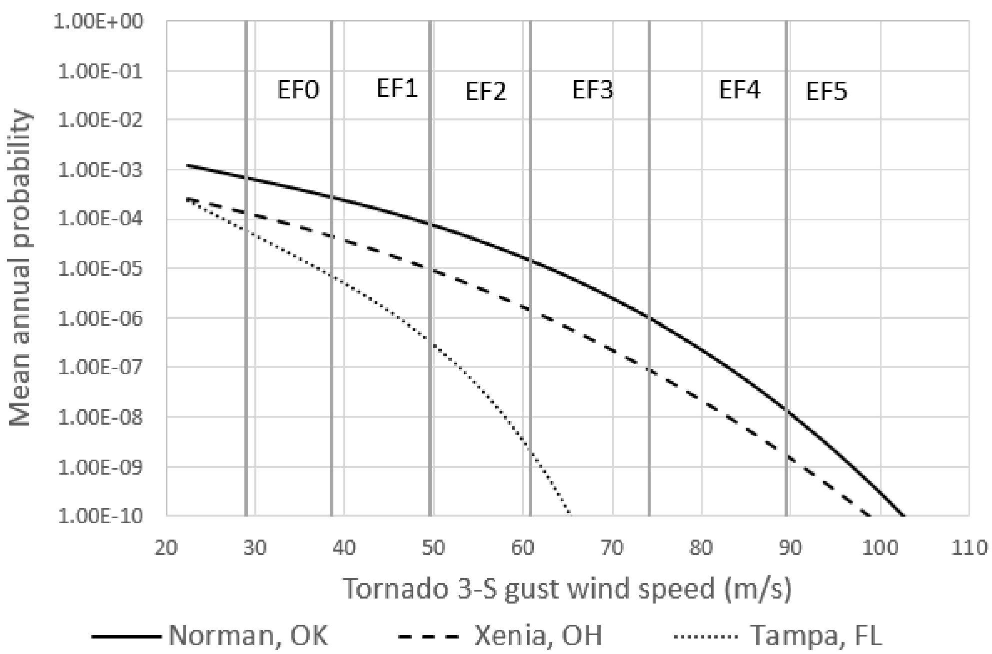

Figure 11: Tornado occurrence curves

Table 5: Values for d_1, d_2, d_3, and d_4 parameters

City	d_1	d_2	d_3	d_4
Norman, OK	-2.523	0.244	-8.833×10^{-7}	3.043
Xenia, OH	-4.397	0.1467	-6.024×10^{-5}	2.28
Tampa, FL	-0.8397	0.5854	-1.507×10^{-11}	5.403

As shown in Figure 11, The probabilities for Norman are higher than those for Xenia, which in turn are higher than those for Tampa for all EF velocity ranges. The low probability values in Figure 11 even for regions with high frequency of tornado occurrence like Norman can be explained by knowing that the hazard maps provided by Standohar-Alfano et al (2014) estimate the probability of tornado occurrence by dividing the path area of the tornadoes hitting some specified region by the total area of the region, and because the path area of the tornado is small compared to the total area of the region, the ratio will always be relatively small. However, it is important to mention that the relatively small area that consists of the cities of Norman and Moore in Oklahoma was hit by 7 tornadoes in the period between 1999 and 2013, of which two where F/EF5 tornadoes and one was EF4 tornado (NWS 2018), resulting in high numbers of fatalities and losses estimated in billions of dollars. This is one of the shortcomings of performing life-cycle cost analysis when studying tornadoes, since it depends on the annual probability of tornadoes hitting a specific point, and this small probability could fail to reflect the high frequency of damaging tornadoes in tornado-active regions.

4.5.1.2. Annual Probability of Failure

After generating the tornado occurrence curves, the annual probability of failure of wood, steel, and PC utility poles can be obtained by Equation (35) (Li et al 2006):

$$P_f(\mathrm{v}) = \int_0^\infty F_R(\mathrm{v}) f_{\mathrm{v}}(\mathrm{v}) d\mathrm{v} \tag{35}$$

Where $F_R(\mathrm{v})$ is the fragility of the pole (Equation (32)), and $f_{\mathrm{v}}(\mathrm{v})$ is the PDF of the tornado wind speed (Equation (34)). The annual probabilities of failure of poles are plotted in Figure 12 as a function of time. For the city of Norman, the probability values are close for all types of poles with the wood being slightly higher, while the values for steel poles are considerably higher for Xenia, and those of wood poles are considerably higher for Tampa. This can be explained by examining the deterioration curves in Figure 7, as it can be seen that the deterioration of the steel pole in Xenia and the deterioration of the wood pole in Tampa occur at higher rates.

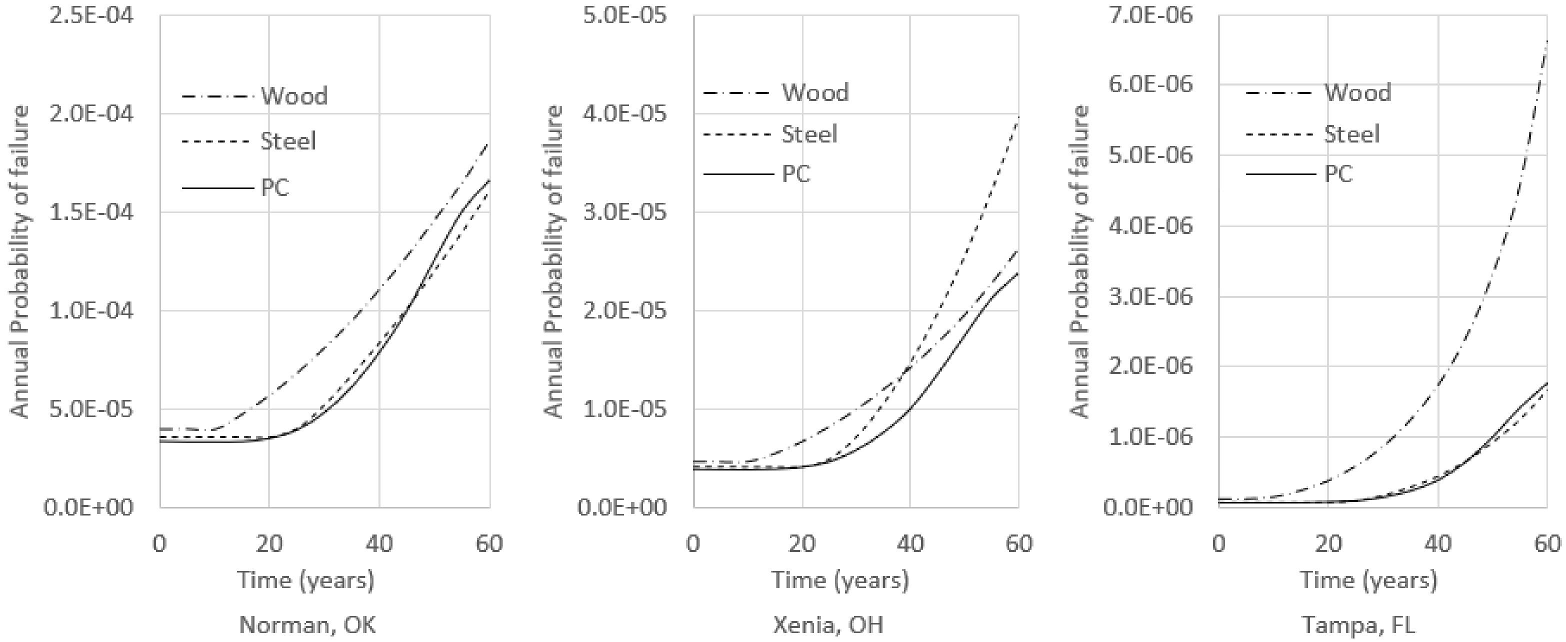

Figure 12: Annual probability of failure over time

4.5.1.3. Life-cycle cost analysis results

The Life cycle cost (LCC) of the poles can be calculated using Equation (36) (Wen et al 2001):

$$LCC = nC_o + \sum_{t=1}^{\tau} nP_f(t) \frac{C_{rep}}{(1+r)^t} + \int_0^{\tau} \frac{C_m}{(1+r)^t} dt \qquad (36)$$

Where $P_f(t)$ is the annual probability of failure of the pole at time t; τ is the design life of the pole; C_o is the initial cost of the poles; C_{rep} is the replacement cost; and C_m is the periodic maintenance cost. The initial cost C_o in this study is equal to the sum of the purchase cost and the installation cost. In general, the purchase cost of wood poles is less than steel poles, mainly because of the higher transportation cost of steel poles. The cost of PC poles is higher than other materials, also because of its higher transportation cost associated with its heavy weight (Lu et al 2017). The purchase price of poles changes with time and depends on the specific project, but the following values are used in this study for demonstration of the framework: $498.35 for wood poles (ATS 2018), $686 for steel poles (Salman et al 2016), and $720 for PC poles, assumed 5% higher than that of steel poles (Lu et al 2017). The installation and replacement costs vary between different types of poles. For example, the replacement cost of steel poles is usually less than that of wood poles because of its salvage value (Lacoursiere et al 1999). Still, due to the lack of data, the installation cost is assumed $2,500 per pole and C_{rep} is assumed equal to $4,000 per pole for all types of poles (Salman et al

2016; Xu et al 2008). Moreover, since the periodic maintenance was not included in generating the age dependent fragility curves, C_m is not considered in the cost analysis. The discount rate r is estimated to be equal to 5% (FEMA 1992), and the number of poles n used in this study is 10^5.

To evaluate the LCC , the service life of the poles is required. The actual service life of wood poles depends on several factors, such as the type of the pole and the quality of treatment, the environmental conditions affecting the poles, and the quality and frequency of maintenance (Morrell 2008). Most power utilities estimate the life of wood poles to be between 30 and 40 years, while the producers usually estimate it between 51 and 70 years (Mankowski et al 2002). Pole removal data shows that wood poles actually have a life longer than what is estimated by utilities, and some recent research papers show that 60-80 years is a more accurate estimate for the service life of utility poles (Bolin et al 2011; Morrell 2008; Pope 2004; Stewart 1996). Bolin et al (2011) recommended the use of 60 years as the expected life of wood, steel, and PC poles. Therefore, the service life of all poles in this study is assumed to be 60 years.

Table 6 shows the initial cost of the poles and their life cycle cost over the design life, and Figure 13 shows the life cycle cost over time. The values are generated for the 3 cities considered in this study for all types of poles. As can be seen from the results, the replacement cost due to pole failure caused by tornadoes has little effect on the LLC, especially for cities of low tornado occurrence probability. The initial cost is the major factor. Unless the initial cost is reduced for the steel and PC poles, or unless they are proven to have longer service life than that of wood poles, the wood poles are the most economic options even if they become more vulnerable to tornadoes over time. Therefore, since the probability that a tornado will strike a specific point is low even in tornado-active regions, and the effect of this probability of failure on the life cycle cost analysis will be small, the decision-making process based on the tornado-poles interaction is best performed through scenario-based analysis rather than life-cycle cost analysis.

Table 6: Comparison of LCC

	Initial cost ($/wood pole)	Initial cost ($/steel pole)	Initial cost ($/PC pole)	LCC ($/wood pole)	LCC ($/steel pole)	LCC ($/PC pole)
Norman, OK	2,998	3,186	3,220	3,003	3,190	3,224
Xenia, OH	2,998	3,186	3,220	3,000	3,188	3,222
Tampa, FL	2,998	3,186	3,220	2,999	3,187	3,221

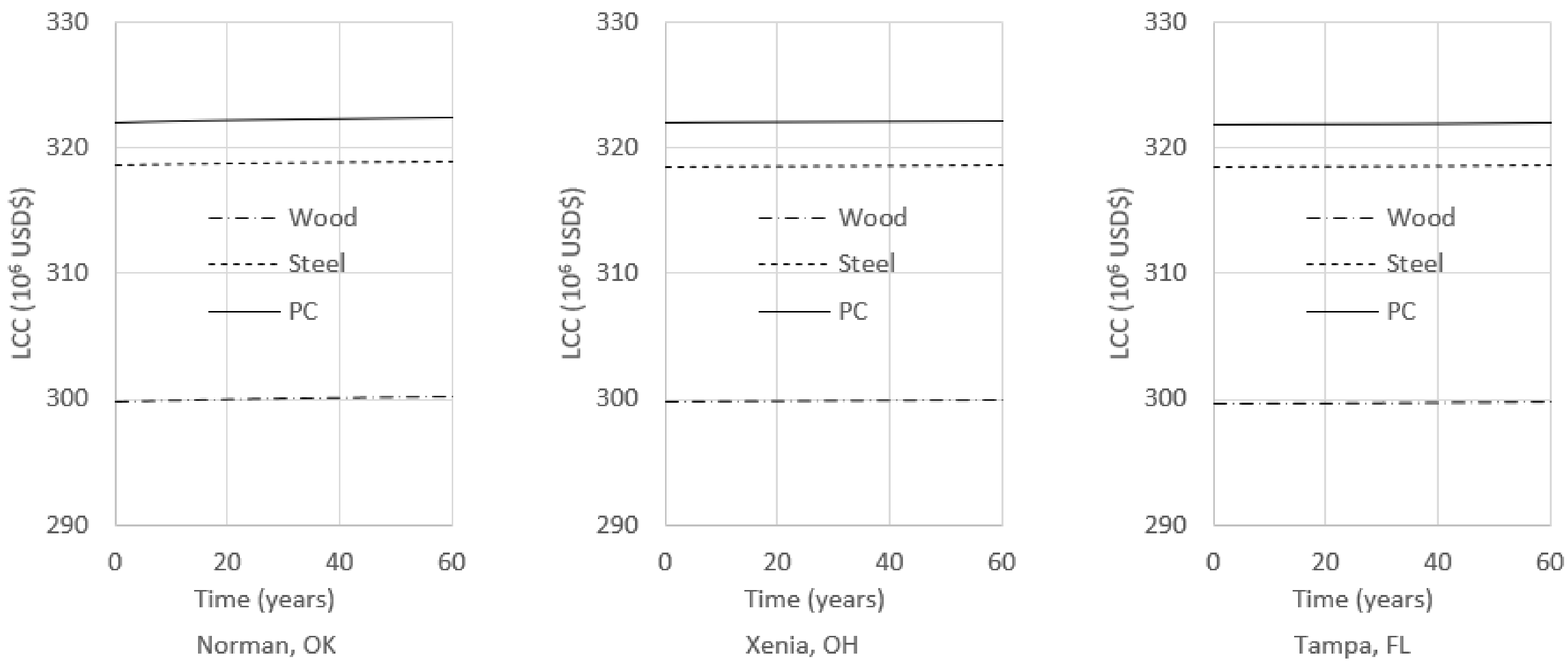

Figure 13: LCC over time

4.5.2. Scenario-based analysis

The tornado intensity, path length, and path width used in this scenario-based analysis are obtained using the data from the tornado that struck near the city of Norman, Oklahoma in May 19, 2013 (NOAA 2013) (see Figure 14). The area struck by the tornado is assumed to have poles of properties similar to those discussed in the previous sections, and distributed uniformly in grids of 46 m in both directions. The fragility curves for the poles are generated using the procedure discussed earlier in this study. Since the width of all intensity areas of the tornado are much larger than the span of the conductors, the effective span subjected to tornado width here is assumed equal to the entire span. The fragility curves for new and 60 years old wood, steel, and PC poles are plotted in Figure 15. The failure of any pole is assumed to be independent from the failure of its adjacent poles.

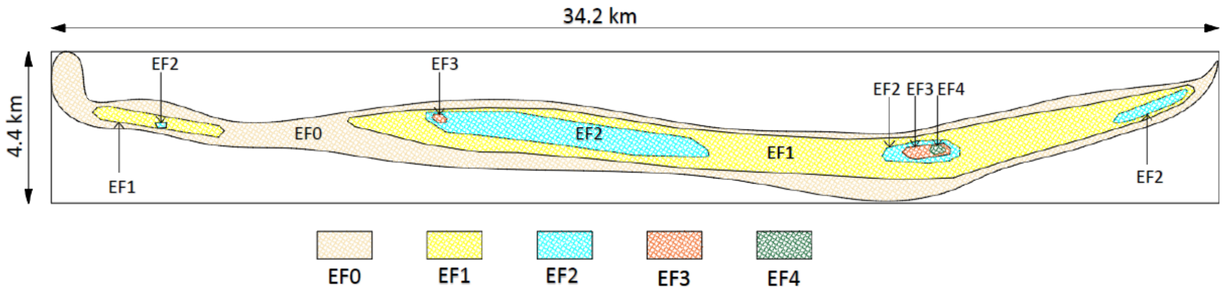

Figure 14: Tornado intensity map

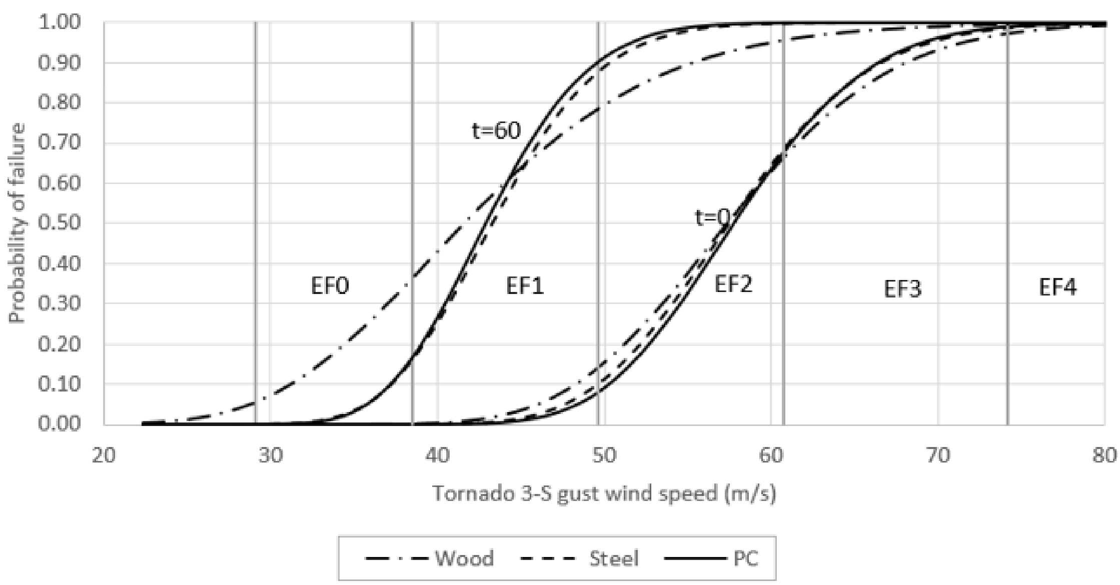

Figure 15: Scenario-based analysis fragility curves for new and 60 years old poles

The number of poles in each intensity area is determined knowing the spacing between poles, and the wind speed that poles in each area are subjected to is assumed equal to the average of the upper and lower bound velocities of the EF category of the area. Using the fragility curves, the probability of failure of the poles in each intensity area can be determined, and the sum of those probabilities is the expected number of failed poles. Finally, the replacement cost of the failed poles is calculated by multiplying the number of failed poles by the replacement cost assumed in the previous section ($4000/pole). The procedure described above is repeated for an assumed age of poles from 0 to 60 years. The expected number of damaged wood, steel, and PC poles and the expected cost of the replacement of the poles are shown in Figure 16 as a function of the assumed age.

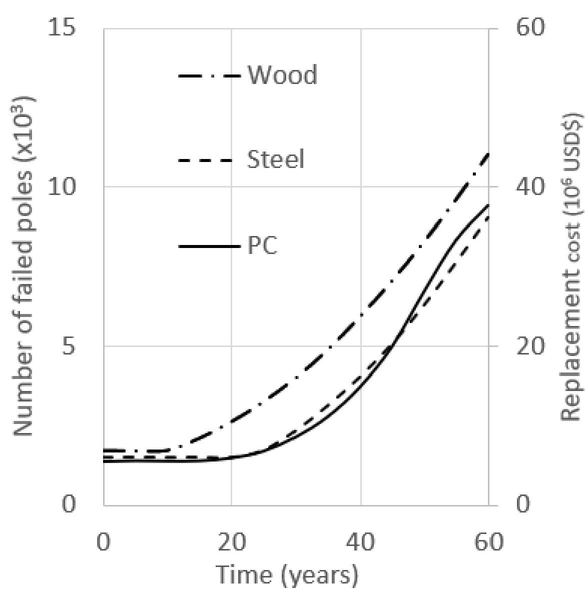

Figure 16: Scenario-based analysis number of failed poles and replacement cost

It can be seen from Figure 16 that the numbers of failed poles and replacement costs are lower for new poles of all materials, while the numbers and costs become considerably higher if the poles are aged. The behavior of the curves versus their assumed age can be explained by examining the behavior of their fragility curves over time. For new poles, the number of failed poles and costs are close for all materials since their fragilities are similar. The aged wood poles are more fragile for weaker tornadoes than other poles, while they are less fragile for moderate tornadoes. Since the area of weaker tornadoes is larger and hence the number of poles subjected to them are higher, this explains the slightly higher number of failed aged wood poles and their associated replacement cost.

5. System Reliability: Reliability and Cost Analysis of Power Distribution Systems Subjected to Tornado Hazard

5.1. Introduction

In the chapter, the component-level reliability method proposed in chapter 4 is used to generate a framework for reliability of power distribution systems when subjected to tornado hazard. The reliability analysis is performed through scenario-based analysis. Wood poles are used for demonstration of the framework, but it can be generalized for other types of poles.

In Section 5.2, the power distribution system used for the demonstration of the framework in this research is defined. Since reliability and cost analysis are performed through scenario-based analysis, the tornado scenarios considered in theis research are defined in Section 5.3. In Section 5.4, probability of failure analysis of power distribution poles subjected to tornadoes is discussed. The analysis is performed based on the fragility method proposed in the previous chapter. After that, the failure of power distribution lines resulting from the failure of poles is discussed in Section 5.4.3, and reliability analysis of power distribution systems is discussed in Section 5.6. The method used to harden the power distribution system and increase its reliability is discussed in Section 5.7, and cost analysis is discussed in Section 5.8. Finally, the results and discussion are presented in section 5.9. A flowchart of the framework is shown in Figure 17.

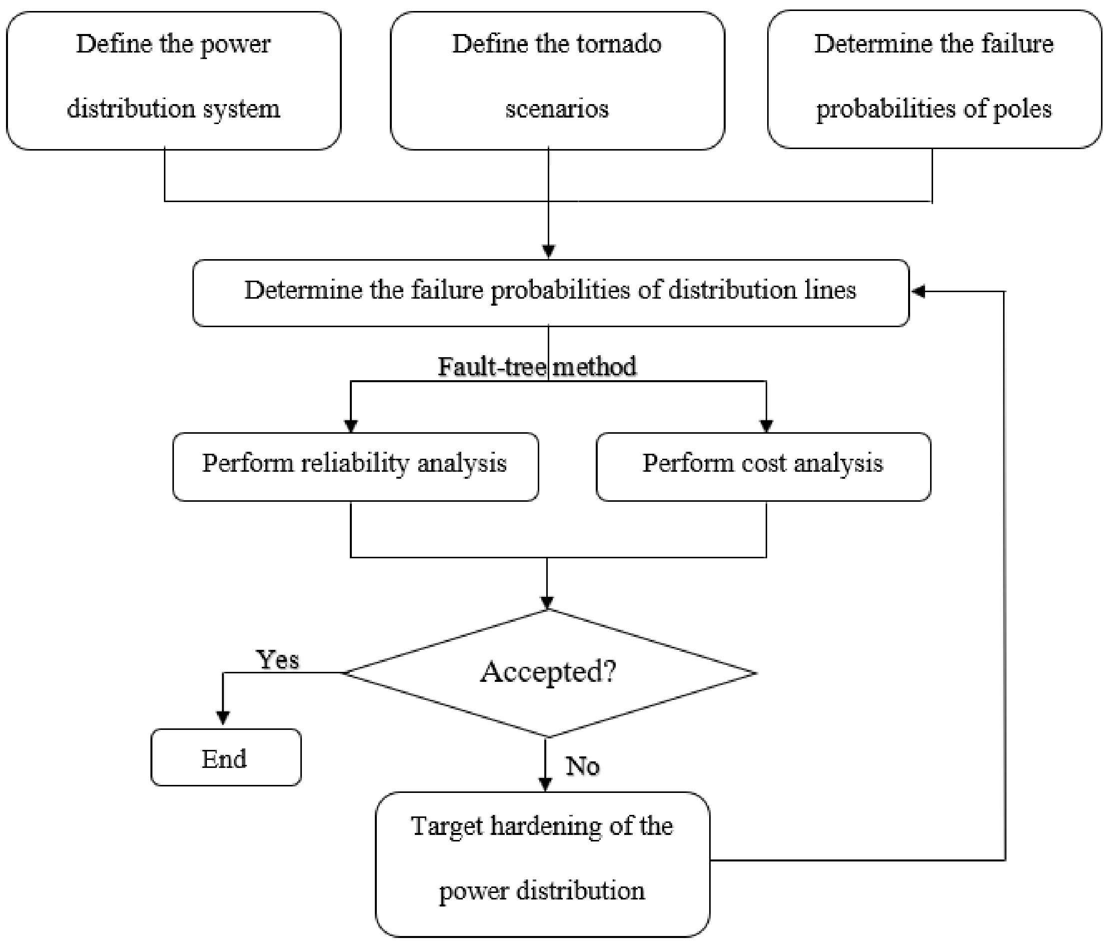

Figure 17: Flowchart of system reliability framework

5.2. Power Distribution System Definition

The power distribution system used in this study is based on the virtual city "Micropolis". This virtual city was created by Brumbelow et al (2007) to simulate an infrastructure system for research purposes and was used to model the power system and other infrastructure systems by other researchers (eg: Bagchi et al 2009; Francis et al 2011; Salman et al 2015). The power distribution system defined and used in this study consists of 38 distribution lines. Most of the lines are overhead distribution lines, but some are buried underground. The system consists of two parts, where each originates from a different feeder, and hence assumed to behave independently. The lines distribute power to 434 residential units, 15 industrial units, and 13 commercial units. The power distribution system is shown in Figure 18. Since the parameters of the decay model used for calculating the deterioration of wood poles require a specific location, this city is assumed to be near the city of Norman, OK. The power consumption of each type of units is assumed constant and equal to the average consumption in the state of Oklahoma within the 5 years period between 2013 and 2017 obtained from EIA (EIA 2018b). The average consumption is 1.53 kWh for each residential unit, 8.51 kWh for each commercial unit, and 110.21 kWh for each industrial unit.

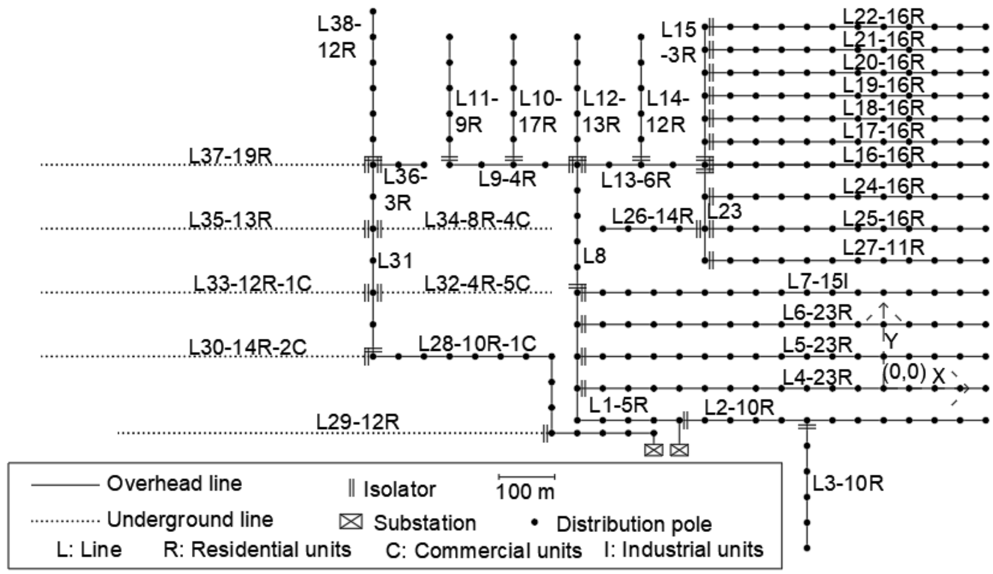

Figure 18: Micropolis power distribution system

5.3. Tornado Scenarios

Reliability of the power distribution system is performed in this research through scenario-based analysis. Each tornado scenario can be created after assuming the tornado intensity scale, starting point, and path angle. Using the previous assumptions, the tornado total path width and length can be estimated using historical data.

Statistics of the total width and length of tornadoes are available from data of 40,000 tornadoes that occurred in the United States between 1971 and 2011 (Standahor-Alfana et al 2014). Those statistics can be used to model the width and length of each EF tornado scale as random variables. Masoomi et al (2018) suggested Weibull distribution to fit the width and length data and determined the scale and shape parameters of the width and length associated with each EF scale. The CDF plots of the length and width of each EF tornado are shown in Figure 19 and Figure 20 respectively. In this study, the mean width and mean length of these random variables are used to define tornado scenarios. The mean width and length of each EF category are shown in Table 7.

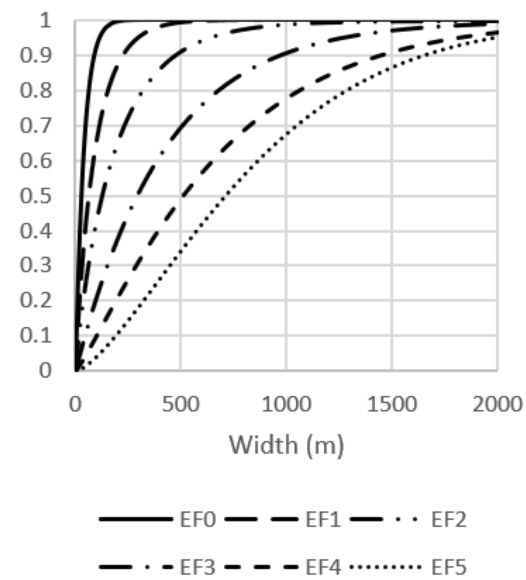

Figure 19: Tornado width CDF

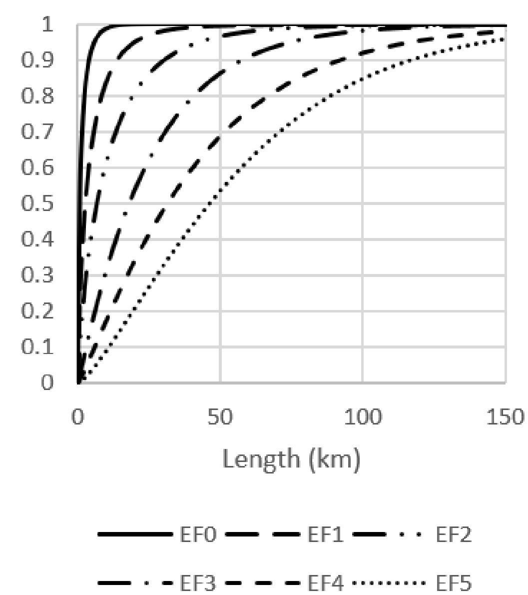

Figure 20: Tornado length CDF

Table 7: EF scale wind speed, tornado mean path width, and tornado mean path length

EF category	3-sec gust wind speed (m/s)	Tornado mean width (m)	Tornado mean Length (km)
EF0	29–38	40	1.5
EF1	38–49	96	5.3
EF2	50–60	197	11.9
EF3	61–74	419	25.2
EF4	74–89	669	41.7
EF5	>89	837	56.7

Standahor-Alfana et al (2014) used the damage data of the Tuscaloosa and Joplin tornadoes in 2011 to estimate the percentages of lengths and widths of the different intensities within the tornado. The percentages of the widths and lengths for different intensities within the EF1 and EF2 tornadoes are shown in Table 8 (Standahor-Alfana et al 2014). Hence, the path and intensities of any assumed tornado can be estimated using Table 7 and Table 8. Although the path of the tornado can have irregular shapes, because of lack of data and for simplicity, it is assumed to be rectangle with the intensity increasing when moving towards its center (Masoomi et al 2018).

Table 8: EF1 and EF2 intensities percentages

	EF0 width %	EF1 width %	EF2 width %	EF0 length %	EF1 length %	EF2 length %
EF1	37.5	62.5	0	57.4	42.6	0
EF2	21.1	31.4	47.5	28.1	35.2	36.7

Most of the tornadoes in the United States are scaled EF2 and below (Wong et al 2010). Hence, 2 tornado scenarios are considered: one for EF2 tornado and another for EF1 tornado. Since the width of those tornadoes is smaller than the size of the power distribution system defined in this study, 6 different paths of parallel tornadoes hitting the system at different points are considered for each scenario. Although other paths could be considered were the tornado hits the system at other points or with different angles, those paths were found after analysis to cover the critical cases when an EF1 and EF2 tornadoes hit the power distribution system. For both the EF2 scenario and the EF1 scenario, the tornado hits the system with its center at the (0,0) point shown in Figure 18 with an angle of 45^{o}. This is the first path of the tornado. Then, another 5 parallel tornado paths are considered where the tornado hits the system with a path angle of 45^{o}, but its center hits the system at a different point. For each path, the tornado center shifts 80 m to the negative X-direction, and 80 m to the positive Y-direction from the location of the center of the previous path. The 6 EF2 scenario paths are shown in Figure 21 through

Figure 26, while the 6 EF1 scenario paths are shown in Figure 27 through Figure 32.

Since the poles of moderate age are vulnerable to EF2 tornadoes, while for EF1 tornadoes, the fragility becomes considerable only for aged poles, different poles' ages are assumed for the two scenarios. For the EF2 scenario, the age of the poles is assumed to be a random variable following a lognormal distribution with a mean of 31.2 years and a coefficient of variation of 0.47 (Darestani et al 2017). On the other hand, the age of the poles in the EF1 scenario is assumed to be a random variable following a uniform distribution between 60 and 80 years, which is the range of service life of wood poles as suggested by some studies (Bolin et al 2011; Morrell 2008; Pope 2004; Stewart 1996). The probability density functions (PDF) of the poles' age for the two scenarios are shown in Figure 33.

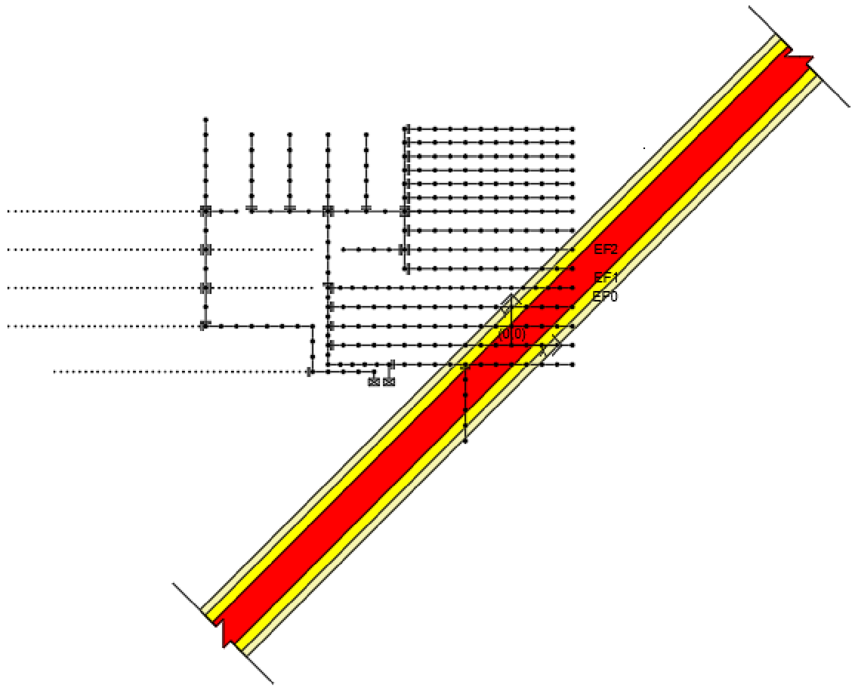

Figure 21: EF2 scenario path 1

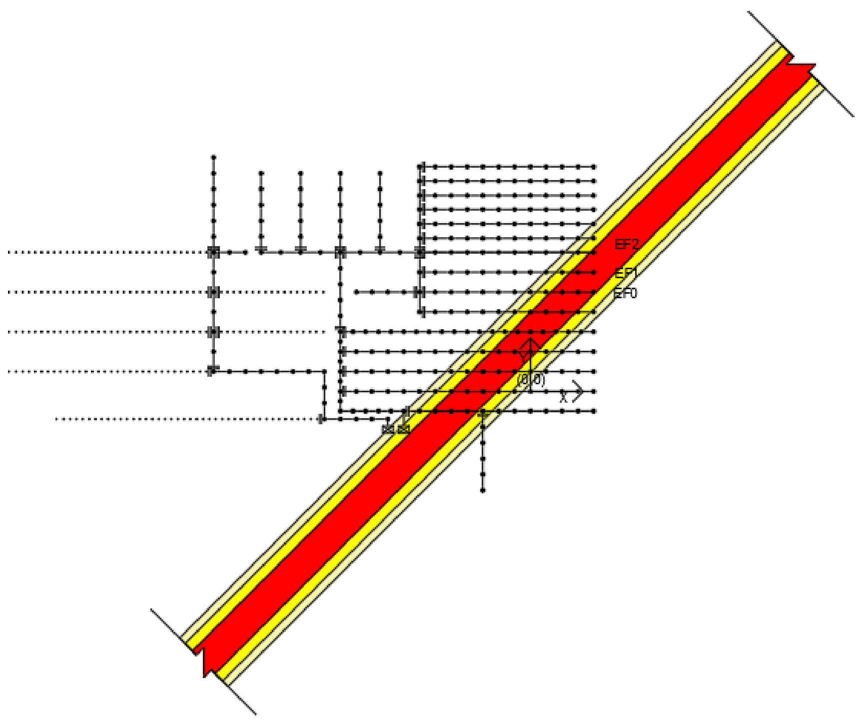

Figure 22: EF2 scenario path 2

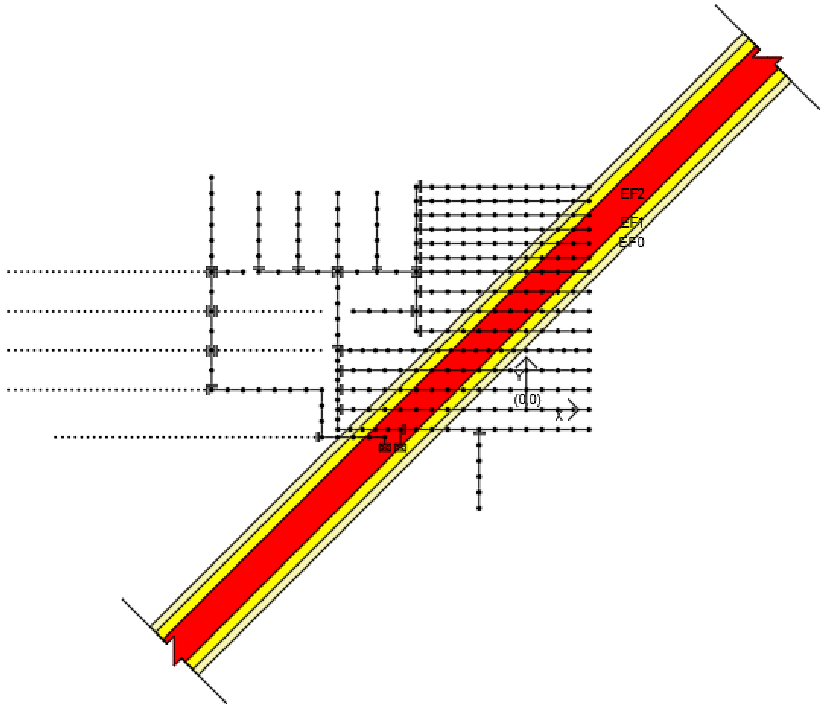

Figure 23: EF2 scenario path 3

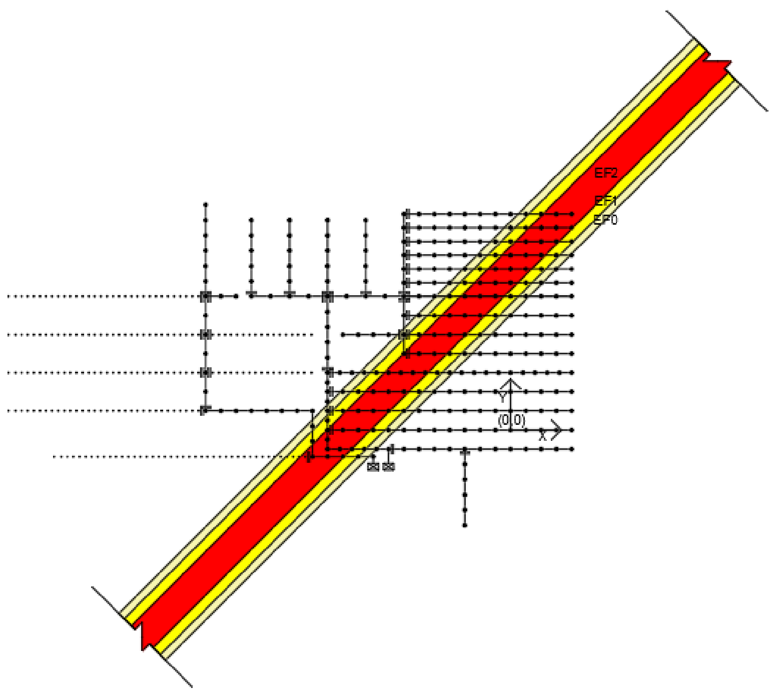

Figure 24: EF2 scenario path 4

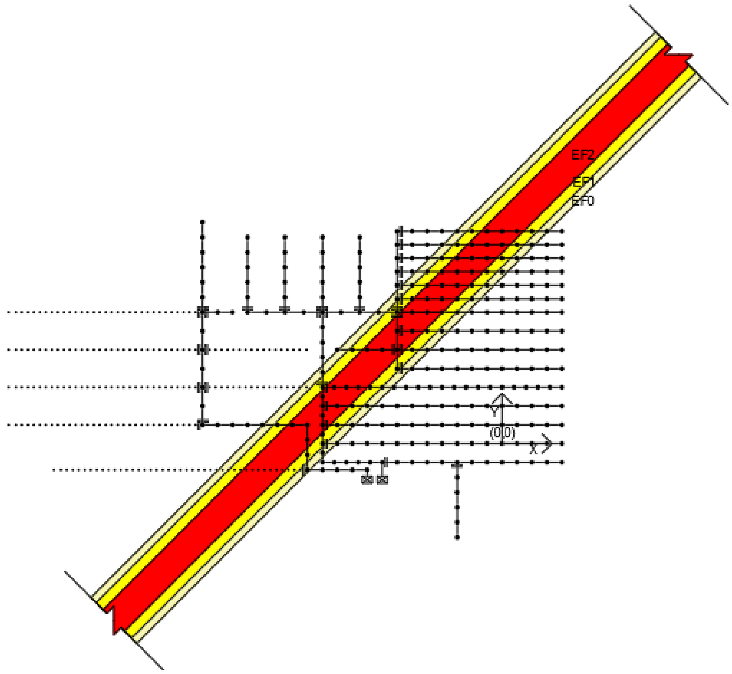

Figure 25: EF2 scenario path 5

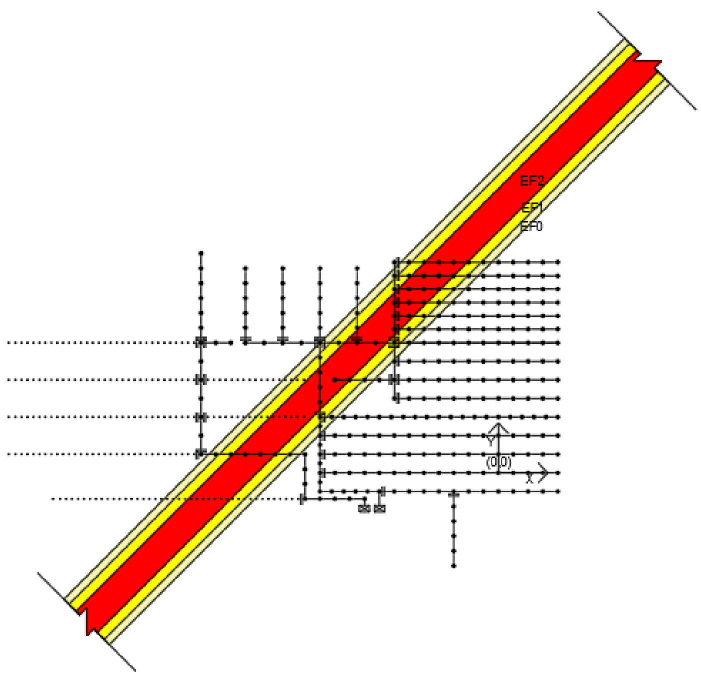

Figure 26: EF2 scenario path 6

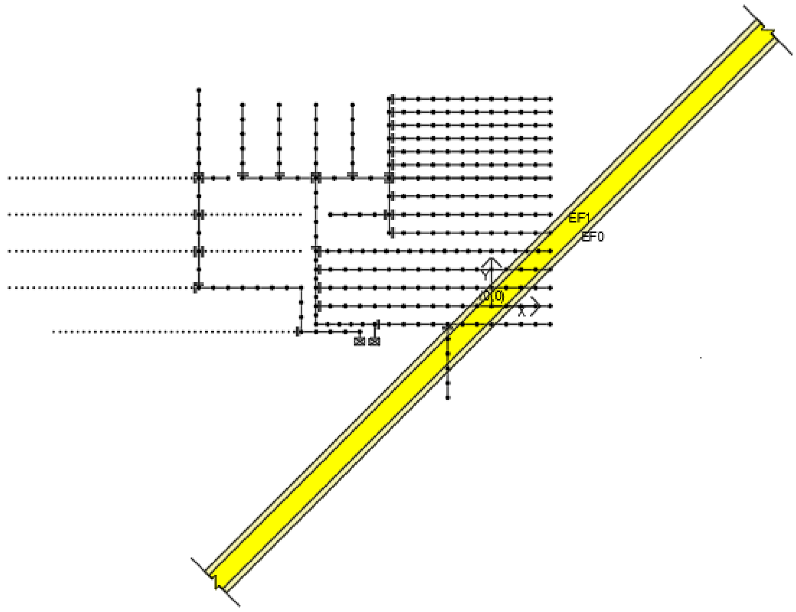

Figure 27: EF1 scenario path 1

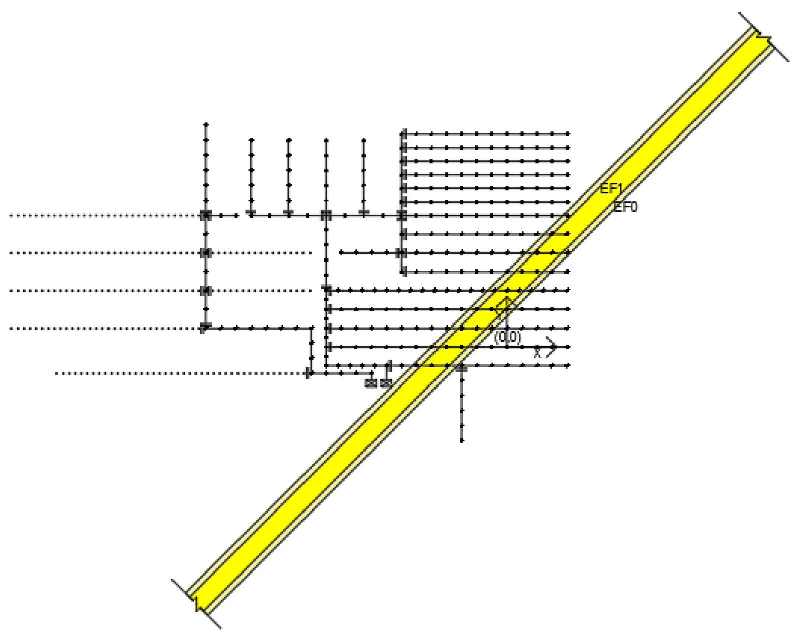

Figure 28: EF1 scenario path 2

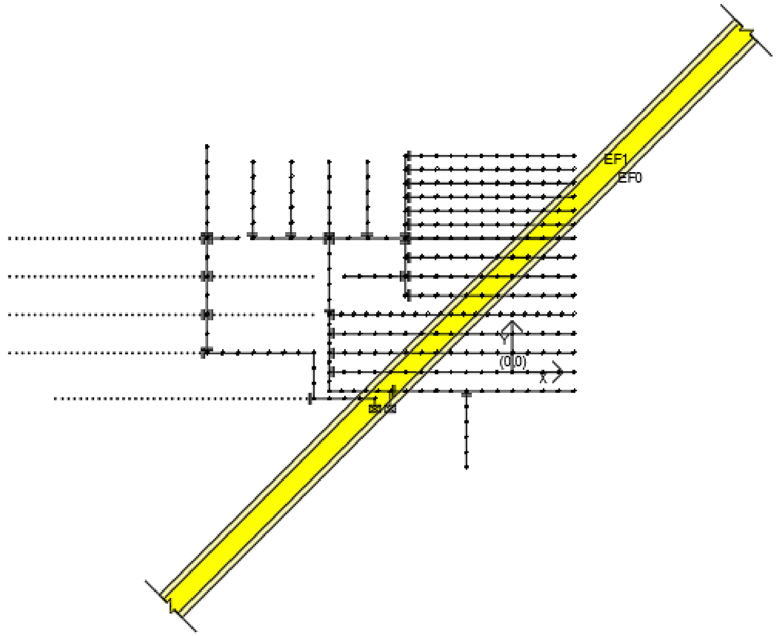

Figure 29: EF1 scenario path 3

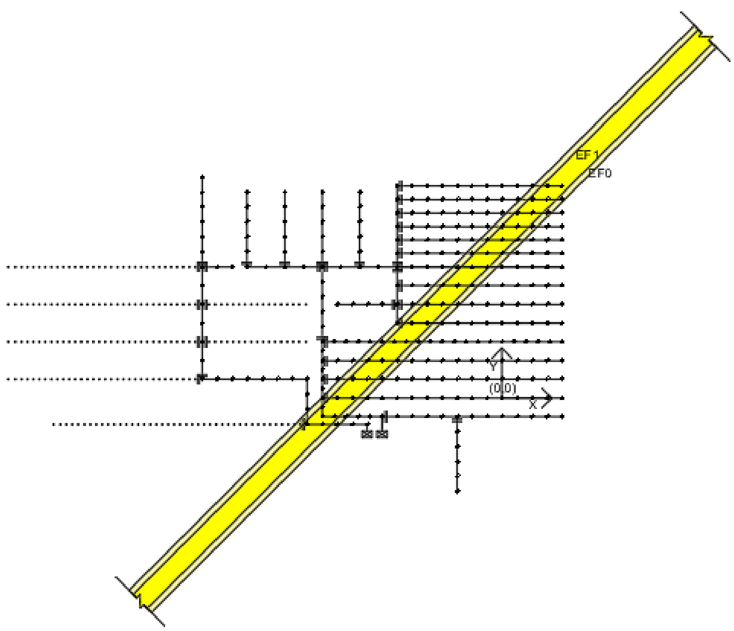

Figure 30: EF1 scenario path 4

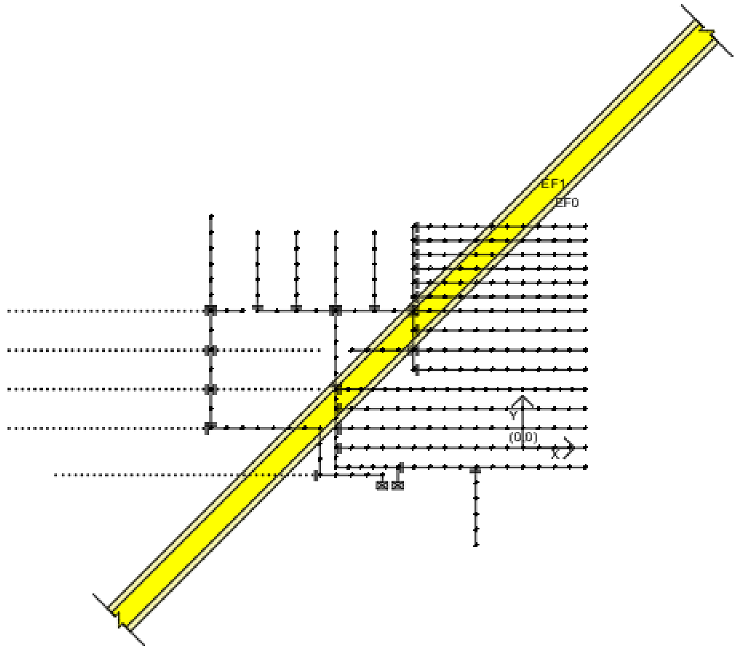

Figure 31: EF1 scenario path 5

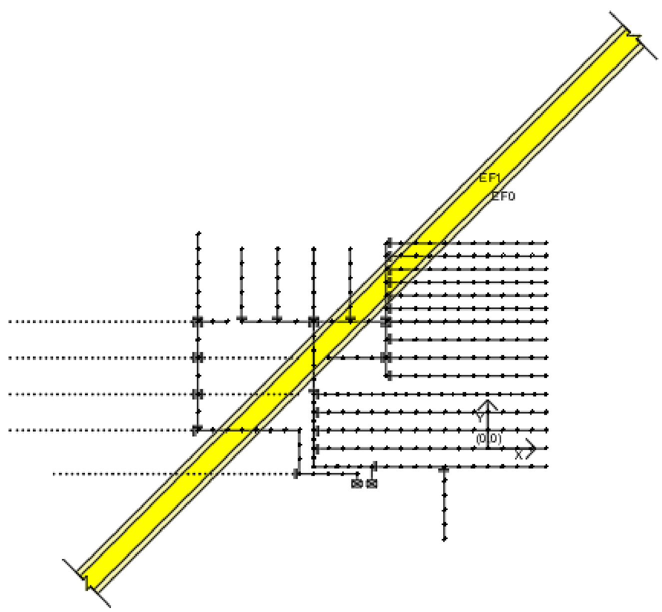

Figure 32: EF1 scenario path 6

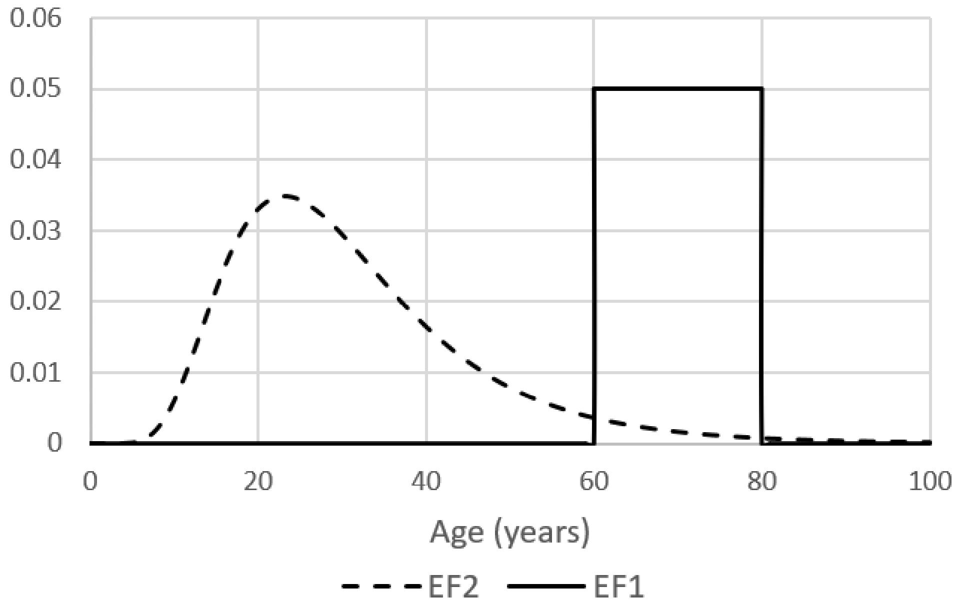

Figure 33: Poles' age PDF

5.4. Failure Probabilities of Poles

5.4.1. Tornado Wind Load

The fragility framework presented in the Chapter 4 is used in this chapter to determine failure probability of poles. In generating the poles fragility curves in Chapter 4, the tornado wind velocity acting on the conductors was assumed equal to that acting on the pole, and the effective span of the conductors subjected to tornado wind was assumed equal to half the span length of the conductors in each side of the pole. Those assumptions were made since the fragility curves were generated to be general. However, in this chapter, a defined power distribution system and defined tornado scenarios are available, and hence, better approximations can be made.

Using the tornado path (that is defined by assuming the tornado EF scale, tornado center location, and tornado path angle as discussed in the previous section) and its EF scales percentages, the maximum tornado wind velocity at each point within the system can be estimated by interpolating between the velocities associated with each EF scale and assuming zero wind velocity outside the path of the tornado. Hence, the pole is assumed to support, in addition to the tornado wind force acting on it, the tornado wind force acting on the conductors it is carrying from both sides (see Figure 34). The tornado wind pressure acting on each conductor varies along its span since the velocity varies from one point to another. The wind load supported by the pole can be estimated by assuming each conductor to be supported by two poles. Moreover, the maximum effective span considered is assumed to not exceed half the width of the tornado, since a span that is larger cannot be subjected to tornado wind acting on the same direction at one specific time. In this procedure, the behavior of the conductors is assumed to be static and the dynamic behavior of vibrating conductors is not considered, which might lead to underestimating the loads. However, the maximum wind pressure is used for the entire length of the conductors' effective span which is unlikely to occur at the same time and hence conservative. The sag of the conductors is usually designed to be very small compared to their lengths except for some extreme cases such as very high temperatures (Darestani et al 2016), and hence, it can be neglected. The tornado demand moment acting on each pole can be calculated using Equation (37):

$$M_s = h_p F_p + h_c \sum F_c \tag{37}$$

Where M_s is the tornado demand moment on the utility pole at the ground level; h_p is the moment arm, equals the distance between the ground and the centroid of the pole; F_p is the tornado wind force on the pole, calculated using Equation (1); h_c is the height of the conductors above the ground level; and $\sum F_c$ is the sum of the forces of the tornado wind acting on the conductors and supported by the pole. Each conductor is divided into 10 segments, and the force on each segment can be determined by using Equation (2) and the tornado wind velocity acting on the segment.

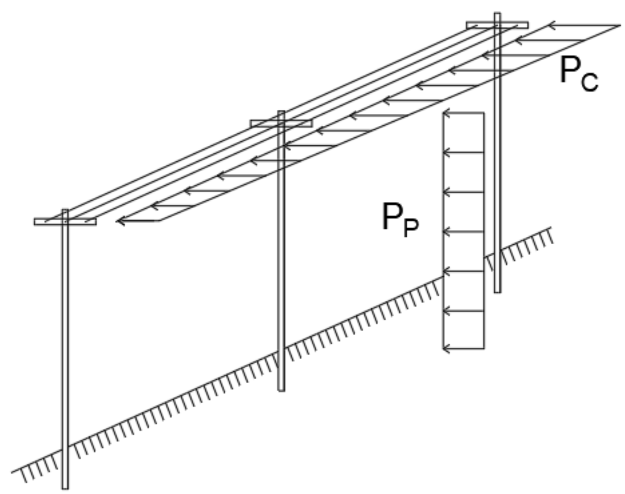

Figure 34: Tornado wind pressure model

5.4.2. Design and Strength Deterioration Models of Poles

The utility poles used to support the conductors are class 4 treated southern pine wood poles. However, class 2, or class 3 treated southern pine wood poles are used for hardening. The strength of the poles has a mean of 55.2 MPa (ANSI-O5.1. 2002), modeled as a lognormally distributed random variable that has a coefficient of variation that varies with age (Dagher et al 2006). Shafieezadeh et al (2014) calculated the coefficient of variation to be 0.17 for new poles, 0.4 for 60 years old poles, and 0.55 for 75 years old poles. After 75 years, the coefficient of variation becomes almost constant.

The dimensions of the poles are modeled as normally distributed random variables with a coefficient of variation assumed equal to 0.04. The length of the poles is 13.7 m, with 2 m buried under the ground (ANSI-O5.1. 2002). The conductors are attached to the pole at a distance 0.6 m below the top of the pole (Short 2014). The class 4 pole has a ground diameter and top diameter of 0.28 m and 0.17 m respectively, the class 3 pole has a ground diameter and top diameter of 0.30 m and 0.19 m respectively, while the class 2 pole has a ground diameter and top diameter of 0.33 m and 0.20 m respectively (ANSI-O5.1. 2002). The moment capacity of the wood pole at ground level and the strength deterioration of the pole cross-section can be calculated using Equation (4) and Equation (5) respectively.

3 conductors of a diameter of 18.3 mm are attached to each pole (Short 2014). The length of the conductors is equal to the distance between poles. The diameter and length of the conductors are also modeled as normally distributed random variables and assumed to have a coefficient of variation of 0.03 and 0.06 respectively. The above values are summarized in Table 9.

Table 9: Summary of random variables used in fragility analysis used for system reliability analysis

	Mean	C.O.V.	Distribution
Strength of wood (MPa)	55.2	Varies with age	Lognormal
Height above ground (m)	11.7	0.04	Normal
Diameter of class 4 pole at ground level (m)	0.28	0.04	Normal
Diameter of class 4 pole at top (m)	0.17	0.04	Normal
Diameter of class 3 pole at ground level (m)	0.30	0.04	Normal
Diameter of class 3 pole at top (m)	0.19	0.04	Normal
Diameter of class 2 pole at ground level (m)	0.33	0.04	Normal
Diameter of class 2 pole at top (m)	0.20	0.04	Normal
Number of conductors	3	-	-
Diameter of conductors (mm)	18.3	0.03	Normal
Length of conductors (m)	Distance between poles	0.06	Normal

5.4.3. Probability of Failure of Poles

For each scenario path, each pole within the power distribution system and the conductors it supports will be subjected to a different tornado wind velocity. Hence, the probability of failure can be calculated using Equation (38):

$$\mathrm{P}_{\mathrm{f-pole}} = P(M_R - M_S < 0) \tag{38}$$

Where $\mathrm{P}_{\mathrm{f-pole}}$ is the probability of failure of the pole; M_R is the moment capacity of the utility pole calculated using Equation (4); and M_S is the moment demand of the tornado load acting on the utility pole calculated using Equation (37).

5.5. Failure of Power Distribution Lines

Taras et al (2004) suggested a simple method to estimate the probability of failure of power distribution lines. In this method, the failure of the line is assumed to occur when 2 adjacent poles fail, and conductors fall to the ground. This is because the span of conductors in distribution lines is relatively small, and the failure of one pole usually doesn't lead to the failure of the line. This is unlike the transmission lines, where the failure of one transmission tower is enough to cause the failure of the line.

When a pole fails within the line, the probability of failure of its two adjacent poles will increase since each will carry part the conductors span that was initially supported by the failed pole. Hence, the probabilities of failure of the two adjacent poles are conditional probabilities depending on the failure of the central pole. The failure of the line resulting from the failure of any pole can be estimated using Equation (39) (See Figure 35):

$$P_{L-a} = P(F_a).P([F_b \cup F_c]|F_a) \tag{39}$$

Where P_{L-a} is the probability that the distribution line will fail because of the failure of pole a; $P(F_a)$ is the probability of failure of pole a; $P([F_b \cup F_c]|F_a)$

is the conditional probability that any of the two adjacent poles b and c will fail if the central pole a fails. Equation (39) can be rewritten as Equation (40):

$$P_{L-a} = P(F_a).[P(F_b|F_a) + P(F_c|F_a) - P(F_b|F_a).P(F_c|F_a)] \quad (40)$$

Where $P(F_b|F_a)$ and $P(F_c|F_a)$ are the conditional probabilities of failure of the adjacent poles b and c if the central pole a fails.

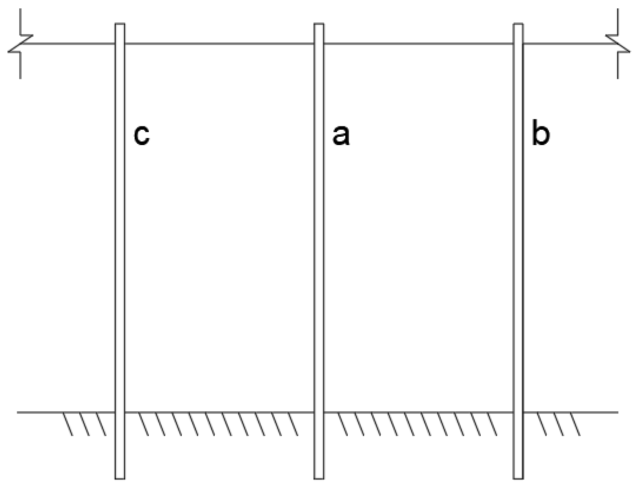

Figure 35: Power distribution line failure model

After determining P_{L-a} for all poles within the line, the probability of failure of the line P_L will depend on the correlation between the poles (Taras et al 2014). The maximum probability of failure will occur if the poles are fully correlated, while the minimum value will occur if the poles are fully independent. The maximum and minimum boundaries of the probability of failure of the line can be calculated by Equation (41) and Equation (42) respectively, where n_a is the number of poles within the line:

$$P_L = 1 - \prod_{a=1}^{n_a} (1 - P_{L-a}) \tag{41}$$

$$P_L = \max(P_{L-a}) \tag{42}$$

In general, the probability of failure of the line will be between that given by Equation (42) which is the lowest possible value, and that given by Equation (41) which is the highest possible value, depending on the correlation coefficient between poles. The correlation coefficient between any two poles a and b can be determined by the exponential decay model shown in Equation (43) (Darestani et al 2017):

$$\rho_{a,b} = \exp\left(-\frac{L_{a,b}}{L_s}\right) \tag{43}$$

Where $\rho_{a,b}$ is the correlation coefficient; $L_{a,b}$ is the distance (positive) between poles a and b; and L_s is the length scale. The correlation will hence depend on the ratio of $L_{a,b}/L_s$ as it will be negligible if the ratio is larger than one, while it will be significant if the ratio is smaller than one. Although Equation (43) can be used to obtain more accurate results, due to the lack of data regarding the length scale, Equation (41) will conservatively be used in this study for the probability of failure of lines within the power distribution system.

In power distribution systems, the lines are connected by isolators. Those isolators will disconnect any line that fails, and hence, each line can be considered as an element that is independent from other lines within the system (Brown 2008).

The analysis of line 7 for path 2, path 3, and path 4 of the EF2 scenario are shown in Table 10, Table 11, and Table 12 respectively. Line 7 consists of 20 poles numbered from left to right. For each scenario path, different poles are subjected to the wind field of the tornado. The upper bounds of the probability of failure of the line using Equation (41) are 0.985, 0.984, and 0.984 for path 2, path 3, and path 4 of the EF2 scenario respectively. Moreover, the lower bounds of the probability of failure of the line using Equation (42) are 0.694, 0.710, and 0.699 for path 2, path 3, and path 4 of the EF2 scenario respectively.

Table 10: Probability of failure results for Line 7 in path 2 of EF2 scenario

Pole	$P(F_a)$	$P(F_b\|F_a)$	$P(F_c\|F_a)$	P_{L-a}
1	0.000	0.000	0.000	0.000
2	0.000	0.000	0.000	0.000
3	0.000	0.000	0.000	0.000
4	0.000	0.000	0.000	0.000
5	0.000	0.000	0.000	0.000
6	0.000	0.000	0.000	0.000
7	0.000	0.000	0.000	0.000
8	0.000	0.000	0.000	0.000
9	0.000	0.000	0.004	0.000
10	0.004	0.000	0.103	0.000
11	0.116	0.074	0.535	0.066
12	0.660	0.659	0.501	0.548
13	0.714	0.950	0.392	0.692
14	0.710	0.970	0.280	0.694
15	0.622	0.964	0.003	0.599
16	0.088	0.902	0.000	0.080
17	0.002	0.379	0.000	0.001
18	0.000	0.007	0.000	0.000
19	0.000	0.000	0.000	0.000
20	0.000	0.000	0.000	0.000

Table 11: Probability of failure results for Line 7 in path 3 of EF2 scenario

Pole	$P(F_a)$	$P(F_b\|F_a)$	$P(F_c\|F_a)$	P_{L-a}
1	0.000	0.000	0.000	0.000
2	0.000	0.000	0.000	0.000
3	0.000	0.000	0.000	0.000
4	0.000	0.000	0.000	0.000
5	0.000	0.000	0.022	0.000
6	0.022	0.001	0.198	0.004
7	0.286	0.283	0.575	0.199
8	0.713	0.821	0.417	0.639
9	0.724	0.968	0.414	0.710
10	0.725	0.973	0.051	0.707
11	0.346	0.955	0.000	0.331
12	0.031	0.768	0.000	0.024
13	0.000	0.126	0.000	0.000
14	0.000	0.000	0.000	0.000
15	0.000	0.000	0.000	0.000
16	0.000	0.000	0.000	0.000
17	0.000	0.000	0.000	0.000
18	0.000	0.000	0.000	0.000
19	0.000	0.000	0.000	0.000
20	0.000	0.000	0.000	0.000

Table 12: Probability of failure results for Line 7 in path 4 of EF2 scenario

Pole	$P(F_a)$	$P(F_b\|F_a)$	$P(F_c\|F_a)$	P_{L-a}
1	0.001	0.000	0.065	0.000
2	0.067	0.027	0.469	0.033
3	0.587	0.540	0.523	0.458
4	0.700	0.930	0.397	0.671
5	0.709	0.968	0.347	0.694
6	0.671	0.966	0.008	0.648
7	0.148	0.927	0.000	0.137
8	0.006	0.529	0.000	0.003
9	0.000	0.024	0.000	0.000
10	0.000	0.000	0.000	0.000
11	0.000	0.000	0.000	0.000
12	0.000	0.000	0.000	0.000
13	0.000	0.000	0.000	0.000
14	0.000	0.000	0.000	0.000
15	0.000	0.000	0.000	0.000
16	0.000	0.000	0.000	0.000
17	0.000	0.000	0.000	0.000
18	0.000	0.000	0.000	0.000
19	0.000	0.000	0.000	0.000
20	0.000	0.000	0.000	0.000

5.6. Reliability Analysis of Power Distribution Systems

Most power distribution systems in the United States are radial (Brown 2008), meaning that there is no redundancy and the failure of any line will result in the failure of all lines downstream of it. The power distribution system in this research is radial. The electricity not reaching any line can result from either the failure of the line itself, or the failure of one of the lines upstream to it. Those upstream lines can be determined using the fault-tree analysis method (Chowdhury et al 2011; Volkanovski 2009). Therefore, the probability of failure of each line within the system can be determined as discussed in the previous section, and then, the probability of electricity not reaching the line can be calculated using Equation (44):

$$P_{LF-x} = 1 - \left[\prod_{j=1}^{m} \left(1 - P_{L-j}\right)\right] (1 - P_{L-x}) \qquad (44)$$

Where P_{LF-x} is the probability of electricity not reaching the line x; P_{L-j} is the probability of failure of the line j upstream of the line x; m is the number of lines upstream of the line x; P_{L-x} is the probability of failure of line x.

The reliability of the entire system can then be calculated using Equation (45) (Volkanovski 2009):

$$R = 1 - \sum_{x=1}^{n_l} \frac{P_{LF-x} k_x}{\sum k} \tag{45}$$

Where R is the reliability of the power distribution system; k_x is the electricity power consumption of the line x. It can be calculated using the average consumption values provided in Section 5.2; $\sum k$ is the total electricity power consumption of the system; and n_l is the number of lines within the system.

The probability of failure for lines used in reliability analysis are shown in Table 13, Table 14, and Table 15 for path 2, path 3, and path 4 of the EF2 scenario respectively. Hence, the reliability of the system is equal to 0.231 ,0.008, and 0.013 for path 2, path 3, and path 4 of the EF2 scenario respectively.

Table 13: Lines probability of failure results for path 2 of EF2 scenario

Line	P_{L-x}	P_{LF-x}
1	0.004	0.004
2	0.989	0.989
3	0.000	0.989
4	0.996	0.996
5	0.996	0.996
6	0.996	0.996
7	0.985	0.985
8	0.000	0.004
9	0.000	0.004
10	0.000	0.004
11	0.000	0.004
12	0.000	0.004
13	0.000	0.004
14	0.000	0.004
15	0.000	0.004
16	0.892	0.892
17	0.520	0.522
18	0.040	0.043
19	0.000	0.004
20	0.000	0.004

21	0.000	0.004
22	0.000	0.004
23	0.000	0.004
24	0.983	0.983
25	0.995	0.995
26	0.000	0.004
27	0.996	0.996
28	0.000	0.000
29	0.000	0.000
30	0.000	0.000
31	0.000	0.000
32	0.000	0.000
33	0.000	0.000
34	0.000	0.000
35	0.000	0.000
36	0.000	0.000
37	0.000	0.000
38	0.000	0.000

Table 14: Lines probability of failure results for path 3 of EF2 scenario

Line	P_{L-x}	P_{LF-x}
1	0.955	0.955
2	0.000	0.955
3	0.000	0.955
4	0.993	1.000
5	0.996	1.000
6	0.996	1.000
7	0.984	0.999
8	0.000	0.955
9	0.000	0.955
10	0.000	0.955
11	0.000	0.955
12	0.000	0.955
13	0.000	0.955
14	0.000	0.955
15	0.000	0.955
16	0.994	1.000
17	0.994	1.000
18	0.991	1.000
19	0.971	0.999
20	0.865	0.994

21	0.451	0.975
22	0.021	0.956
23	0.000	0.955
24	0.995	1.000
25	0.996	1.000
26	0.000	0.955
27	0.996	1.000
28	0.971	0.971
29	0.000	0.971
30	0.000	0.971
31	0.000	0.971
32	0.000	0.971
33	0.000	0.971
34	0.000	0.971
35	0.000	0.971
36	0.000	0.971
37	0.000	0.971
38	0.000	0.971

Table 15: Lines probability of failure results for path 4 of EF2 scenario

Line	P_{L-x}	P_{LF-x}
1	0.875	0.875
2	0.000	0.875
3	0.000	0.875
4	0.305	0.913
5	0.963	0.995
6	0.994	0.999
7	0.984	0.998
8	0.000	0.875
9	0.000	0.875
10	0.000	0.875
11	0.000	0.875
12	0.000	0.875
13	0.000	0.875
14	0.000	0.875
15	0.000	0.875
16	0.996	0.999
17	0.995	0.999
18	0.993	0.999
19	0.993	0.999
20	0.993	0.999

21	0.992	0.999
22	0.988	0.999
23	0.955	0.994
24	0.995	1.000
25	0.974	1.000
26	0.000	0.994
27	0.319	0.996
28	0.969	0.969
29	0.000	0.969
30	0.000	0.969
31	0.000	0.969
32	0.000	0.969
33	0.000	0.969
34	0.000	0.969
35	0.000	0.969
36	0.000	0.969
37	0.000	0.969
38	0.000	0.969

5.7. Hardening of Power Distribution Systems

One of the methods to harden the power distribution system is to replace aged poles with new poles of the same class or a stronger one. Although the highest reliability would be achieved when all the poles within the system are hardened, this is usually expensive and unnecessary, as replacing some poles within the system through target hardening would often result in a reliability high enough with a cost much less than that of hardening the entire system. In this study, hardening the class 4 wood pole is performed through replacing it with a new pole of the same class, or with a new pole of classes 3, or 2. The choice of the pole class used for hardening depends on the scenario.

Although target hardening can be done for each pole separately, the analysis can be simplified by considering the hardening of all poles within the line, or in other words, hardening the lines within the system. Some of the measures used to estimate the worth of hardening a line within the system are the risk achievement worth (RAW) and the risk reduction worth (RRW). RAW and RRW can be calculated for each line within the system using Equation (46) and Equation (47) respectively (Rausand et al 2004):

$$RAW = \frac{1 - R_{P_{LF-x}=1}}{1 - R} \tag{46}$$

$$RRW = \frac{1 - R}{1 - R_{P_{LF-x}=0}} \tag{47}$$

Where R is the original reliability of the system; $R_{P_{LF-x}=1}$ is the reliability of the system by setting the probability of failure of line x to be 1; and $R_{P_{LF-x}=0}$ is the reliability of the system by setting the probability of failure of line x to be 0. As can be seen from Equation (46) and Equation (47), RAW studies the worth of hardening of line x by looking into the effect of the failure of this line, while RRW studies the worth of hardening of line x by looking into the effect of the survival of this line. Since hardening will result in the line having a higher probability of survival, RRW is used in this study as the measure of the worth of hardening each line within the system.

5.8. Cost Analysis

The total direct cost resulting of the power distribution system being hit by a tornado results from the cost of replacement of failed poles in addition to cost of the interruption of electricity service. Moreover, the cost of hardening is also added to the total cost in order to analyze the worth of hardening. Hence, the total cost is calculated using Equation (48):

$$C_{total} = C_R + C_L + C_H \tag{48}$$

Where C_{total} is the total cost; C_R is the cost of poles replacement; C_L is the cost resulting from the loss of power service; and C_H is the cost of hardening. C_R, C_L, and C_H are calculated using Equation (49), Equation (50), and Equation (51) respectively as explained in the next sections.

The failure of the power distribution lines when hit by a tornado causes, in addition to the direct costs mentioned above, other indirect costs resulting from the cascading failure of other infrastructure systems. For example, the water distribution system and the road network could be significantly affected when the electric power distribution is interrupted, and even after the recovery of the power system, it could take longer time to recover the other infrastructure systems (Zimmerman et al 2017). However, this research considers only the direct costs, and the indirect costs are not considered here.

5.8.1. Replacement Cost

The replacement cost of the failed poles equals the summation of the probabilities of failures of all poles within the system, multiplied by the replacement cost of the failed pole. Hence, the replacement cost of any line within the system can be calculated using Equation (49):

$$C_{R-line} = \sum_{p=1}^{n} C_r P_{f-p} \tag{49}$$

Where C_r is the average replacement cost per pole. The replacement cost of poles after hazards is usually considerably higher than the replacement cost under normal condition, and it is assumed to be 4000$/pole in this study as suggested by Xu et al (2008); P_{f-p} is the probability of failure of the pole p determined from the fragility analysis discussed earlier; and n is the number of poles in the line. The replacement cost of poles within the system C_R can then be calculated by adding the replacement costs of lines C_{R-line} within the system.

5.8.2. Service Interruption Cost

The service interruption cost is the cost consumers suffer from during the loss of power service, in addition to the cost resulting from the loss of revenue utility companies incur. Since the cost consumer incur is usually much higher than that utilities incur during blackouts, the cost of revenue loss is ignored in this study. The service interruption cost is hence equal to the cost each unit incur per hour during the loss of power service multiplied by the duration of the loss as shown in Equation (50):

$$C_L = \sum_{x=1}^{n_l} P_{f-x} C_x t_x \tag{50}$$

Where P_{f-x} is the probability of electricity not reaching the line x; n_l is the number of distribution lines in the system; C_x is the average cost customers incur per hour when electricity is not reaching the line x, and is equal to the sum of the costs incurred by units supported by this line. LaCommare et al (2006) estimated this cost to be 2.7$/h for residential units, 886$/h for commercial units, and 3253$/h for industrial units; and t_x is the recovery time of the line x.

The time of power restoration for lines depends on many factors, such as the number of crew units available, the accessibility to broken element, and the time required to repair or replace the elements. The number of crew units available immediately after tornadoes is usually less than that required for post-hazards recovery. The tornado warning lead time is between 1 to 2 hours, and the fake warnings are more than 75% (Hoekstra et al 2011), making it difficult for utilities to immediately provide enough crew units. Moreover, the broken trees and poles can block the streets and prevent the crew units from reaching the broken distribution poles, and the situation could worsen when the traffic signals go off resulting in traffic congestion and chaos, and hence delaying the recovery (Miles et al 2013; Smith et al 2013). When a crew unit reaches a failed pole, the time required to replace the pole will vary depending on the situation, but was estimated to take 4 hours on average to replace a single pole by Brown et al (2009). Because of the high variability in the factors discussed above, it is difficult to estimate the time required for power restoration. However, in this paper, the time of power restoration of the system is estimated equal to 25.5 hours using the average of the restoration times of nine blackouts resulting from tornadoes recorded between the years 2003-2013 (EIA 2018a). This value is assumed for simplicity to be the restoration time for all lines within the system.

5.8.3. Hardening Cost

The cost of hardening a pole is the sum of the purchase price of the pole and the installation cost of the pole. The purchase price is assumed 498$/pole for class 4, 564$/pole for class 3, and 619$/pole for class 2 (ATS 2018). The installation cost of any pole is assumed 2500$/pole (Taras et al 2004). Hence, the cost of hardening the pole using a new class 4 pole is 2998$/pole, while it is 3064$/pole and 3119$/pole for classes 3 and 2 respectively. The total hardening cost of the system can be calculated using Equation (51):

$$C_H = C_h . n_{p-h} \tag{51}$$

Where C_h is the cost of hardening the pole before the occurrence of the hazard; and n_{p-h} is the number of hardened poles within the system.

5.9. Analysis, Results, and Discussion

As explained in Section 5.3, two scenarios are considered in this study, where the power distribution system is subjected to both EF2 and EF1 tornadoes, and 6 different tornado paths are considered for each scenario. For both scenarios, the reliability of the system is calculated for all the 6 paths following the procedure explained in Section 5.6. Then, the replacement costs, service interruption costs, and total costs of each tornado path are calculated as explained in Section 5.8. After that, RRW is determined for each line within the system as explained in Section 5.7 and the lines with the high values of RRW (larger than 1.1 in this study) are considered for hardening. Hardening in the EF2 scenario is done by replacing the poles with new poles of class 2, while in the EF1 scenario class 3 is used for hardening. After hardening the system, the reliability, replacement costs, service interruption costs, hardening cost, and total costs for all tornado paths are calculated again and compared to the results before hardening. The results of the EF2 scenario are shown in Table 16 and Table 17, while those of the EF1 scenario are shown in Table 18 and Table 19.

5.9.1. EF2 Scenario: Results and Discussion

As shown in Table 16, the reliability of the power distribution system can be as low as 0.008 for path 3, while it is highest for path 6 with R equals to 0.741. However, after target hardening the poles of the distribution lines L1, L7, L8, and L28, the reliability of the system increases to become in the range of 0.8-0.9 for all scenarios as shown in Table 17. Moreover, the total cost decreased considerably for all scenario paths after hardening, mainly because of the reduction in the cost of service interruption. It is worth mentioning that the hardened lines contribute to less than 20% of the total utility poles in the system. Figure 36 shows the costs of the EF2 scenario paths before and after hardening.

Table 16: EF2 scenario before hardening results

path	R	C_R (10^3 \$)	C_L (10^3 \$)	C_H (10^3 \$)	C_{Total} (10^3 \$)	Lines with RRW>1.1
1	0.271	66.4	1216.8	0.0	1283.2	L7
2	0.231	93.7	1236.7	0.0	1330.4	L7
3	0.008	141.3	1535.9	0.0	1677.2	L1/L28
4	0.013	147.8	1533.2	0.0	1681.0	L1/L7/L28
5	0.126	95.5	1364.9	0.0	1460.3	L1/L7/L28
6	0.741	65.4	291.9	0.0	357.3	L8/L28

Table 17: EF2 scenario after hardening results

path	R	C_R (10^3 \$)	C_L (10^3 \$)	C_H (10^3 \$)	C_{Total} (10^3 \$)
1	0.899	57.4	54.2	168.4	280.0
2	0.870	83.2	70.0	168.4	321.6
3	0.813	115.4	130.3	168.4	414.2
4	0.823	122.6	88.5	168.4	379.5
5	0.873	79.6	41.0	168.4	289.0
6	0.866	46.8	40.1	168.4	255.3

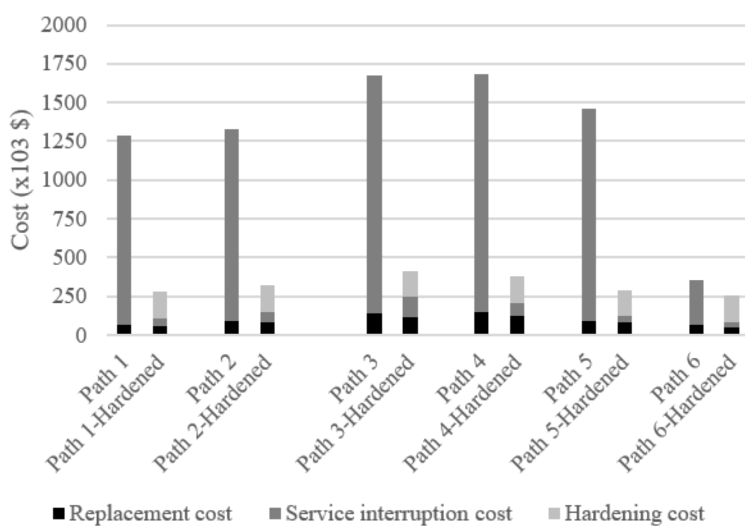

Figure 36: EF2 scenario costs

5.9.2. EF1 Scenario: Results and Discussion

It can be seen from Table 18 that the reliability of the power distribution system can be as low as 0.073 for path 3, while it is highest for path 6 with R equals to 0.78. However, after target hardening the poles of the distribution lines L1, L7, L8, and L28, the reliability of the system increases to become in the range of 0.90-0.95 for all scenarios as shown in Table 19. The lines worth hardening in both the EF2 scenario and the EF1 scenario are the same. Also, the total cost was reduced considerably for all scenarios after hardening, mainly because of the reduction in the cost of service interruption. Figure 37 shows the costs of the EF2 scenario paths before and after hardening.

Table 18: EF1 scenario before hardening results

path	R	C_R (10^3 \$)	C_L (10^3 \$)	C_H (10^3 \$)	C_{Total} (10^3 \$)	Lines with RRW>1.1
1	0.369	27.7	1067.7	0.0	1095.4	L7
2	0.347	39.6	1071.4	0.0	1111.0	L7
3	0.073	60.1	1426.8	0.0	1486.9	L1/L7/L28
4	0.078	60.0	1415.6	0.0	1475.6	L1/L7/L28
5	0.364	36.6	972.0	0.0	1008.6	L1 /L28
6	0.780	27.2	215.9	0.0	243.2	L8/L28

Table 19: EF1 scenario after hardening results

path	R	C_R (10^3 \$)	C_L (10^3 \$)	C_H (10^3 \$)	C_{Total} (10^3 \$)
1	0.950	22.1	5.4	165.5	193.0
2	0.929	33.9	7.8	165.5	207.2
3	0.911	45.2	9.8	165.5	220.5
4	0.905	45.8	10.4	165.5	221.6
5	0.945	29.3	6.0	165.5	200.7
6	0.901	18.7	11.5	165.5	195.7

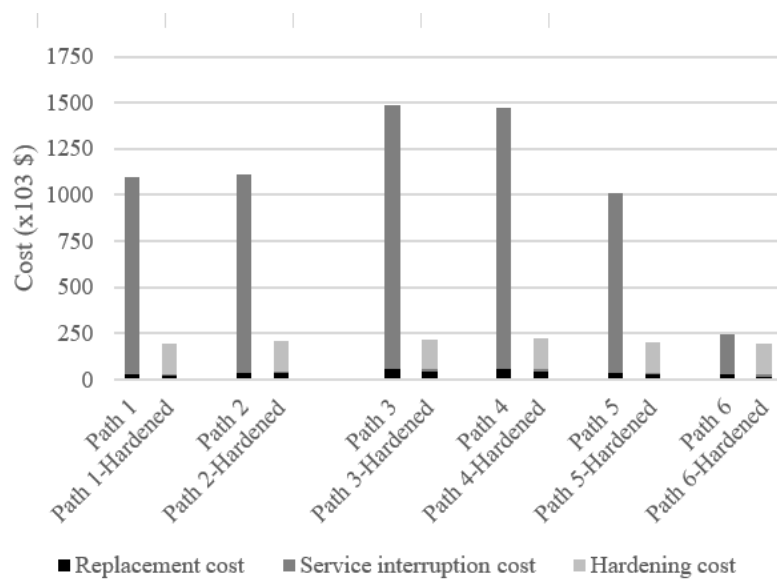

Figure 37: EF1 scenario costs

6. Conclusions

Chapter 4 of this research proposes a framework to compare the reliability of wood, steel, and prestressed concrete utility poles at component-level when subjected to tornadoes. Age-dependent fragility curves were generated for different types of poles based on their designs and strength deterioration models. Also, Life-cycle cost analysis and scenario-based analysis were performed based on the fragility analysis. It was shown that utility poles, whether they are made of wood, steel, or prestressed concrete, are vulnerable to tornadoes, even to the weaker tornadoes of EF1 and EF2 scales. Considering that EF1 and EF2 tornadoes have a considerable probability of occurrence, especially in tornado-active regions, this supports the direction towards designing the utility poles against those tornadoes considering the huge direct and indirect losses associated with the mass failure of utility poles when subjected to tornadoes. Moreover, the age of utility poles is shown to have a big impact on their resistance to tornadoes, as aging poles are vulnerable to tornadoes that are much weaker than those the new poles can resist. Because of the low probability of occurrence of tornadoes, especially in regions that are not tornado-active, the effect of tornadoes on the LCC was shown to be small compared to that of the initial cost. However, the scenario-based analysis was shown to be a useful method to study the impact of tornadoes on the critical components of the power distribution system in tornado-prone regions, compare different types of materials, and help in decision-making process.

Chapter 5 of this research proposes a framework to perform reliability and cost analysis on power distribution systems subjected to tornadoes through scenario-based analysis and using the age-dependent fragility method proposed in chapter 4. The results show that power distribution systems that include wood poles of average age are very vulnerable to moderate-intensity EF2 tornadoes, while those with aged wood poles are vulnerable to even week tornadoes of EF1 rating. Moreover, it was shown that hardening of less than 20% of the poles within the system can considerably increase the reliability of the system and reduce the costs when hit by tornadoes. This shows that target hardening is a useful tool to increase the reliability of power distribution systems in tornado-active regions.

Since many factors used in the analysis in addition to the costs depend mainly on the materials, climatic conditions, and region and can differ significantly from one case to another, site-specific models can be generated, and region-specific costs can be used to obtain more accurate results that can help in the decision-making process.

Since this study didn't take into consideration the structural dependency between poles, this can be considered in future research. Moreover, periodic maintenance of poles could be considered in generating age-dependent fragility curves. The current research could be expanded to study the behavior of other sub-systems within the electric power network when subjected to tornadoes, such as the power transmission system. Additionally, the indirect effect on the other infrastructure systems that could be affected when the power system fails, such as the water distribution network and the road network could be considered in future work.

Appendix A

1) programming code for generating fragility curves using MATLAB:

```
%Material Type: (wood,steel,concrete)
Material="wood";
%
%Hazard Type: (tornado,hurricane)
Hazard="tornado";
%
%City: (Norman,Xenia,Tampa)
City="Norman";
%Number of MCS values:
n_rows=10^5;
n_columns=1;
%Age
t=0;
%3-S gust wind speed range: mph
Vi=50;
Vo=250;
Vinc=1;
%

%Dimensions of poles:
%1-wood:
m_totalheight_w=45; %ft
cov_totalheight_w=0.04;
st_totalheight_w=cov_totalheight_w*m_totalheight_w;
totalheight_w=normrnd(m_totalheight_w,st_totalheight_w,n_rows,n_columns);
m_burriedheight_w=6.5; %ft
cov_burriedheight_w=0.04;
st_burriedheight_w=cov_burriedheight_w*m_burriedheight_w;
burriedheight_w=normrnd(m_burriedheight_w,st_burriedheight_w,n_rows,n_columns);
height_w=totalheight_w-burriedheight_w;
m_grdiameter_w=11.15; %in
cov_grdiameter_w=0.04;
st_grdiameter_w=cov_grdiameter_w*m_grdiameter_w;
grdiameter_w=normrnd(m_grdiameter_w,st_grdiameter_w,n_rows,n_columns);
m_topdiameter_w=6.7; %in
cov_topdiameter_w=0.04;
st_topdiameter_w=cov_topdiameter_w*m_topdiameter_w;
topdiameter_w=normrnd(m_topdiameter_w,st_topdiameter_w,n_rows,n_columns);
area_w=0.5*(grdiameter_w+topdiameter_w).*height_w/12; %ft^2
%2-steel:
m_totalheight_s=45; %ft
cov_totalheight_s=0.025;
st_totalheight_s=cov_totalheight_s*m_totalheight_s;
totalheight_s=normrnd(m_totalheight_s,st_totalheight_s,n_rows,n_columns);
m_burriedheight_s=6.5; %ft
cov_burriedheight_s=0.025;
st_burriedheight_s=cov_burriedheight_s*m_burriedheight_s;
burriedheight_s=normrnd(m_burriedheight_s,st_burriedheight_s,n_rows,n_columns);
```

```
height_s=totalheight_s-burriedheight_s;
m_grdiameter_s=11.15; %in
cov_grdiameter_s=0.025;
st_grdiameter_s=cov_grdiameter_s*m_grdiameter_s;
grdiameter_s=normrnd(m_grdiameter_s,st_grdiameter_s,n_rows,n_columns);
m_topdiameter_s=6.7; %in
cov_topdiameter_s=0.025;
st_topdiameter_s=cov_topdiameter_s*m_topdiameter_s;
topdiameter_s=normrnd(m_topdiameter_s,st_topdiameter_s,n_rows,n_columns);
area_s=0.5*(grdiameter_s+topdiameter_s).*height_s/12; %ft^2
Thickness_s=0.18; %inch
grdiameter_i_s=grdiameter_s-2*Thickness_s;
%3-concrete:
m_totalheight_c=45; %ft
cov_totalheight_c=0.025;
st_totalheight_c=cov_totalheight_c*m_totalheight_c;
totalheight_c=normrnd(m_totalheight_c,st_totalheight_c,n_rows,n_columns);
m_burriedheight_c=6.5; %ft
cov_burriedheight_c=0.025;
st_burriedheight_c=cov_burriedheight_c*m_burriedheight_c;
burriedheight_c=normrnd(m_burriedheight_c,st_burriedheight_c,n_rows,n_columns);
height_c=totalheight_c-burriedheight_c;
m_grdiameter_c=11.15; %in
cov_grdiameter_c=0.025;
st_grdiameter_c=cov_grdiameter_c*m_grdiameter_c;
grdiameter_c=normrnd(m_grdiameter_c,st_grdiameter_c,n_rows,n_columns);
grradius_co=grdiameter_c/2;
m_t_c=3; %in
cov_t_c=0.025;
st_t_c=cov_t_c*m_t_c;
t_c=normrnd(m_t_c,st_t_c,n_rows,n_columns);
grradius_ci=grradius_co-t_c;
m_topdiameter_c=6.7; %in
cov_topdiameter_c=0.025;
st_topdiameter_c=cov_topdiameter_c*m_topdiameter_c;
topdiameter_c=normrnd(m_topdiameter_c,st_topdiameter_c,n_rows,n_columns);
area_c=0.5*(grdiameter_c+topdiameter_c).*height_c/12; %ft^2


%Strength of poles:
%1-wood:
m_strength_w=8*10^3; %psi
S_w=3.1416*(grdiameter_w.^3)/32;
S_w_age=S_w;
%
%cov curve fitting using data from Shafieezadeh et al (2014):
t_Shafieezadeh=[0;10;20;30;40;50;60];
cov_Shafieezadeh=[0.17;0.171;0.186;0.210;0.251;0.315;0.399];
curve_fit_Shafieezadeh=fit(t_Shafieezadeh,cov_Shafieezadeh,'exp2');
cov_strength_w=curve_fit_Shafieezadeh(t);
%
z_strength_w=sqrt(log(1+cov_strength_w^2));
L_strength_w=log(m_strength_w)-0.5*z_strength_w^2;
strength_w=lognrnd(L_strength_w,z_strength_w,n_rows,n_columns);
%Age_Model_w:
if City=="Norman"
```

```
rain=987;
temperature=15.58;
N_dry_months=0;
elseif City=="Xenia"
rain=1065;
temperature=11.86;
N_dry_months=0;
elseif City=="Tampa"
rain=1176;
temperature=22.97;
N_dry_months=0;
else
rain=1270;
temperature=21.72;
N_dry_months=0;
end
f_rain_o=10*(1-exp(-0.001*max(rain-250,0)));
f_rain=max(f_rain_o*(1-N_dry_months/6),0);
if temperature<5
   g_temperature=0;
else if temperature<20
   g_temperature=-1+0.2*temperature;
else
   g_temperature=-25+1.4*temperature;
   end
end
k_climate=f_rain^0.3*g_temperature^0.2;
k_wood=5.44;
r_untreated=k_climate*k_wood;
B_treat=45;
D_treat=617;
C_creosote=D_treat/100;
C_CCA_eq=0.07*C_creosote;
r_treated=r_untreated/(1+B_treat*C_CCA_eq);
t_lag=5.5*r_treated^-0.95;
d_age=r_treated/25.4*max(t-t_lag,0);
S_w_age=3.1416*((grdiameter_w-2*d_age).^3)/32;
Resisting_Moment_w=strength_w.*S_w_age/12; %lb-ft
%2-steel:
grdiameter_s_age=grdiameter_s;
m_strength_s=65000; %psi
cov_strength_s=0.15;
z_strength_s=sqrt(log(1+cov_strength_s^2));
L_strength_s=log(m_strength_s)-0.5*z_strength_s^2;
strength_s=lognrnd(L_strength_s,z_strength_s,n_rows,1);
if City=="Norman"
   k_steel_corr=0.144;
   alpha_steel_corr=0.734;
   t_steel_corr=2.57;
elseif City=="Xenia"
   k_steel_corr=0.163;
   alpha_steel_corr=0.793;
elseif City=="Tampa"
   k_steel_corr=0.144;
   alpha_steel_corr=0.734;
else
```

```
    k_steel_corr=0.163;
    alpha_steel_corr=0.793;
end
t_steel_min=((rand(n_rows,n_columns)*10+20));
t_steel_effective=max(t-t_steel_min,0);
d_age_s=k_steel_corr.*t_steel_effective.^alpha_steel_corr./25.4;
grdiameter_s_age=grdiameter_s-2*d_age_s;
S_s=3.1416*(grdiameter_s_age.^4-grdiameter_i_s.^4)./32./grdiameter_s_age;
Resisting_Moment_s=strength_s.*S_s/12; %lb-ft
%3-concrete:
P_Loss=0.2;
m_Fs_c=270000*(1-P_Loss);
cov_Fs_c=0.15;
z_Fs_c=sqrt(log(1+cov_Fs_c^2));
L_Fs_c=log(m_Fs_c)-0.5*z_Fs_c^2;
Fs_c=lognrnd(L_Fs_c,z_Fs_c,n_rows,n_columns);
m_Fc_c=11000;
cov_Fc_c=0.15;
z_Fc_c=sqrt(log(1+cov_Fc_c^2));
L_Fc_c=log(m_Fc_c)-0.5*z_Fc_c^2;
Fc_c=lognrnd(L_Fc_c,z_Fc_c,n_rows,n_columns);
beta1=min(0.85,max(0.65,0.85-0.05*(m_Fc_c-4000)));
m_Astrand=0.115; %in2
cov_Astrand=0.04;
st_Astrand=cov_Astrand*m_Astrand;
Astrand=normrnd(m_Astrand,st_Astrand,n_rows,n_columns);
N_strands=12;
N_wires=7;
D_wire_strand=sqrt(Astrand/N_wires*4/pi());
%
%
D0=D_wire_strand*25.4;      %mm
L0=totalheight_c*304.8; %mm
w_c_ratio=27./(Fc_c*0.006895+13.5);
Cover_Concrete=(t_c-1)/2*25.4; %mm
f_icorr=27;
icorr=f_icorr*(1-w_c_ratio).^-1.64./Cover_Concrete;
X_chloride=(t_c-1)/2*2.54; %cm
m_D_chloride_s=10.^(-10+4.66*w_c_ratio); %psi
cov_D_chloride_s=0.75;
z_D_chloride_s=sqrt(log(1+cov_D_chloride_s^2));
L_D_chloride_s=log(m_D_chloride_s)-0.5*z_D_chloride_s^2;
D_chloride_s=lognrnd(L_D_chloride_s,z_D_chloride_s,n_rows,n_columns);
D_chloride_year=3.154e+7*D_chloride_s;
m_C0_chloride=3.5; %psi
cov_C0_chloride=0.5;
z_C0_chloride=sqrt(log(1+cov_C0_chloride^2));
L_C0_chloride=log(m_C0_chloride)-0.5*z_C0_chloride^2;
C0_chloride=lognrnd(L_C0_chloride,z_C0_chloride,n_rows,n_columns);
Ccr_chloride=(rand(n_rows,n_columns)*0.6+0.6);
t_i_c=X_chloride.^2/4./D_chloride_year.*erfinv(mean((C0_chloride-Ccr_chloride)./C0_chloride)).^-2;
t_concrete_effective=max(t-t_i_c,0);
%
T0_exp=0.03836;  %years
icorr_exp=186;   %MicroAmper/cm2
L0_exp=650;      %mm
```

```
a_corr_mm=normrnd(0.91,0.17*0.91,n_rows,n_columns);  %mm
M0_exp=0.84;
alpha0_exp=8.1;
N=96;
%
alpha_corr=alpha0_exp;
M_corr=M0_exp+(alpha0_exp^-1)*log(L0/L0_exp);
%
k_corr_re=0.85;
theta_corr_re=-0.29;
icorr_T=icorr.*k_corr_re.*mean(t_concrete_effective).^theta_corr_re;
%
T0=2.71.^((theta_corr_re+1)^-1*log(((theta_corr_re+1)*(icorr_exp*T0_exp)+(k_corr_re-theta_corr_re-
1)*icorr)./k_corr_re./icorr));
lambda_corr=(D0.^2-(D0-
0.0232.*icorr.*(1+k_corr_re./(theta_corr_re+1).*(t_concrete_effective.^(theta_corr_re+1)-1))).^2)./(D0.^2-
(D0-0.0232*icorr.*(1+k_corr_re./(theta_corr_re+1).*((T0).^(theta_corr_re+1)-1))).^2);
lambda_corr_mean=max(mean(lambda_corr),0.0000001);
a_corr_mm=-evrnd(-M_corr,1/alpha_corr,n_rows,n_columns); %mm
P_corr=a_corr_mm./25.4.*lambda_corr_mean^0.54;
b_corr_in=2*P_corr.*mean((1-(P_corr./D_wire_strand).^2))^0.5;
theta1_corr=2*asin(mean((b_corr_in./D_wire_strand)));
theta2_corr=2*asin(mean((b_corr_in./2./P_corr)));
A1_corr=0.5*(theta1_corr*(D_wire_strand/2).^2-b_corr_in.*abs(D_wire_strand/2-
P_corr.^2./D_wire_strand));
A2_corr=0.5*(theta2_corr.*P_corr.^2-b_corr_in.*P_corr.^2./D_wire_strand);

if mean(P_corr)<mean(D_wire_strand)/sqrt(2)
   A_corr=pi()/4*D_wire_strand.^2-A1_corr-A2_corr;
else if  mean(P_corr)<mean(D_wire_strand)
       A_corr=A1_corr-A2_corr;
   else
       A_corr=0;
   end
end

Reduction_Astrand=(mean(A_corr)*6+mean(Astrand/7))/mean(Astrand);

Astrand_t=Astrand*Reduction_Astrand;
%
%
r_strands=(grradius_co+grradius_ci)/2;
theta_c=10*pi()/180;
P_total=10^6;
while abs(mean(P_total))>=100000;
a_c=grradius_co*(1-cos(theta_c/2));
c_c=a_c/beta1;
if mean(a_c)<mean(t_c)
   Ac=(theta_c-sin(theta_c))/2.*grradius_co.^2;
else
   thetai=2*acos((mean(grradius_co)-mean(a_c))/mean(grradius_co));
   Ac=(theta_c-sin(theta_c))./2.*grradius_co.^2-(thetai-sin(thetai))./2.*grradius_ci.^2;
end
n_strands_c=0;
n_strands_t=0;
Mstrand=0;
```

```
for angle=90-360/N_strands/2:-360/N_strands:-(90-360/N_strands/2)
   n_strand=2;
   r_strand=r_strands*sin(angle*pi()/180);
   Fstrands=n_strand.*Astrand_t.*Fs_c;
   Mstrand=Mstrand+abs(r_strand-c_c).*Fstrands;
   if mean(r_strand)>mean(grradius_co)-mean(c_c)
      n_strands_c=n_strands_c+n_strand;
   else
      n_strands_t=n_strands_t+n_strand;
   end
end
P_Cc=0.85*Ac.*Fc_c;
P_Cs=Fs_c.*Astrand_t*n_strands_c;
P_Ts=Fs_c.*Astrand_t*n_strands_t;
P_total=P_Cc+P_Cs-P_Ts;
theta_c=theta_c+0.1*pi()/180;
end
Resisting_Moment_c=(P_Cc.*(4*grradius_co*sin(theta_c/2)^3/3/(theta_c-sin(theta_c))-(grradius_co-
c_c))+Mstrand)/12;
%4-Resisting_Moment:
if Material=="wood"
   Resisting_Moment=Resisting_Moment_w;
elseif Material=="steel"
   Resisting_Moment=Resisting_Moment_s;
elseif Material=="concrete"
   Resisting_Moment=Resisting_Moment_c;
end
%

%Wind load factors:
%1-Kz:
%1-1)Kz_pole:
Kz_pole_t=1;
m_Kz_pole_h=0.951;
cov_Kz_pole_h=0.06;
st_G_pole_h=cov_Kz_pole_h*m_Kz_pole_h;
Kz_pole_h=normrnd(m_Kz_pole_h,st_G_pole_h,n_rows,n_columns);
if Hazard=="tornado"
   Kz_pole=Kz_pole_t;
elseif Hazard=="hurricane"
    Kz_pole=Kz_pole_h;
end
%1-2)Kz_wire:
Kz_wire_t=1;
m_Kz_wire_h=1.024;
cov_Kz_wire_h=0.06;
st_Kz_wire_h=cov_Kz_wire_h*m_Kz_wire_h;
Kz_wire_h=normrnd(m_Kz_wire_h,st_Kz_wire_h,n_rows,n_columns);
if Hazard=="tornado"
   Kz_wire=Kz_wire_t;
elseif Hazard=="hurricane"
    Kz_wire=Kz_wire_h;
end
%
%2-G:
%2-1)G_pole:
```

```
G_pole_t=1;
m_G_pole_h=0.948;
cov_G_pole_h=0.11;
st_G_pole_h=cov_G_pole_h*m_G_pole_h;
G_pole_h=normrnd(m_G_pole_h,st_G_pole_h,n_rows,n_columns);
if Hazard=="tornado"
   G_pole=G_pole_t;
elseif Hazard=="hurricane"
    G_pole=G_pole_h;
end
%2-2)G_wire:
G_wire_t=1;
m_G_wire_h=0.801;
cov_G_wire_h=0.11;
st_G_wire_h=cov_G_wire_h*m_G_wire_h;
G_wire_h=normrnd(m_G_wire_h,st_G_wire_h,n_rows,n_columns);
if Hazard=="tornado"
   G_wire=G_wire_t;
elseif Hazard=="hurricane"
    G_wire=G_wire_h;
end
%
%3-Cf:
%3-1)Cf_pole:
m_Cf_pole=0.9;
cov_Cf_pole=0.12;
st_Cf_pole=cov_Cf_pole*m_Cf_pole;
Cf_pole=normrnd(m_Cf_pole,st_Cf_pole,n_rows,n_columns);
%3-2)Cf_wire:
m_Cf_wire=1.0;
cov_Cf_wire=0.12;
st_Cf_wire=cov_Cf_wire*m_Cf_wire;
Cf_wire=normrnd(m_Cf_wire,st_Cf_wire,n_rows,n_columns);
%
%4-A:
%4-1)A_pole:
if Material=="wood"
   A_pole=area_w;
elseif Material=="steel"
   A_pole=area_s;
elseif Material=="concrete"
   A_pole=area_c;
end
%4-2)A_wire:
N_wire=3;
m_D_wire=0.724; %in
cov_D_wire=0.03;
st_D_wire=cov_D_wire*m_D_wire;
D_wire=normrnd(m_D_wire,st_D_wire,n_rows,n_columns);
m_L_wire=151; %ft
cov_L_wire=0.06;
st_L_wire=cov_L_wire*m_L_wire;
L_wire=normrnd(m_L_wire,st_L_wire,n_rows,n_columns);
A_wire=L_wire.*D_wire/12*N_wire;
%
%5-Q:
```

```
Q=0.00256;
%
%6-Kzt:
Kzt=1;
%
%7-wind factor:
%7-1): f_pole:
f_pole=Kzt*Q.*Kz_pole.*G_pole.*Cf_pole.*A_pole;
%7-2): f_wire:
if Hazard=="tornado"
f_wire=((rand(n_rows,n_columns)*0.36+1).^2+(rand(n_rows,n_columns)*0.17+0.47).^2).*Kzt*Q.*Kz_wi
re.*G_wire.*Cf_wire.*A_wire;
elseif Hazard=="hurricane"
f_wire=Kzt*Q.*Kz_wire.*G_wire.*Cf_wire.*A_wire;
end
%

% Heights:
%1)h_pole:
h_centroid_pole_w=height_w.*((grdiameter_w-topdiameter_w)/6+topdiameter_w/2)./((grdiameter_w-
topdiameter_w)/2+topdiameter_w);
h_centroid_pole_s=height_s.*((grdiameter_s-topdiameter_s)/6+topdiameter_s/2)./((grdiameter_s-
topdiameter_s)/2+topdiameter_s);
 h_centroid_pole_c=height_c.*((grdiameter_c-topdiameter_c)/6+topdiameter_c/2)./((grdiameter_c-
topdiameter_c)/2+topdiameter_c);
if Material=="wood"
    h_centroid_pole=h_centroid_pole_w;
elseif Material=="steel"
    h_centroid_pole=h_centroid_pole_s;
elseif Material=="concrete"
   h_centroid_pole=h_centroid_pole_c;
end
%2)h_wire:
h_wire_top=2; %ft
if Material=="wood"
    h_wire=height_w-h_wire_top;
elseif Material=="steel"
    h_wire=height_s-h_wire_top;
elseif Material=="concrete"
    h_wire=height_c-h_wire_top;
end
%

% MCS:
for V=Vi:Vinc:Vo
%1-Wind Forces:
%1-1)wind force on pole:
F_pole=f_pole.*V^2;    %lb
%1-2)wind force on wire1:
if Hazard=="tornado"
if V<75
maximum_effictive_span=65;
else if V<98
maximum_effictive_span=65+(157-65)*(V-75)/(98-75);
else if V<123
maximum_effictive_span=157+(323-157)*(V-98)/(123-98);
```

```
else if V<150.5
maximum_effictive_span=323+(688-323)*(V-123)/(150.5-123);
else if V<183
maximum_effictive_span=688+(1098-688)*(V-150.5)/(183-150.5);
else
maximum_effictive_span=1373;
end
end
end
end
end
elseif Hazard=="hurricane"
maximum_effictive_span=m_L_wire;
end

m_L_wire_ef=min(m_L_wire,maximum_effictive_span);
F_wire=(m_L_wire_ef/m_L_wire)*f_wire.*V^2;   %lb
%2-Wind Moments::
%2-1)wind moment on pole:
M_pole=F_pole.*h_centroid_pole;
%2-2)wind moment on wire:
M_wire=F_wire.*h_wire;
%2-4)wind total moment:
M_total=M_pole+M_wire;   %lb-ft
%
%4-Limit state:
G=Resisting_Moment-M_total;
Z=sum(G<0);
%
%5-Probability of failure:
Pf=Z/n_rows;

%
V_P((V-Vi)/(Vinc)+1,1)=V;
P_P((V-Vi)/(Vinc)+1,1)=Pf;
%
end
```

2) programming code for calculating system reliability using MATLAB:

```
System__Properties; %Script
Lines__Properties;  %Script
Constants;          %Script
[System_Properties_Modified,Lines_Properties_Modified]=System_Lines(System_Properties,Lines_Prope
rties);


%
EF_Tornado=System_Properties_Modified(1,1);
Angle_Tornado=System_Properties_Modified(2,1);
X_Center_Tornado=System_Properties_Modified(3,1);
Y_Center_Tornado=System_Properties_Modified(4,1);
X_0_System=System_Properties_Modified(5,1);
Y_0_System=System_Properties_Modified(6,1);
Number_Lines_System=System_Properties_Modified(11,1);
%

System_Pf_L=zeros(Number_Lines_System,1);
System_Pf_U=zeros(Number_Lines_System,1);
Number_Poles_System=0;
for i=1:Number_Lines_System
t_M=Lines_Properties_Modified(i,12);
t_Sd=Lines_Properties_Modified(i,13);
Tornado_Properties=[t_M;t_Sd;EF_Tornado;Angle_Tornado;X_Center_Tornado;Y_Center_Tornado];
if Lines_Properties_Modified(i,2)<1
if Lines_Properties_Modified(i,17)>0&&Lines_Properties_Modified(i,20)>0
Line_Poles_Properties=[[[1:Lines_Properties_Modified(i,14)]',ones(Lines_Properties_Modified(i,14),1)*Li
nes_Properties_Modified(i,4),ones(Lines_Properties_Modified(i,14),1)*Lines_Properties_Modified(i,5),on
es(Lines_Properties_Modified(i,14),1)*Lines_Properties_Modified(i,6),ones(Lines_Properties_Modified(i,
14),1)*Lines_Properties_Modified(i,7),ones(Lines_Properties_Modified(i,14),1)*Lines_Properties_Modifi
ed(i,7),[0;ones(Lines_Properties_Modified(i,14)-
1,1)*Lines_Properties_Modified(i,16)],[ones(Lines_Properties_Modified(i,14)-
1,1)*Lines_Properties_Modified(i,16);0],ones(Lines_Properties_Modified(i,14),1)*Lines_Properties_Modi
fied(i,8),ones(Lines_Properties_Modified(i,14),1)*Lines_Properties_Modified(i,8),ones(Lines_Properties_
Modified(i,14),1)*Lines_Properties_Modified(i,9),ones(Lines_Properties_Modified(i,14),1)*Lines_Propert
ies_Modified(i,10),ones(Lines_Properties_Modified(i,14),1)*Lines_Properties_Modified(i,11),([1:Lines_P
roperties_Modified(i,14)]'-1)*(Lines_Properties_Modified(i,25)-
Lines_Properties_Modified(i,23))/(Lines_Properties_Modified(i,14)-
1)+Lines_Properties_Modified(i,23),([1:Lines_Properties_Modified(i,14)]'-
1)*(Lines_Properties_Modified(i,26)-Lines_Properties_Modified(i,24))/(Lines_Properties_Modified(i,14)-
1)+Lines_Properties_Modified(i,24)];

[[1:Lines_Properties_Modified(i,17)]',ones(Lines_Properties_Modified(i,17),1)*Lines_Properties_Modifie
d(i,4),ones(Lines_Properties_Modified(i,17),1)*Lines_Properties_Modified(i,5),ones(Lines_Properties_Mo
dified(i,17),1)*Lines_Properties_Modified(i,6),ones(Lines_Properties_Modified(i,17),1)*Lines_Properties
_Modified(i,7),ones(Lines_Properties_Modified(i,17),1)*Lines_Properties_Modified(i,7),[ones(Lines_Prop
erties_Modified(i,17),1)*Lines_Properties_Modified(i,19)],[ones(Lines_Properties_Modified(i,17)-
1,1)*Lines_Properties_Modified(i,19);0],ones(Lines_Properties_Modified(i,17),1)*Lines_Properties_Modi
fied(i,8),ones(Lines_Properties_Modified(i,17),1)*Lines_Properties_Modified(i,8),ones(Lines_Properties_
Modified(i,17),1)*Lines_Properties_Modified(i,9),ones(Lines_Properties_Modified(i,17),1)*Lines_Propert
ies_Modified(i,10),ones(Lines_Properties_Modified(i,17),1)*Lines_Properties_Modified(i,11),([1:Lines_P
```

roperties_Modified(i,17)]')*(Lines_Properties_Modified(i,27)-
Lines_Properties_Modified(i,25))/(Lines_Properties_Modified(i,17))+Lines_Properties_Modified(i,25),([1:
Lines_Properties_Modified(i,17)]')*(Lines_Properties_Modified(i,28)-
Lines_Properties_Modified(i,26))/(Lines_Properties_Modified(i,17))+Lines_Properties_Modified(i,26)];

[[1:Lines_Properties_Modified(i,20)]',ones(Lines_Properties_Modified(i,20),1)*Lines_Properties_Modified(i,4),ones(Lines_Properties_Modified(i,20),1)*Lines_Properties_Modified(i,5),ones(Lines_Properties_Modified(i,20),1)*Lines_Properties_Modified(i,6),ones(Lines_Properties_Modified(i,20),1)*Lines_Properties_Modified(i,7),ones(Lines_Properties_Modified(i,20),1)*Lines_Properties_Modified(i,7),[ones(Lines_Properties_Modified(i,20),1)*Lines_Properties_Modified(i,22)],[ones(Lines_Properties_Modified(i,20)-
1,1)*Lines_Properties_Modified(i,22);0],ones(Lines_Properties_Modified(i,20),1)*Lines_Properties_Modified(i,8),ones(Lines_Properties_Modified(i,20),1)*Lines_Properties_Modified(i,8),ones(Lines_Properties_Modified(i,20),1)*Lines_Properties_Modified(i,9),ones(Lines_Properties_Modified(i,20),1)*Lines_Properties_Modified(i,10),ones(Lines_Properties_Modified(i,20),1)*Lines_Properties_Modified(i,11),([1:Lines_Properties_Modified(i,20)]')*(Lines_Properties_Modified(i,29)-
Lines_Properties_Modified(i,27))/(Lines_Properties_Modified(i,20))+Lines_Properties_Modified(i,27),([1:
Lines_Properties_Modified(i,20)]')*(Lines_Properties_Modified(i,30)-
Lines_Properties_Modified(i,28))/(Lines_Properties_Modified(i,20))+Lines_Properties_Modified(i,28)]];
else if Lines_Properties_Modified(i,20)==0&&Lines_Properties_Modified(i,17)>0
Line_Poles_Properties=[[[1:Lines_Properties_Modified(i,14)]',ones(Lines_Properties_Modified(i,14),1)*Lines_Properties_Modified(i,4),ones(Lines_Properties_Modified(i,14),1)*Lines_Properties_Modified(i,5),ones(Lines_Properties_Modified(i,14),1)*Lines_Properties_Modified(i,6),ones(Lines_Properties_Modified(i,14),1)*Lines_Properties_Modified(i,7),ones(Lines_Properties_Modified(i,14),1)*Lines_Properties_Modified(i,7),[0;ones(Lines_Properties_Modified(i,14)-
1,1)*Lines_Properties_Modified(i,16)],[ones(Lines_Properties_Modified(i,14)-
1,1)*Lines_Properties_Modified(i,16);0],ones(Lines_Properties_Modified(i,14),1)*Lines_Properties_Modified(i,8),ones(Lines_Properties_Modified(i,14),1)*Lines_Properties_Modified(i,8),ones(Lines_Properties_Modified(i,14),1)*Lines_Properties_Modified(i,9),ones(Lines_Properties_Modified(i,14),1)*Lines_Properties_Modified(i,10),ones(Lines_Properties_Modified(i,14),1)*Lines_Properties_Modified(i,11),([1:Lines_Properties_Modified(i,14)]'-1)*(Lines_Properties_Modified(i,25)-
Lines_Properties_Modified(i,23))/(Lines_Properties_Modified(i,14)-
1)+Lines_Properties_Modified(i,23),([1:Lines_Properties_Modified(i,14)]'-
1)*(Lines_Properties_Modified(i,26)-Lines_Properties_Modified(i,24))/(Lines_Properties_Modified(i,14)-
1)+Lines_Properties_Modified(i,24)];

[[1:Lines_Properties_Modified(i,17)]',ones(Lines_Properties_Modified(i,17),1)*Lines_Properties_Modified(i,4),ones(Lines_Properties_Modified(i,17),1)*Lines_Properties_Modified(i,5),ones(Lines_Properties_Modified(i,17),1)*Lines_Properties_Modified(i,6),ones(Lines_Properties_Modified(i,17),1)*Lines_Properties_Modified(i,7),ones(Lines_Properties_Modified(i,17),1)*Lines_Properties_Modified(i,7),[ones(Lines_Properties_Modified(i,17),1)*Lines_Properties_Modified(i,19)],[ones(Lines_Properties_Modified(i,17)-
1,1)*Lines_Properties_Modified(i,19);0],ones(Lines_Properties_Modified(i,17),1)*Lines_Properties_Modified(i,8),ones(Lines_Properties_Modified(i,17),1)*Lines_Properties_Modified(i,8),ones(Lines_Properties_Modified(i,17),1)*Lines_Properties_Modified(i,9),ones(Lines_Properties_Modified(i,17),1)*Lines_Properties_Modified(i,10),ones(Lines_Properties_Modified(i,17),1)*Lines_Properties_Modified(i,11),([1:Lines_Properties_Modified(i,17)]')*(Lines_Properties_Modified(i,27)-
Lines_Properties_Modified(i,25))/(Lines_Properties_Modified(i,17))+Lines_Properties_Modified(i,25),([1:
Lines_Properties_Modified(i,17)]')*(Lines_Properties_Modified(i,28)-
Lines_Properties_Modified(i,26))/(Lines_Properties_Modified(i,17))+Lines_Properties_Modified(i,26)]];
else if Lines_Properties_Modified(i,20)==0&&Lines_Properties_Modified(i,17)==0
Line_Poles_Properties=[[1:Lines_Properties_Modified(i,14)]',ones(Lines_Properties_Modified(i,14),1)*Lines_Properties_Modified(i,4),ones(Lines_Properties_Modified(i,14),1)*Lines_Properties_Modified(i,5),ones(Lines_Properties_Modified(i,14),1)*Lines_Properties_Modified(i,6),ones(Lines_Properties_Modified(i,14),1)*Lines_Properties_Modified(i,7),ones(Lines_Properties_Modified(i,14),1)*Lines_Properties_Modified(i,7),[ones(Lines_Properties_Modified(i,14),1)*Lines_Properties_Modified(i,16)],[ones(Lines_Properties_Modified(i,14)-
1,1)*Lines_Properties_Modified(i,16);0],ones(Lines_Properties_Modified(i,14),1)*Lines_Properties_Modi

```
fied(i,8),ones(Lines_Properties_Modified(i,14),1)*Lines_Properties_Modified(i,8),ones(Lines_Properties_
Modified(i,14),1)*Lines_Properties_Modified(i,9),ones(Lines_Properties_Modified(i,14),1)*Lines_Propert
ies_Modified(i,10),ones(Lines_Properties_Modified(i,14),1)*Lines_Properties_Modified(i,11),([1:Lines_P
roperties_Modified(i,14)]'-1)*(Lines_Properties_Modified(i,25)-
Lines_Properties_Modified(i,23))/(Lines_Properties_Modified(i,14)-
1)+Lines_Properties_Modified(i,23),([1:Lines_Properties_Modified(i,14)]'-
1)*(Lines_Properties_Modified(i,26)-Lines_Properties_Modified(i,24))/(Lines_Properties_Modified(i,14)-
1)+Lines_Properties_Modified(i,24)];
end
end
end
else
if Lines_Properties_Modified(i,17)>0&&Lines_Properties_Modified(i,20)>0
Line_Poles_Properties=[[[1:Lines_Properties_Modified(i,14)]',ones(Lines_Properties_Modified(i,14),1)*Li
nes_Properties_Modified(i,4),ones(Lines_Properties_Modified(i,14),1)*Lines_Properties_Modified(i,5),on
es(Lines_Properties_Modified(i,14),1)*Lines_Properties_Modified(i,6),ones(Lines_Properties_Modified(i,
14),1)*Lines_Properties_Modified(i,7),ones(Lines_Properties_Modified(i,14),1)*Lines_Properties_Modifi
ed(i,7),[ones(Lines_Properties_Modified(i,14),1)*Lines_Properties_Modified(i,16)],[ones(Lines_Propertie
s_Modified(i,14)-
1,1)*Lines_Properties_Modified(i,16);0],ones(Lines_Properties_Modified(i,14),1)*Lines_Properties_Modi
fied(i,8),ones(Lines_Properties_Modified(i,14),1)*Lines_Properties_Modified(i,8),ones(Lines_Properties_
Modified(i,14),1)*Lines_Properties_Modified(i,9),ones(Lines_Properties_Modified(i,14),1)*Lines_Propert
ies_Modified(i,10),ones(Lines_Properties_Modified(i,14),1)*Lines_Properties_Modified(i,11),([1:Lines_P
roperties_Modified(i,14)]'-1)*(Lines_Properties_Modified(i,25)-
Lines_Properties_Modified(i,23))/(Lines_Properties_Modified(i,14)-
1)+Lines_Properties_Modified(i,23),([1:Lines_Properties_Modified(i,14)]'-
1)*(Lines_Properties_Modified(i,26)-Lines_Properties_Modified(i,24))/(Lines_Properties_Modified(i,14)-
1)+Lines_Properties_Modified(i,24)];

[[1:Lines_Properties_Modified(i,17)]',ones(Lines_Properties_Modified(i,17),1)*Lines_Properties_Modifie
d(i,4),ones(Lines_Properties_Modified(i,17),1)*Lines_Properties_Modified(i,5),ones(Lines_Properties_Mo
dified(i,17),1)*Lines_Properties_Modified(i,6),ones(Lines_Properties_Modified(i,17),1)*Lines_Properties
_Modified(i,7),ones(Lines_Properties_Modified(i,17),1)*Lines_Properties_Modified(i,7),[ones(Lines_Prop
erties_Modified(i,17),1)*Lines_Properties_Modified(i,19)],[ones(Lines_Properties_Modified(i,17)-
1,1)*Lines_Properties_Modified(i,19);0],ones(Lines_Properties_Modified(i,17),1)*Lines_Properties_Modi
fied(i,8),ones(Lines_Properties_Modified(i,17),1)*Lines_Properties_Modified(i,8),ones(Lines_Properties_
Modified(i,17),1)*Lines_Properties_Modified(i,9),ones(Lines_Properties_Modified(i,17),1)*Lines_Propert
ies_Modified(i,10),ones(Lines_Properties_Modified(i,17),1)*Lines_Properties_Modified(i,11),([1:Lines_P
roperties_Modified(i,17)]')*(Lines_Properties_Modified(i,27)-
Lines_Properties_Modified(i,25))/(Lines_Properties_Modified(i,17))+Lines_Properties_Modified(i,25),([1:
Lines_Properties_Modified(i,17)]')*(Lines_Properties_Modified(i,28)-
Lines_Properties_Modified(i,26))/(Lines_Properties_Modified(i,17))+Lines_Properties_Modified(i,26)];

[[1:Lines_Properties_Modified(i,20)]',ones(Lines_Properties_Modified(i,20),1)*Lines_Properties_Modifie
d(i,4),ones(Lines_Properties_Modified(i,20),1)*Lines_Properties_Modified(i,5),ones(Lines_Properties_Mo
dified(i,20),1)*Lines_Properties_Modified(i,6),ones(Lines_Properties_Modified(i,20),1)*Lines_Properties
_Modified(i,7),ones(Lines_Properties_Modified(i,20),1)*Lines_Properties_Modified(i,7),[ones(Lines_Prop
erties_Modified(i,20),1)*Lines_Properties_Modified(i,22)],[ones(Lines_Properties_Modified(i,20)-
1,1)*Lines_Properties_Modified(i,22);0],ones(Lines_Properties_Modified(i,20),1)*Lines_Properties_Modi
fied(i,8),ones(Lines_Properties_Modified(i,20),1)*Lines_Properties_Modified(i,8),ones(Lines_Properties_
Modified(i,20),1)*Lines_Properties_Modified(i,9),ones(Lines_Properties_Modified(i,20),1)*Lines_Propert
ies_Modified(i,10),ones(Lines_Properties_Modified(i,20),1)*Lines_Properties_Modified(i,11),([1:Lines_P
roperties_Modified(i,20)]')*(Lines_Properties_Modified(i,29)-
Lines_Properties_Modified(i,27))/(Lines_Properties_Modified(i,20))+Lines_Properties_Modified(i,27),([1:
Lines_Properties_Modified(i,20)]')*(Lines_Properties_Modified(i,30)-
Lines_Properties_Modified(i,28))/(Lines_Properties_Modified(i,20))+Lines_Properties_Modified(i,28)]];
```

```
else if Lines_Properties_Modified(i,20)==0&&Lines_Properties_Modified(i,17)>0
Line_Poles_Properties=[[[1:Lines_Properties_Modified(i,14)]',ones(Lines_Properties_Modified(i,14),1)*Lines_Properties_Modified(i,4),ones(Lines_Properties_Modified(i,14),1)*Lines_Properties_Modified(i,5),ones(Lines_Properties_Modified(i,14),1)*Lines_Properties_Modified(i,6),ones(Lines_Properties_Modified(i,14),1)*Lines_Properties_Modified(i,7),ones(Lines_Properties_Modified(i,14),1)*Lines_Properties_Modified(i,7),[ones(Lines_Properties_Modified(i,14),1)*Lines_Properties_Modified(i,16)],[ones(Lines_Properties_Modified(i,14)-
1,1)*Lines_Properties_Modified(i,16);0],ones(Lines_Properties_Modified(i,14),1)*Lines_Properties_Modified(i,8),ones(Lines_Properties_Modified(i,14),1)*Lines_Properties_Modified(i,8),ones(Lines_Properties_Modified(i,14),1)*Lines_Properties_Modified(i,9),ones(Lines_Properties_Modified(i,14),1)*Lines_Properties_Modified(i,10),ones(Lines_Properties_Modified(i,14),1)*Lines_Properties_Modified(i,11),([1:Lines_Properties_Modified(i,14)]'-1)*(Lines_Properties_Modified(i,25)-
Lines_Properties_Modified(i,23))/(Lines_Properties_Modified(i,14)-
1)+Lines_Properties_Modified(i,23),([1:Lines_Properties_Modified(i,14)]'-
1)*(Lines_Properties_Modified(i,26)-Lines_Properties_Modified(i,24))/(Lines_Properties_Modified(i,14)-
1)+Lines_Properties_Modified(i,24)];

[[1:Lines_Properties_Modified(i,17)]',ones(Lines_Properties_Modified(i,17),1)*Lines_Properties_Modified(i,4),ones(Lines_Properties_Modified(i,17),1)*Lines_Properties_Modified(i,5),ones(Lines_Properties_Modified(i,17),1)*Lines_Properties_Modified(i,6),ones(Lines_Properties_Modified(i,17),1)*Lines_Properties_Modified(i,7),ones(Lines_Properties_Modified(i,17),1)*Lines_Properties_Modified(i,7),[ones(Lines_Properties_Modified(i,17),1)*Lines_Properties_Modified(i,19)],[ones(Lines_Properties_Modified(i,17)-
1,1)*Lines_Properties_Modified(i,19);0],ones(Lines_Properties_Modified(i,17),1)*Lines_Properties_Modified(i,8),ones(Lines_Properties_Modified(i,17),1)*Lines_Properties_Modified(i,8),ones(Lines_Properties_Modified(i,17),1)*Lines_Properties_Modified(i,9),ones(Lines_Properties_Modified(i,17),1)*Lines_Properties_Modified(i,10),ones(Lines_Properties_Modified(i,17),1)*Lines_Properties_Modified(i,11),([1:Lines_Properties_Modified(i,17)]')*(Lines_Properties_Modified(i,27)-
Lines_Properties_Modified(i,25))/(Lines_Properties_Modified(i,17))+Lines_Properties_Modified(i,25),([1:Lines_Properties_Modified(i,17)]')*(Lines_Properties_Modified(i,28)-
Lines_Properties_Modified(i,26))/(Lines_Properties_Modified(i,17))+Lines_Properties_Modified(i,26)]];
else if Lines_Properties_Modified(i,20)==0&&Lines_Properties_Modified(i,17)==0
Line_Poles_Properties=[[1:Lines_Properties_Modified(i,14)]',ones(Lines_Properties_Modified(i,14),1)*Lines_Properties_Modified(i,4),ones(Lines_Properties_Modified(i,14),1)*Lines_Properties_Modified(i,5),ones(Lines_Properties_Modified(i,14),1)*Lines_Properties_Modified(i,6),ones(Lines_Properties_Modified(i,14),1)*Lines_Properties_Modified(i,7),ones(Lines_Properties_Modified(i,14),1)*Lines_Properties_Modified(i,7),[ones(Lines_Properties_Modified(i,14),1)*Lines_Properties_Modified(i,16)],[ones(Lines_Properties_Modified(i,14)-
1,1)*Lines_Properties_Modified(i,16);0],ones(Lines_Properties_Modified(i,14),1)*Lines_Properties_Modified(i,8),ones(Lines_Properties_Modified(i,14),1)*Lines_Properties_Modified(i,8),ones(Lines_Properties_Modified(i,14),1)*Lines_Properties_Modified(i,9),ones(Lines_Properties_Modified(i,14),1)*Lines_Properties_Modified(i,10),ones(Lines_Properties_Modified(i,14),1)*Lines_Properties_Modified(i,11),([1:Lines_Properties_Modified(i,14)]'-1)*(Lines_Properties_Modified(i,25)-
Lines_Properties_Modified(i,23))/(Lines_Properties_Modified(i,14)-
1)+Lines_Properties_Modified(i,23),([1:Lines_Properties_Modified(i,14)]'-
1)*(Lines_Properties_Modified(i,26)-Lines_Properties_Modified(i,24))/(Lines_Properties_Modified(i,14)-
1)+Lines_Properties_Modified(i,24)];
end
end
end
end
end

[ Line_Poles_Properties__Modified ] = Line_Poles_Properties_Modified( Line_Poles_Properties );

if Lines_Properties_Modified(i,3)==1
[Line_PF_Pole,Line_PF_L,Line_PF_U]=Line_PF( Tornado_Properties,Line_Poles_Properties__Modified
);
```

```
Number_Poles=size(Line_Poles_Properties,1);
System_Pf_L(i,1)=Line_PF_L;
System_Pf_U(i,1)=Line_PF_U;
for j=1:Number_Poles
System_Pf_Poles(Number_Poles_System+j,1)=Line_PF_Pole(j,1);
end
Number_Poles_System=Number_Poles_System+Number_Poles;
else if Lines_Properties_Modified(i,3)==2
System_Pf_L(i,1)=0;
System_Pf_U(i,1)=0;
end
end
end

%
Number_Lines_System=size(Lines_Properties_Modified,1);
Connectivity_s=Lines_Properties_Modified(2:Number_Lines_System,2);
Connectivity_t=Lines_Properties_Modified(2:Number_Lines_System,1);

System_Consumption=0;
for i=1:Number_Lines_System
System_Consumption=System_Consumption+(Lines_Properties_Modified(i,33)*Lines_Properties_Modifi
ed(i,34)+Lines_Properties_Modified(i,35)*Lines_Properties_Modified(i,36));
end

System_Pf_L_Com = zeros(Number_Lines_System,1);
System_Pf_U_Com = zeros(Number_Lines_System,1);
System_R_L_Inv = zeros(Number_Lines_System,1);
System_R_U_Inv = zeros(Number_Lines_System,1);
for i=1:Number_Lines_System
if Lines_Properties_Modified(i,2)<1
System_Pf_L_Com(i,1)=System_Pf_L(i,1);
System_Pf_U_Com(i,1)=System_Pf_U(i,1);
else
Connect=Connectivity_s(find(Connectivity_t==i),1);
System_Pf_L_Com(i,1)=1-(1-System_Pf_L(i,1))*(1-System_Pf_L_Com(Connect,1));
System_Pf_U_Com(i,1)=1-(1-System_Pf_U(i,1))*(1-System_Pf_U_Com(Connect,1));
end
System_R_L_Inv(i,1)=System_Pf_L_Com(i,1)*(Lines_Properties_Modified(i,33)*Lines_Properties_Modif
ied(i,34)+Lines_Properties_Modified(i,35)*Lines_Properties_Modified(i,36))/System_Consumption;
System_R_U_Inv(i,1)=System_Pf_U_Com(i,1)*(Lines_Properties_Modified(i,33)*Lines_Properties_Modi
fied(i,34)+Lines_Properties_Modified(i,35)*Lines_Properties_Modified(i,36))/System_Consumption;
end
%
System_R_L_Com=1-sum(System_R_L_Inv);
System_R_U_Com=1-sum(System_R_U_Inv);


System_Pf_L_Com_RRW = zeros(Number_Lines_System,1);
System_Pf_U_Com_RRW = zeros(Number_Lines_System,1);
System_R_L_Inv_RRW = zeros(Number_Lines_System,1);
System_R_U_Inv_RRW = zeros(Number_Lines_System,1);
System_R_L_Com_RRW= zeros(Number_Lines_System,1);
System_R_U_Com_RRW= zeros(Number_Lines_System,1);
System_L_RRW= zeros(Number_Lines_System,1);
System_U_RRW= zeros(Number_Lines_System,1);
```

```
for j=1:Number_Lines_System
System_Pf_L_RRW=System_Pf_L;
System_Pf_U_RRW=System_Pf_U;
System_Pf_L_RRW(j,1)=0;
System_Pf_U_RRW(j,1)=0;
for i=1:Number_Lines_System
if Lines_Properties_Modified(i,2)<1
System_Pf_L_Com_RRW(i,1)=System_Pf_L_RRW(i,1);
System_Pf_U_Com_RRW(i,1)=System_Pf_U_RRW(i,1);
else
Connect=Connectivity_s(find(Connectivity_t==i),1);
System_Pf_L_Com_RRW(i,1)=1-(1-System_Pf_L_RRW(i,1))*(1-System_Pf_L_Com_RRW(Connect,1));
System_Pf_U_Com_RRW(i,1)=1-(1-System_Pf_U_RRW(i,1))*(1-
System_Pf_U_Com_RRW(Connect,1));
end
System_R_L_Inv_RRW(i,1)=System_Pf_L_Com_RRW(i,1)*(Lines_Properties_Modified(i,33)*Lines_Pro
perties_Modified(i,34)+Lines_Properties_Modified(i,35)*Lines_Properties_Modified(i,36))/System_Consu
mption;
System_R_U_Inv_RRW(i,1)=System_Pf_U_Com_RRW(i,1)*(Lines_Properties_Modified(i,33)*Lines_Pr
operties_Modified(i,34)+Lines_Properties_Modified(i,35)*Lines_Properties_Modified(i,36))/System_Cons
umption;
end
System_R_L_Com_RRW=1-sum(System_R_L_Inv_RRW);
System_R_U_Com_RRW=1-sum(System_R_U_Inv_RRW);
System_L_RRW(j,1)=((1-System_R_L_Com_RRW)/(1-System_R_L_Com))^-1;
System_U_RRW(j,1)=((1-System_R_U_Com_RRW)/(1-System_R_U_Com))^-1;
end

%
C_Repair_Poles_System=sum(System_Pf_Poles,1)*C_repair_Pole;
C_harden_Poles_System_vector=zeros(Number_Lines_System,1);
for i=1:1:Number_Lines_System
N_harden=Lines_Properties_Modified(i,14)+Lines_Properties_Modified(i,17)+Lines_Properties_Modified
(i,20);
if Lines_Properties_Modified(i,6)==1 &&   Lines_Properties_Modified(i,12)==0
C_harden_Pole=C_harden_Pole_1;
else if Lines_Properties_Modified(i,6)==2 &&   Lines_Properties_Modified(i,12)==0
C_harden_Pole=C_harden_Pole_2;
else if Lines_Properties_Modified(i,6)==3 &&   Lines_Properties_Modified(i,12)==0
C_harden_Pole=C_harden_Pole_3;
else if Lines_Properties_Modified(i,6)==4 &&   Lines_Properties_Modified(i,12)==0
C_harden_Pole=C_harden_Pole_4;
else
C_harden_Pole=0;
end
end
end
end
C_harden_Poles_System_vector(i,1)=N_harden*C_harden_Pole;
end
C_harden_Poles_System=sum(C_harden_Poles_System_vector,1);
C_serviceloss_System_vector_U=t_restoration*(Lines_Properties_Modified(:,33).*Lines_Properties_Modi
fied(:,37)+Lines_Properties_Modified(:,35).*Lines_Properties_Modified(:,38)).*System_Pf_U_Com;
C_serviceloss_System_U=sum(C_serviceloss_System_vector_U,1);
C_total_System_U=[C_Repair_Poles_System;C_serviceloss_System_U;C_harden_Poles_System];
```

```
C_serviceloss_System_vector_L=t_restoration*(Lines_Properties_Modified(:,33).*Lines_Properties_Modified(:,37)+Lines_Properties_Modified(:,35).*Lines_Properties_Modified(:,38)).*System_Pf_L_Com;
C_serviceloss_System_L=sum(C_serviceloss_System_vector_L,1);
C_total_System_L=[C_Repair_Poles_System;C_serviceloss_System_L;C_harden_Poles_System];
%

function
[System_Properties_Modified,Lines_Properties_Modified]=System_Lines(System_Properties,Lines_Properties)

Constants;

%
EF_Tornado=System_Properties(1,1);
Angle_Tornado=System_Properties(2,1);
X_Center_Tornado=System_Properties(3,1);
Y_Center_Tornado=System_Properties(4,1);
X_0_System_1=System_Properties(5,1);
Y_0_System_1=System_Properties(6,1);
X_0_System_2=System_Properties(7,1);
Y_0_System_2=System_Properties(8,1);
X_0_System_3=System_Properties(9,1);
Y_0_System_3=System_Properties(10,1);
%
Number_Lines_System=size(Lines_Properties,1);
System_Properties_Modified=System_Properties;
System_Properties_Modified(11,1)=Number_Lines_System;
%
Connectivity_s=Lines_Properties(1:Number_Lines_System,2);
Connectivity_t=Lines_Properties(1:Number_Lines_System,1);

Lines_Properties_Modified=Lines_Properties;



for i=1:Number_Lines_System
if Lines_Properties_Modified(i,2)<1
if Lines_Properties_Modified(i,2)==0.1
Lines_Properties_Modified(i,23)=X_0_System_1;
Lines_Properties_Modified(i,24)=Y_0_System_1;
else if Lines_Properties_Modified(i,2)==0.2
Lines_Properties_Modified(i,23)=X_0_System_2;
Lines_Properties_Modified(i,24)=Y_0_System_2;
else if Lines_Properties_Modified(i,2)==0.3
Lines_Properties_Modified(i,23)=X_0_System_3;
Lines_Properties_Modified(i,24)=Y_0_System_3;
end
end
end
Lines_Properties_Modified(i,25)=Lines_Properties_Modified(i,23)+Lines_Properties(i,16)*(Lines_Properties(i,14)-1)*cosd(Lines_Properties(i,15))*0.000189394;
Lines_Properties_Modified(i,26)=Lines_Properties_Modified(i,24)+Lines_Properties(i,16)*(Lines_Properties(i,14)-1)*sind(Lines_Properties(i,15))*0.000189394;
Lines_Properties_Modified(i,27)=Lines_Properties_Modified(i,25)+Lines_Properties(i,19)*(Lines_Properties(i,17))*cosd(Lines_Properties(i,18))*0.000189394;
```

```
Lines_Properties_Modified(i,28)=Lines_Properties_Modified(i,26)+Lines_Properties(i,19)*(Lines_Propert
ies(i,17))*sind(Lines_Properties(i,18))*0.000189394;
Lines_Properties_Modified(i,29)=Lines_Properties_Modified(i,27)+Lines_Properties(i,22)*(Lines_Propert
ies(i,20))*cosd(Lines_Properties(i,21))*0.000189394;
Lines_Properties_Modified(i,30)=Lines_Properties_Modified(i,28)+Lines_Properties(i,22)*(Lines_Propert
ies(i,20))*sind(Lines_Properties(i,21))*0.000189394;
else
Connect=Connectivity_s(find(Connectivity_t==i),1);
if Lines_Properties_Modified(i,32)==1
if Lines_Properties_Modified(Connect,2)<1
Lines_Properties_Modified(i,23)=Lines_Properties_Modified(Connect,23)+(Lines_Properties_Modified(C
onnect,25)-
Lines_Properties_Modified(Connect,23))*Lines_Properties_Modified(i,31)+Lines_Properties_Modified(i,1
6)*cosd(Lines_Properties_Modified(i,15))*0.000189394;
Lines_Properties_Modified(i,24)=Lines_Properties_Modified(Connect,24)+(Lines_Properties_Modified(C
onnect,26)-
Lines_Properties_Modified(Connect,24))*Lines_Properties_Modified(i,31)+Lines_Properties_Modified(i,1
6)*sind(Lines_Properties_Modified(i,15))*0.000189394;
else
Lines_Properties_Modified(i,23)=Lines_Properties_Modified(Connect,23)+(Lines_Properties_Modified(C
onnect,25)-
Lines_Properties_Modified(Connect,23))*Lines_Properties_Modified(i,31)+Lines_Properties_Modified(i,1
6)*cosd(Lines_Properties_Modified(i,15))*0.000189394-
Lines_Properties_Modified(Connect,16)*cosd(Lines_Properties_Modified(Connect,15))*0.000189394*(1-
Lines_Properties_Modified(i,31));
Lines_Properties_Modified(i,24)=Lines_Properties_Modified(Connect,24)+(Lines_Properties_Modified(C
onnect,26)-
Lines_Properties_Modified(Connect,24))*Lines_Properties_Modified(i,31)+Lines_Properties_Modified(i,1
6)*sind(Lines_Properties_Modified(i,15))*0.000189394-
Lines_Properties_Modified(Connect,16)*sind(Lines_Properties_Modified(Connect,15))*0.000189394*(1-
Lines_Properties_Modified(i,31));
end
else if Lines_Properties_Modified(i,32)==2
Lines_Properties_Modified(i,23)=Lines_Properties_Modified(Connect,25)+(Lines_Properties_Modified(C
onnect,27)-
Lines_Properties_Modified(Connect,25))*Lines_Properties_Modified(i,31)+Lines_Properties_Modified(i,1
6)*cosd(Lines_Properties_Modified(i,15))*0.000189394;
Lines_Properties_Modified(i,24)=Lines_Properties_Modified(Connect,26)+(Lines_Properties_Modified(C
onnect,28)-
Lines_Properties_Modified(Connect,26))*Lines_Properties_Modified(i,31)+Lines_Properties_Modified(i,1
6)*sind(Lines_Properties_Modified(i,15))*0.000189394;
else if Lines_Properties_Modified(i,32)==3
Lines_Properties_Modified(i,23)=Lines_Properties_Modified(Connect,27)+(Lines_Properties_Modified(C
onnect,29)-
Lines_Properties_Modified(Connect,27))*Lines_Properties_Modified(i,31)+Lines_Properties_Modified(i,1
6)*cosd(Lines_Properties_Modified(i,15))*0.000189394;
Lines_Properties_Modified(i,24)=Lines_Properties_Modified(Connect,28)+(Lines_Properties_Modified(C
onnect,30)-
Lines_Properties_Modified(Connect,28))*Lines_Properties_Modified(i,31)+Lines_Properties_Modified(i,1
6)*sind(Lines_Properties_Modified(i,15))*0.000189394;
end
end
end
Lines_Properties_Modified(i,25)=Lines_Properties_Modified(i,23)+Lines_Properties(i,16)*(Lines_Propert
ies(i,14)-1)*cosd(Lines_Properties(i,15))*0.000189394;
```

```
Lines_Properties_Modified(i,26)=Lines_Properties_Modified(i,24)+Lines_Properties(i,16)*(Lines_Propert
ies(i,14)-1)*sind(Lines_Properties(i,15))*0.000189394;
Lines_Properties_Modified(i,27)=Lines_Properties_Modified(i,25)+Lines_Properties(i,19)*Lines_Properti
es(i,17)*cosd(Lines_Properties(i,18))*0.000189394;
Lines_Properties_Modified(i,28)=Lines_Properties_Modified(i,26)+Lines_Properties(i,19)*Lines_Properti
es(i,17)*sind(Lines_Properties(i,18))*0.000189394;
Lines_Properties_Modified(i,29)=Lines_Properties_Modified(i,27)+Lines_Properties(i,22)*Lines_Properti
es(i,20)*cosd(Lines_Properties(i,21))*0.000189394;
Lines_Properties_Modified(i,30)=Lines_Properties_Modified(i,28)+Lines_Properties(i,22)*Lines_Properti
es(i,20)*sind(Lines_Properties(i,21))*0.000189394;
end
end

end

function
[EF_Coordinates_Adjusted_Abs,EF_Coordinates_mean]=EF_Coordinates(EF_Tornado,Angle_Tornado,X
_Center_Tornado,Y_Center_Tornado)

Constants;

%
if EF_Tornado==5
   k_Length_Tornado=1.291;
   lambda_Length_Tornado=38.074;
   k_Width_Tornado=1.423;
   lambda_Width_Tornado=.572;
   Length_Tornado=lambda_Length_Tornado*gamma(1+1/k_Length_Tornado);
   Width_Tornado=lambda_Width_Tornado*gamma(1+1/k_Width_Tornado);
   %Length_Tornado=wblrnd(lambda_Length_Tornado,k_Length_Tornado,n_rows,n_columns);
   %Width_Tornado=wblrnd(lambda_Width_Tornado,k_Width_Tornado,n_rows,n_columns);
   Length_Tornado_EF5=14.9/100*Length_Tornado;
   Length_Tornado_EF4=18.5/100*Length_Tornado;
   Length_Tornado_EF3=24.2/100*Length_Tornado;
   Length_Tornado_EF2=18.9/100*Length_Tornado;
   Length_Tornado_EF1=10.3/100*Length_Tornado;
   Length_Tornado_EF0=13.2/100*Length_Tornado;
   Width_Tornado_EF5=27.3/100*Width_Tornado;
   Width_Tornado_EF4=19.9/100*Width_Tornado;
   Width_Tornado_EF3=13.6/100*Width_Tornado;
   Width_Tornado_EF2=13.8/100*Width_Tornado;
   Width_Tornado_EF1=12.7/100*Width_Tornado;
   Width_Tornado_EF0=12.7/100*Width_Tornado;
else if EF_Tornado==4
   k_Length_Tornado=1.117;
   lambda_Length_Tornado=26.997;
   k_Width_Tornado=1.150;
   lambda_Width_Tornado=.437;
   Length_Tornado=lambda_Length_Tornado*gamma(1+1/k_Length_Tornado);
   Width_Tornado=lambda_Width_Tornado*gamma(1+1/k_Width_Tornado);
   %Length_Tornado=wblrnd(lambda_Length_Tornado,k_Length_Tornado,n_rows,n_columns);
   %Width_Tornado=wblrnd(lambda_Width_Tornado,k_Width_Tornado,n_rows,n_columns);
   Length_Tornado_EF5=0/100*Length_Tornado;
   Length_Tornado_EF4=21.2/100*Length_Tornado;
   Length_Tornado_EF3=21.0/100*Length_Tornado;
   Length_Tornado_EF2=27.8/100*Length_Tornado;
```

```
    Length_Tornado_EF1=15.8/100*Length_Tornado;
    Length_Tornado_EF0=14.2/100*Length_Tornado;
    Width_Tornado_EF5=0/100*Length_Tornado;
    Width_Tornado_EF4=27.3/100*Width_Tornado;
    Width_Tornado_EF3=18.7/100*Width_Tornado;
    Width_Tornado_EF2=19.0/100*Width_Tornado;
    Width_Tornado_EF1=17.5/100*Width_Tornado;
    Width_Tornado_EF0=17.5/100*Width_Tornado;
  else if EF_Tornado==3
    k_Length_Tornado=1.031;
    lambda_Length_Tornado=15.865;
    k_Width_Tornado=1.004;
    lambda_Width_Tornado=0.261;
    Length_Tornado=lambda_Length_Tornado*gamma(1+1/k_Length_Tornado);
    Width_Tornado=lambda_Width_Tornado*gamma(1+1/k_Width_Tornado);
    %Length_Tornado=wblrnd(lambda_Length_Tornado,k_Length_Tornado,n_rows,n_columns);
    %Width_Tornado=wblrnd(lambda_Width_Tornado,k_Width_Tornado,n_rows,n_columns);
    Length_Tornado_EF5=0/100*Length_Tornado;
    Length_Tornado_EF4=0/100*Length_Tornado;
    Length_Tornado_EF3=32.1/100*Length_Tornado;
    Length_Tornado_EF2=31.8/100*Length_Tornado;
    Length_Tornado_EF1=24.4/100*Length_Tornado;
    Length_Tornado_EF0=11.7/100*Length_Tornado;
    Width_Tornado_EF5=0/100*Length_Tornado;
    Width_Tornado_EF4=0/100*Width_Tornado;
    Width_Tornado_EF3=33.8/100*Width_Tornado;
    Width_Tornado_EF2=20.2/100*Width_Tornado;
    Width_Tornado_EF1=26.2/100*Width_Tornado;
    Width_Tornado_EF0=19.8/100*Width_Tornado;
  else if EF_Tornado==2
    k_Length_Tornado=0.796;
    lambda_Length_Tornado=6.514;
    k_Width_Tornado=0.912;
    lambda_Width_Tornado=0.117;
    Length_Tornado=lambda_Length_Tornado*gamma(1+1/k_Length_Tornado);
    Width_Tornado=lambda_Width_Tornado*gamma(1+1/k_Width_Tornado);
    %Length_Tornado=wblrnd(lambda_Length_Tornado,k_Length_Tornado,n_rows,n_columns);
    %Width_Tornado=wblrnd(lambda_Width_Tornado,k_Width_Tornado,n_rows,n_columns);
    Length_Tornado_EF5=0/100*Length_Tornado;
    Length_Tornado_EF4=0/100*Length_Tornado;
    Length_Tornado_EF3=0/100*Length_Tornado;
    Length_Tornado_EF2=36.7/100*Length_Tornado;
    Length_Tornado_EF1=35.2/100*Length_Tornado;
    Length_Tornado_EF0=28.1/100*Length_Tornado;
    Width_Tornado_EF5=0/100*Length_Tornado;
    Width_Tornado_EF4=0/100*Width_Tornado;
    Width_Tornado_EF3=0/100*Width_Tornado;
    Width_Tornado_EF2=47.5/100*Width_Tornado;
    Width_Tornado_EF1=31.4/100*Width_Tornado;
    Width_Tornado_EF0=21.1/100*Width_Tornado;
  else if EF_Tornado==1
    k_Length_Tornado=0.727;
    lambda_Length_Tornado=2.671;
    k_Width_Tornado=0.943;
    lambda_Width_Tornado=0.058;
    Length_Tornado=lambda_Length_Tornado*gamma(1+1/k_Length_Tornado);
```

```
    Width_Tornado=lambda_Width_Tornado*gamma(1+1/k_Width_Tornado);
    %Length_Tornado=wblrnd(lambda_Length_Tornado,k_Length_Tornado,n_rows,n_columns);
    %Width_Tornado=wblrnd(lambda_Width_Tornado,k_Width_Tornado,n_rows,n_columns);
    Length_Tornado_EF5=0/100*Length_Tornado;
    Length_Tornado_EF4=0/100*Length_Tornado;
    Length_Tornado_EF3=0/100*Length_Tornado;
    Length_Tornado_EF2=0/100*Length_Tornado;
    Length_Tornado_EF1=42.6/100*Length_Tornado;
    Length_Tornado_EF0=57.4/100*Length_Tornado;
    Width_Tornado_EF5=0/100*Length_Tornado;
    Width_Tornado_EF4=0/100*Width_Tornado;
    Width_Tornado_EF3=0/100*Width_Tornado;
    Width_Tornado_EF2=0/100*Width_Tornado;
    Width_Tornado_EF1=62.5/100*Width_Tornado;
    Width_Tornado_EF0=37.5/100*Width_Tornado;
else if EF_Tornado==0
    k_Length_Tornado=0.675;
    lambda_Length_Tornado=0.718;
    k_Width_Tornado=1.043;
    lambda_Width_Tornado=0.025;
    Length_Tornado=lambda_Length_Tornado*gamma(1+1/k_Length_Tornado);
    Width_Tornado=lambda_Width_Tornado*gamma(1+1/k_Width_Tornado);
    %Length_Tornado=wblrnd(lambda_Length_Tornado,k_Length_Tornado,n_rows,n_columns);
    %Width_Tornado=wblrnd(lambda_Width_Tornado,k_Width_Tornado,n_rows,n_columns);
    Length_Tornado_EF5=0/100*Length_Tornado;
    Length_Tornado_EF4=0/100*Length_Tornado;
    Length_Tornado_EF3=0/100*Length_Tornado;
    Length_Tornado_EF2=0/100*Length_Tornado;
    Length_Tornado_EF1=0/100*Length_Tornado;
    Length_Tornado_EF0=100/100*Length_Tornado;
    Width_Tornado_EF5=0/100*Length_Tornado;
    Width_Tornado_EF4=0/100*Width_Tornado;
    Width_Tornado_EF3=0/100*Width_Tornado;
    Width_Tornado_EF2=0/100*Width_Tornado;
    Width_Tornado_EF1=0/100*Width_Tornado;
    Width_Tornado_EF0=100/100*Width_Tornado;
    end
    end
    end
    end
    end
end
%

%
Length_Tornado_EF5_Com=Length_Tornado_EF5;
Length_Tornado_EF4_Com=Length_Tornado_EF5_Com+Length_Tornado_EF4;
Length_Tornado_EF3_Com=Length_Tornado_EF4_Com+Length_Tornado_EF3;
Length_Tornado_EF2_Com=Length_Tornado_EF3_Com+Length_Tornado_EF2;
Length_Tornado_EF1_Com=Length_Tornado_EF2_Com+Length_Tornado_EF1;
Length_Tornado_EF0_Com=Length_Tornado_EF1_Com+Length_Tornado_EF0;
Width_Tornado_EF5_Com=Width_Tornado_EF5;
Width_Tornado_EF4_Com=Width_Tornado_EF5_Com+Width_Tornado_EF4;
Width_Tornado_EF3_Com=Width_Tornado_EF4_Com+Width_Tornado_EF3;
Width_Tornado_EF2_Com=Width_Tornado_EF3_Com+Width_Tornado_EF2;
Width_Tornado_EF1_Com=Width_Tornado_EF2_Com+Width_Tornado_EF1;
```

```
Width_Tornado_EF0_Com=Width_Tornado_EF1_Com+Width_Tornado_EF0;
Area_Tornado=Length_Tornado.*Width_Tornado;
Area_Tornado_EF5=Length_Tornado_EF5_Com.*Width_Tornado_EF5_Com;
Area_Tornado_EF4=Length_Tornado_EF4_Com.*Width_Tornado_EF4_Com-
Length_Tornado_EF5_Com.*Width_Tornado_EF5_Com;
Area_Tornado_EF3=Length_Tornado_EF3_Com.*Width_Tornado_EF3_Com-
Length_Tornado_EF4_Com.*Width_Tornado_EF4_Com;
Area_Tornado_EF2=Length_Tornado_EF2_Com.*Width_Tornado_EF2_Com-
Length_Tornado_EF3_Com.*Width_Tornado_EF3_Com;
Area_Tornado_EF1=Length_Tornado_EF1_Com.*Width_Tornado_EF1_Com-
Length_Tornado_EF2_Com.*Width_Tornado_EF2_Com;
Area_Tornado_EF0=Length_Tornado_EF0_Com.*Width_Tornado_EF0_Com-
Length_Tornado_EF1_Com.*Width_Tornado_EF1_Com;
%

%
EF0_Coordinates_Adjusted_Abs=[Length_Tornado_EF0_Com/2,Width_Tornado_EF0_Com/2];
EF1_Coordinates_Adjusted_Abs=[Length_Tornado_EF1_Com/2,Width_Tornado_EF1_Com/2];
EF2_Coordinates_Adjusted_Abs=[Length_Tornado_EF2_Com/2,Width_Tornado_EF2_Com/2];
EF3_Coordinates_Adjusted_Abs=[Length_Tornado_EF3_Com/2,Width_Tornado_EF3_Com/2];
EF4_Coordinates_Adjusted_Abs=[Length_Tornado_EF4_Com/2,Width_Tornado_EF4_Com/2];
EF5_Coordinates_Adjusted_Abs=[Length_Tornado_EF5_Com/2,Width_Tornado_EF5_Com/2];
EF_Coordinates_Adjusted_Abs=[EF0_Coordinates_Adjusted_Abs,EF1_Coordinates_Adjusted_Abs,EF2_
Coordinates_Adjusted_Abs,EF3_Coordinates_Adjusted_Abs,EF4_Coordinates_Adjusted_Abs,EF5_Coordi
nates_Adjusted_Abs];
%

%
EF0_Coordinates=[X_Center_Tornado-
Length_Tornado_EF0_Com/2.*cosd(Angle_Tornado)+Width_Tornado_EF0_Com/2.*sind(Angle_Tornado
),Y_Center_Tornado-Length_Tornado_EF0_Com/2.*sind(Angle_Tornado)-
Width_Tornado_EF0_Com/2.*cosd(Angle_Tornado),X_Center_Tornado+Length_Tornado_EF0_Com/2.*
cosd(Angle_Tornado)+Width_Tornado_EF0_Com/2.*sind(Angle_Tornado),Y_Center_Tornado+Length_T
ornado_EF0_Com/2.*sind(Angle_Tornado)-
Width_Tornado_EF0_Com/2.*cosd(Angle_Tornado),X_Center_Tornado+Length_Tornado_EF0_Com/2.*
cosd(Angle_Tornado)-
Width_Tornado_EF0_Com/2.*sind(Angle_Tornado),Y_Center_Tornado+Length_Tornado_EF0_Com/2.*s
ind(Angle_Tornado)+Width_Tornado_EF0_Com/2.*cosd(Angle_Tornado),X_Center_Tornado-
Length_Tornado_EF0_Com/2.*cosd(Angle_Tornado)-
Width_Tornado_EF0_Com/2.*sind(Angle_Tornado),Y_Center_Tornado-
Length_Tornado_EF0_Com/2.*sind(Angle_Tornado)+Width_Tornado_EF0_Com/2.*cosd(Angle_Tornado
),];
EF1_Coordinates=[X_Center_Tornado-
Length_Tornado_EF1_Com/2.*cosd(Angle_Tornado)+Width_Tornado_EF1_Com/2.*sind(Angle_Tornado
),Y_Center_Tornado-Length_Tornado_EF1_Com/2.*sind(Angle_Tornado)-
Width_Tornado_EF1_Com/2.*cosd(Angle_Tornado),X_Center_Tornado+Length_Tornado_EF1_Com/2.*
cosd(Angle_Tornado)+Width_Tornado_EF1_Com/2.*sind(Angle_Tornado),Y_Center_Tornado+Length_T
ornado_EF1_Com/2.*sind(Angle_Tornado)-
Width_Tornado_EF1_Com/2.*cosd(Angle_Tornado),X_Center_Tornado+Length_Tornado_EF1_Com/2.*
cosd(Angle_Tornado)-
Width_Tornado_EF1_Com/2.*sind(Angle_Tornado),Y_Center_Tornado+Length_Tornado_EF1_Com/2.*s
ind(Angle_Tornado)+Width_Tornado_EF1_Com/2.*cosd(Angle_Tornado),X_Center_Tornado-
Length_Tornado_EF1_Com/2.*cosd(Angle_Tornado)-
Width_Tornado_EF1_Com/2.*sind(Angle_Tornado),Y_Center_Tornado-
Length_Tornado_EF1_Com/2.*sind(Angle_Tornado)+Width_Tornado_EF1_Com/2.*cosd(Angle_Tornado
),];
```

```
EF2_Coordinates=[X_Center_Tornado-
Length_Tornado_EF2_Com/2.*cosd(Angle_Tornado)+Width_Tornado_EF2_Com/2.*sind(Angle_Tornado
),Y_Center_Tornado-Length_Tornado_EF2_Com/2.*sind(Angle_Tornado)-
Width_Tornado_EF2_Com/2.*cosd(Angle_Tornado),X_Center_Tornado+Length_Tornado_EF2_Com/2.*
cosd(Angle_Tornado)+Width_Tornado_EF2_Com/2.*sind(Angle_Tornado),Y_Center_Tornado+Length_T
ornado_EF2_Com/2.*sind(Angle_Tornado)-
Width_Tornado_EF2_Com/2.*cosd(Angle_Tornado),X_Center_Tornado+Length_Tornado_EF2_Com/2.*
cosd(Angle_Tornado)-
Width_Tornado_EF2_Com/2.*sind(Angle_Tornado),Y_Center_Tornado+Length_Tornado_EF2_Com/2.*s
ind(Angle_Tornado)+Width_Tornado_EF2_Com/2.*cosd(Angle_Tornado),X_Center_Tornado-
Length_Tornado_EF2_Com/2.*cosd(Angle_Tornado)-
Width_Tornado_EF2_Com/2.*sind(Angle_Tornado),Y_Center_Tornado-
Length_Tornado_EF2_Com/2.*sind(Angle_Tornado)+Width_Tornado_EF2_Com/2.*cosd(Angle_Tornado
),];
EF3_Coordinates=[X_Center_Tornado-
Length_Tornado_EF3_Com/2.*cosd(Angle_Tornado)+Width_Tornado_EF3_Com/2.*sind(Angle_Tornado
),Y_Center_Tornado-Length_Tornado_EF3_Com/2.*sind(Angle_Tornado)-
Width_Tornado_EF3_Com/2.*cosd(Angle_Tornado),X_Center_Tornado+Length_Tornado_EF3_Com/2.*
cosd(Angle_Tornado)+Width_Tornado_EF3_Com/2.*sind(Angle_Tornado),Y_Center_Tornado+Length_T
ornado_EF3_Com/2.*sind(Angle_Tornado)-
Width_Tornado_EF3_Com/2.*cosd(Angle_Tornado),X_Center_Tornado+Length_Tornado_EF3_Com/2.*
cosd(Angle_Tornado)-
Width_Tornado_EF3_Com/2.*sind(Angle_Tornado),Y_Center_Tornado+Length_Tornado_EF3_Com/2.*s
ind(Angle_Tornado)+Width_Tornado_EF3_Com/2.*cosd(Angle_Tornado),X_Center_Tornado-
Length_Tornado_EF3_Com/2.*cosd(Angle_Tornado)-
Width_Tornado_EF3_Com/2.*sind(Angle_Tornado),Y_Center_Tornado-
Length_Tornado_EF3_Com/2.*sind(Angle_Tornado)+Width_Tornado_EF3_Com/2.*cosd(Angle_Tornado
),];
EF4_Coordinates=[X_Center_Tornado-
Length_Tornado_EF4_Com/2.*cosd(Angle_Tornado)+Width_Tornado_EF4_Com/2.*sind(Angle_Tornado
),Y_Center_Tornado-Length_Tornado_EF4_Com/2.*sind(Angle_Tornado)-
Width_Tornado_EF4_Com/2.*cosd(Angle_Tornado),X_Center_Tornado+Length_Tornado_EF4_Com/2.*
cosd(Angle_Tornado)+Width_Tornado_EF4_Com/2.*sind(Angle_Tornado),Y_Center_Tornado+Length_T
ornado_EF4_Com/2.*sind(Angle_Tornado)-
Width_Tornado_EF4_Com/2.*cosd(Angle_Tornado),X_Center_Tornado+Length_Tornado_EF4_Com/2.*
cosd(Angle_Tornado)-
Width_Tornado_EF4_Com/2.*sind(Angle_Tornado),Y_Center_Tornado+Length_Tornado_EF4_Com/2.*s
ind(Angle_Tornado)+Width_Tornado_EF4_Com/2.*cosd(Angle_Tornado),X_Center_Tornado-
Length_Tornado_EF4_Com/2.*cosd(Angle_Tornado)-
Width_Tornado_EF4_Com/2.*sind(Angle_Tornado),Y_Center_Tornado-
Length_Tornado_EF4_Com/2.*sind(Angle_Tornado)+Width_Tornado_EF4_Com/2.*cosd(Angle_Tornado
),];
EF5_Coordinates=[X_Center_Tornado-
Length_Tornado_EF5_Com/2.*cosd(Angle_Tornado)+Width_Tornado_EF5_Com/2.*sind(Angle_Tornado
),Y_Center_Tornado-Length_Tornado_EF5_Com/2.*sind(Angle_Tornado)-
Width_Tornado_EF5_Com/2.*cosd(Angle_Tornado),X_Center_Tornado+Length_Tornado_EF5_Com/2.*
cosd(Angle_Tornado)+Width_Tornado_EF5_Com/2.*sind(Angle_Tornado),Y_Center_Tornado+Length_T
ornado_EF5_Com/2.*sind(Angle_Tornado)-
Width_Tornado_EF5_Com/2.*cosd(Angle_Tornado),X_Center_Tornado+Length_Tornado_EF5_Com/2.*
cosd(Angle_Tornado)-
Width_Tornado_EF5_Com/2.*sind(Angle_Tornado),Y_Center_Tornado+Length_Tornado_EF5_Com/2.*s
ind(Angle_Tornado)+Width_Tornado_EF5_Com/2.*cosd(Angle_Tornado),X_Center_Tornado-
Length_Tornado_EF5_Com/2.*cosd(Angle_Tornado)-
Width_Tornado_EF5_Com/2.*sind(Angle_Tornado),Y_Center_Tornado-
Length_Tornado_EF5_Com/2.*sind(Angle_Tornado)+Width_Tornado_EF5_Com/2.*cosd(Angle_Tornado
),];
```

```
EF__Coordinates=[EF0_Coordinates,EF1_Coordinates,EF2_Coordinates,EF3_Coordinates,EF4_Coordinat
es,EF5_Coordinates];
%EF_Coordinates_mean=mean(EF_Coordinates);
EF_Coordinates_mean=EF__Coordinates;
%



end

function
[EF__Velocity]=EF_Velocity(EF_Tornado,Angle_Tornado,X_Center_Tornado,Y_Center_Tornado,X_Cen
ter_Pole,Y_Center_Pole)

Constants;

%
[EF_Coordinates_Adjusted_Abs,EF_Coordinates_mean]=EF_Coordinates(EF_Tornado,Angle_Tornado,X
_Center_Tornado,Y_Center_Tornado);
%EF_Coordinates_Adjusted_Abs_mean=mean(EF_Coordinates_Adjusted_Abs);
EF_Coordinates_Adjusted_Abs_mean=EF_Coordinates_Adjusted_Abs;
%

%
X_Center_Pole_Rotated=Y_Center_Pole*sind(Angle_Tornado)+X_Center_Pole*cosd(Angle_Tornado);
X_Center_Tornado_Rotated=Y_Center_Tornado*sind(Angle_Tornado)+X_Center_Tornado*cosd(Angle_
Tornado);
X_Center_Pole_Adjusted=X_Center_Pole_Rotated-X_Center_Tornado_Rotated;
Y_Center_Pole_Rotated=Y_Center_Pole*cosd(Angle_Tornado)-X_Center_Pole*sind(Angle_Tornado);
Y_Center_Tornado_Rotated=Y_Center_Tornado*cosd(Angle_Tornado)-
X_Center_Tornado*sind(Angle_Tornado);
Y_Center_Pole_Adjusted=Y_Center_Pole_Rotated-Y_Center_Tornado_Rotated;
%

%
if
abs(X_Center_Pole_Adjusted)>EF_Coordinates_Adjusted_Abs_mean(1,1)|abs(Y_Center_Pole_Adjusted)>
EF_Coordinates_Adjusted_Abs_mean(1,2)
  EF_Velocity_Cat="EF_";
  if
abs(X_Center_Pole_Adjusted)>EF_Coordinates_Adjusted_Abs_mean(1,1)&abs(Y_Center_Pole_Adjusted)
<EF_Coordinates_Adjusted_Abs_mean(1,2)
    Border_Pole="X";
  else if
abs(X_Center_Pole_Adjusted)<EF_Coordinates_Adjusted_Abs_mean(1,1)&abs(Y_Center_Pole_Adjusted)
>EF_Coordinates_Adjusted_Abs_mean(1,2)
    Border_Pole="Y";
  else
    Border_Pole="XY";
  end
  end
else if
abs(X_Center_Pole_Adjusted)>EF_Coordinates_Adjusted_Abs_mean(1,3)|abs(Y_Center_Pole_Adjusted)>
EF_Coordinates_Adjusted_Abs_mean(1,4)
  EF_Velocity_Cat="EF0";
```

```
   if
abs(X_Center_Pole_Adjusted)>EF_Coordinates_Adjusted_Abs_mean(1,3)&abs(Y_Center_Pole_Adjusted)
<EF_Coordinates_Adjusted_Abs_mean(1,4)
      Border_Pole="X";
   else if
abs(X_Center_Pole_Adjusted)<EF_Coordinates_Adjusted_Abs_mean(1,3)&abs(Y_Center_Pole_Adjusted)
>EF_Coordinates_Adjusted_Abs_mean(1,4)
      Border_Pole="Y";
   else
      Border_Pole="XY";
   end
   end
else if
abs(X_Center_Pole_Adjusted)>EF_Coordinates_Adjusted_Abs_mean(1,5)|abs(Y_Center_Pole_Adjusted)>
EF_Coordinates_Adjusted_Abs_mean(1,6)
   EF_Velocity_Cat="EF1";
   if
abs(X_Center_Pole_Adjusted)>EF_Coordinates_Adjusted_Abs_mean(1,5)&abs(Y_Center_Pole_Adjusted)
<EF_Coordinates_Adjusted_Abs_mean(1,6)
      Border_Pole="X";
   else if
abs(X_Center_Pole_Adjusted)<EF_Coordinates_Adjusted_Abs_mean(1,5)&abs(Y_Center_Pole_Adjusted)
>EF_Coordinates_Adjusted_Abs_mean(1,6)
      Border_Pole="Y";
   else
      Border_Pole="XY";
   end
   end
else if
abs(X_Center_Pole_Adjusted)>EF_Coordinates_Adjusted_Abs_mean(1,7)|abs(Y_Center_Pole_Adjusted)>
EF_Coordinates_Adjusted_Abs_mean(1,8)
   EF_Velocity_Cat="EF2";
   if
abs(X_Center_Pole_Adjusted)>EF_Coordinates_Adjusted_Abs_mean(1,7)&abs(Y_Center_Pole_Adjusted)
<EF_Coordinates_Adjusted_Abs_mean(1,8)
      Border_Pole="X";
   else if
abs(X_Center_Pole_Adjusted)<EF_Coordinates_Adjusted_Abs_mean(1,7)&abs(Y_Center_Pole_Adjusted)
>EF_Coordinates_Adjusted_Abs_mean(1,8)
      Border_Pole="Y";
   else
      Border_Pole="XY";
   end
   end
else if
abs(X_Center_Pole_Adjusted)>EF_Coordinates_Adjusted_Abs_mean(1,9)|abs(Y_Center_Pole_Adjusted)>
EF_Coordinates_Adjusted_Abs_mean(1,10)
   EF_Velocity_Cat="EF3";
   if
abs(X_Center_Pole_Adjusted)>EF_Coordinates_Adjusted_Abs_mean(1,9)&abs(Y_Center_Pole_Adjusted)
<EF_Coordinates_Adjusted_Abs_mean(1,10)
      Border_Pole="X";
   else if
abs(X_Center_Pole_Adjusted)<EF_Coordinates_Adjusted_Abs_mean(1,9)&abs(Y_Center_Pole_Adjusted)
>EF_Coordinates_Adjusted_Abs_mean(1,10)
      Border_Pole="Y";
```

```
   else
      Border_Pole="XY";
   end
   end
else if
abs(X_Center_Pole_Adjusted)>EF_Coordinates_Adjusted_Abs_mean(1,11)|abs(Y_Center_Pole_Adjusted)
>EF_Coordinates_Adjusted_Abs_mean(1,12)
   EF_Velocity_Cat="EF4";
   if
abs(X_Center_Pole_Adjusted)>EF_Coordinates_Adjusted_Abs_mean(1,11)&abs(Y_Center_Pole_Adjuste
d)<EF_Coordinates_Adjusted_Abs_mean(1,12)
      Border_Pole="X";
   else if
abs(X_Center_Pole_Adjusted)<EF_Coordinates_Adjusted_Abs_mean(1,11)&abs(Y_Center_Pole_Adjuste
d)>EF_Coordinates_Adjusted_Abs_mean(1,12)
      Border_Pole="Y";
   else
      Border_Pole="XY";
   end
   end
else
   EF_Velocity_Cat="EF5";
   end
   end
   end
   end
   end
end
%

%
if EF_Velocity_Cat=="EF_"
   EF__Velocity=0;
else if EF_Velocity_Cat=="EF0"
   if Border_Pole=="X"
      EF__Velocity=-(abs(X_Center_Pole_Adjusted)-
EF_Coordinates_Adjusted_Abs_mean(1,3))/(EF_Coordinates_Adjusted_Abs_mean(1,1)-
EF_Coordinates_Adjusted_Abs_mean(1,3))*(Velocity_Tornado_EF01-
Velocity_Tornado_EF0_L)+Velocity_Tornado_EF01;
   else if Border_Pole=="Y"
      EF__Velocity=-(abs(Y_Center_Pole_Adjusted)-
EF_Coordinates_Adjusted_Abs_mean(1,4))/(EF_Coordinates_Adjusted_Abs_mean(1,2)-
EF_Coordinates_Adjusted_Abs_mean(1,4))*(Velocity_Tornado_EF01-
Velocity_Tornado_EF0_L)+Velocity_Tornado_EF01;
   else if Border_Pole=="XY"
      EF__Velocity=max(-(abs(X_Center_Pole_Adjusted)-
EF_Coordinates_Adjusted_Abs_mean(1,3))/(EF_Coordinates_Adjusted_Abs_mean(1,1)-
EF_Coordinates_Adjusted_Abs_mean(1,3))*(Velocity_Tornado_EF01-
Velocity_Tornado_EF0_L)+Velocity_Tornado_EF01,-(abs(Y_Center_Pole_Adjusted)-
EF_Coordinates_Adjusted_Abs_mean(1,4))/(EF_Coordinates_Adjusted_Abs_mean(1,2)-
EF_Coordinates_Adjusted_Abs_mean(1,4))*(Velocity_Tornado_EF01-
Velocity_Tornado_EF0_L)+Velocity_Tornado_EF01);
      end
      end
   end
else if EF_Velocity_Cat=="EF1"
```

```
    if Border_Pole=="X"
        EF__Velocity=-(abs(X_Center_Pole_Adjusted)-
EF_Coordinates_Adjusted_Abs_mean(1,5))/(EF_Coordinates_Adjusted_Abs_mean(1,3)-
EF_Coordinates_Adjusted_Abs_mean(1,5))*(Velocity_Tornado_EF12-
Velocity_Tornado_EF01)+Velocity_Tornado_EF12;
    else if Border_Pole=="Y"
        EF__Velocity=-(abs(Y_Center_Pole_Adjusted)-
EF_Coordinates_Adjusted_Abs_mean(1,6))/(EF_Coordinates_Adjusted_Abs_mean(1,4)-
EF_Coordinates_Adjusted_Abs_mean(1,6))*(Velocity_Tornado_EF12-
Velocity_Tornado_EF01)+Velocity_Tornado_EF12;
    else if Border_Pole=="XY"
        EF__Velocity=max(-(abs(X_Center_Pole_Adjusted)-
EF_Coordinates_Adjusted_Abs_mean(1,5))/(EF_Coordinates_Adjusted_Abs_mean(1,3)-
EF_Coordinates_Adjusted_Abs_mean(1,5))*(Velocity_Tornado_EF12-
Velocity_Tornado_EF01)+Velocity_Tornado_EF12,-(abs(Y_Center_Pole_Adjusted)-
EF_Coordinates_Adjusted_Abs_mean(1,6))/(EF_Coordinates_Adjusted_Abs_mean(1,4)-
EF_Coordinates_Adjusted_Abs_mean(1,6))*(Velocity_Tornado_EF12-
Velocity_Tornado_EF01)+Velocity_Tornado_EF12);
        end
        end
    end
else if EF_Velocity_Cat=="EF2"
    if Border_Pole=="X"
        EF__Velocity=-(abs(X_Center_Pole_Adjusted)-
EF_Coordinates_Adjusted_Abs_mean(1,7))/(EF_Coordinates_Adjusted_Abs_mean(1,5)-
EF_Coordinates_Adjusted_Abs_mean(1,7))*(Velocity_Tornado_EF23-
Velocity_Tornado_EF12)+Velocity_Tornado_EF23;
    else if Border_Pole=="Y"
        EF__Velocity=-(abs(Y_Center_Pole_Adjusted)-
EF_Coordinates_Adjusted_Abs_mean(1,8))/(EF_Coordinates_Adjusted_Abs_mean(1,6)-
EF_Coordinates_Adjusted_Abs_mean(1,8))*(Velocity_Tornado_EF23-
Velocity_Tornado_EF12)+Velocity_Tornado_EF23;
    else if Border_Pole=="XY"
        EF__Velocity=max(-(abs(X_Center_Pole_Adjusted)-
EF_Coordinates_Adjusted_Abs_mean(1,7))/(EF_Coordinates_Adjusted_Abs_mean(1,5)-
EF_Coordinates_Adjusted_Abs_mean(1,7))*(Velocity_Tornado_EF23-
Velocity_Tornado_EF12)+Velocity_Tornado_EF23,-(abs(Y_Center_Pole_Adjusted)-
EF_Coordinates_Adjusted_Abs_mean(1,8))/(EF_Coordinates_Adjusted_Abs_mean(1,6)-
EF_Coordinates_Adjusted_Abs_mean(1,8))*(Velocity_Tornado_EF23-
Velocity_Tornado_EF12)+Velocity_Tornado_EF23);
        end
        end
    end
else if EF_Velocity_Cat=="EF3"
    if Border_Pole=="X"
        EF__Velocity=-(abs(X_Center_Pole_Adjusted)-
EF_Coordinates_Adjusted_Abs_mean(1,9))/(EF_Coordinates_Adjusted_Abs_mean(1,7)-
EF_Coordinates_Adjusted_Abs_mean(1,9))*(Velocity_Tornado_EF34-
Velocity_Tornado_EF23)+Velocity_Tornado_EF34;
    else if Border_Pole=="Y"
        EF__Velocity=-(abs(Y_Center_Pole_Adjusted)-
EF_Coordinates_Adjusted_Abs_mean(1,10))/(EF_Coordinates_Adjusted_Abs_mean(1,8)-
EF_Coordinates_Adjusted_Abs_mean(1,10))*(Velocity_Tornado_EF34-
Velocity_Tornado_EF23)+Velocity_Tornado_EF34;
    else if Border_Pole=="XY"
```

```
        EF__Velocity=max(-(abs(X_Center_Pole_Adjusted)-
EF_Coordinates_Adjusted_Abs_mean(1,9))/(EF_Coordinates_Adjusted_Abs_mean(1,7)-
EF_Coordinates_Adjusted_Abs_mean(1,9))*(Velocity_Tornado_EF34-
Velocity_Tornado_EF23)+Velocity_Tornado_EF34,-(abs(Y_Center_Pole_Adjusted)-
EF_Coordinates_Adjusted_Abs_mean(1,10))/(EF_Coordinates_Adjusted_Abs_mean(1,8)-
EF_Coordinates_Adjusted_Abs_mean(1,10))*(Velocity_Tornado_EF34-
Velocity_Tornado_EF23)+Velocity_Tornado_EF34);
        end
        end
    end
else if EF_Velocity_Cat=="EF4"
    if Border_Pole=="X"
        EF__Velocity=-(abs(X_Center_Pole_Adjusted)-
EF_Coordinates_Adjusted_Abs_mean(1,11))/(EF_Coordinates_Adjusted_Abs_mean(1,9)-
EF_Coordinates_Adjusted_Abs_mean(1,11))*(Velocity_Tornado_EF45-
Velocity_Tornado_EF34)+Velocity_Tornado_EF45;
    else if Border_Pole=="Y"
        EF__Velocity=-(abs(Y_Center_Pole_Adjusted)-
EF_Coordinates_Adjusted_Abs_mean(1,12))/(EF_Coordinates_Adjusted_Abs_mean(1,10)-
EF_Coordinates_Adjusted_Abs_mean(1,12))*(Velocity_Tornado_EF45-
Velocity_Tornado_EF34)+Velocity_Tornado_EF45;
    else if Border_Pole=="XY"
        EF__Velocity=max(-(abs(X_Center_Pole_Adjusted)-
EF_Coordinates_Adjusted_Abs_mean(1,11))/(EF_Coordinates_Adjusted_Abs_mean(1,9)-
EF_Coordinates_Adjusted_Abs_mean(1,11))*(Velocity_Tornado_EF45-
Velocity_Tornado_EF34)+Velocity_Tornado_EF45,-(abs(Y_Center_Pole_Adjusted)-
EF_Coordinates_Adjusted_Abs_mean(1,12))/(EF_Coordinates_Adjusted_Abs_mean(1,10)-
EF_Coordinates_Adjusted_Abs_mean(1,12))*(Velocity_Tornado_EF45-
Velocity_Tornado_EF34)+Velocity_Tornado_EF45);
        end
        end
    end
else if EF_Velocity_Cat=="EF5"
    EF__Velocity=-
(sqrt(abs(X_Center_Pole_Adjusted)^2+abs(Y_Center_Pole_Adjusted)^2)/(sqrt(EF_Coordinates_Adjusted_
Abs_mean(1,11)^2+EF_Coordinates_Adjusted_Abs_mean(1,12)^2)))*(Velocity_Tornado_EF5_U-
Velocity_Tornado_EF45)+Velocity_Tornado_EF5_U;
    end
    end
    end
    end
    end
    end
end
end
%

function [M_Capacity_RV] = M__Capacity(t,Pole_Material,Pole_Length,Pole_Class)

Constants;
[Burried_Depth,Diameter_G,Diameter_Top,t_Pole_S]=ANSI(Pole_Length,Pole_Class);
[d_age]=Decay( t,Pole_Material );

%COV DIM:
if Pole_Material=="Wood"
    Cov_dim=Cov_dim_W;
```

```
else if Pole_Material=="Steel"
   Cov_dim=Cov_dim_S;
   end
end
%
%
Diameter_G_RV=normrnd(Diameter_G,Diameter_G*Cov_dim,n_rows,n_columns);
if Pole_Material=="Wood"
   t_Shafieezadeh=[0;10;20;30;40;50;60;75];
   cov_Shafieezadeh=[0.17;0.171;0.186;0.210;0.251;0.315;0.399;0.55];
   curve_fit_Shafieezadeh=fit(t_Shafieezadeh,cov_Shafieezadeh,'exp2');
   if mean(t)<=75
   Cov_Strength_W=curve_fit_Shafieezadeh(mean(t));
   else
   Cov_Strength_W=0.55;
   end
   z_strength=sqrt(log(1+Cov_Strength_W^2));
   L_strength=log(Strength_Pole_W)-0.5*z_strength^2;
   Strength_Pole_RV=lognrnd(L_strength,z_strength,n_rows,n_columns);
else if Pole_Material=="Steel"
   z_strength=sqrt(log(1+Cov_Strength_S^2));
   L_strength=log(Strength_Pole_S)-0.5*z_strength^2;
   Strength_Pole_RV=lognrnd(L_strength,z_strength,n_rows,n_columns);
   end
end
%
if Pole_Material=="Wood"
   S_Pole_RV=pi()*((Diameter_G_RV-2*d_age).^3)/32;
else if Pole_Material=="Steel"
   t_Pole_S_RV=normrnd(t_Pole_S,t_Pole_S*Cov_dim,n_rows,n_columns);
   Diameter_Gi_RV=Diameter_G_RV-2*t_Pole_S_RV;
   S_Pole_RV=pi()*((Diameter_G_RV-2*d_age).^4-Diameter_Gi_RV.^4)./32./(Diameter_G_RV-
2*d_age);
   end
end
%
M_Capacity_RV=S_Pole_RV.*Strength_Pole_RV/12;
%

end

function [M_Demand_RV] =
M__Demand(Tornado_Properties,X_Center_Pole,Y_Center_Pole,X_Center_Pole_Before,Y_Center_Pole_
Before,X_Center_Pole_After,Y_Center_Pole_After,Pole_Material,Pole_Length,Pole_Class,N_wire1,D_wi
re1,L_wire1,N_wire2,D_wire2,L_wire2,height_Wire_top)

Constants;
EF_Tornado=Tornado_Properties(3,1);
Angle_Tornado=Tornado_Properties(4,1);
X_Center_Tornado=Tornado_Properties(5,1);
Y_Center_Tornado=Tornado_Properties(6,1);

[Burried_Depth,Diameter_G,Diameter_Top,t_Pole_S]=ANSI(Pole_Length,Pole_Class);

%COV DIM:
if Pole_Material=="Wood"
```

```
   Cov_dim=Cov_dim_W;
else if Pole_Material=="Steel"
   Cov_dim=Cov_dim_S;
   end
end
%

%
Pole_Length_RV=normrnd(Pole_Length,Pole_Length*Cov_dim,n_rows,n_columns);
Burried_Depth_RV=normrnd(Burried_Depth,Burried_Depth*Cov_dim,n_rows,n_columns);
Pole_Height_G_RV=Pole_Length_RV-Burried_Depth_RV;
Diameter_G_RV=normrnd(Diameter_G,Diameter_G*Cov_dim,n_rows,n_columns);
Diameter_Top_RV=normrnd(Diameter_Top,Diameter_Top*Cov_dim,n_rows,n_columns);
Pole_Area_RV=0.5*(Diameter_G_RV+Diameter_Top_RV).*Pole_Height_G_RV/12;
Pole_Centriod_RV=Pole_Height_G_RV.*((Diameter_G_RV-
Diameter_Top_RV)/6+Diameter_Top_RV/2)./((Diameter_G_RV-
Diameter_Top_RV)/2+Diameter_Top_RV);
%

%Wire:
D_wire1_RV=normrnd(D_wire1,D_wire1*Cov_D_wire,n_rows,n_columns);
L_wire1_RV=normrnd(L_wire1,L_wire1*Cov_L_wire,n_rows,n_columns);
Wire_Area1_RV=L_wire1_RV.*D_wire1_RV/12*N_wire1;
D_wire2_RV=normrnd(D_wire2,D_wire2*Cov_D_wire,n_rows,n_columns);
L_wire2_RV=normrnd(L_wire2,L_wire2*Cov_L_wire,n_rows,n_columns);
Wire_Area2_RV=L_wire2_RV.*D_wire2_RV/12*N_wire2;
height_Wire_top_RV=normrnd(height_Wire_top,height_Wire_top*Cov_dim,n_rows,n_columns);
Wire_Centriod_RV=Pole_Height_G_RV-height_Wire_top_RV;
%

%
if Hazard_Type=="Tornado"
Kz_Pole_RV=1;
Kz_Wire_RV=1;
else if Hazard_Type=="Hurricane"
Kz_Pole_RV=normrnd(0.951,0.951*0.06,n_rows,n_columns);
Kz_Wire_RV=normrnd(1.024,1.024*0.06,n_rows,n_columns);
end
end
if Hazard_Type=="Tornado"
Gust_Pole_RV=1;
Gust_Wire_RV=1;
else if Hazard_Type=="Hurricane"
Gust_Pole_RV=normrnd(0.948,0.948*0.11,n_rows,n_columns);
Gust_Wire_RV=normrnd(0.801,0.801*0.11,n_rows,n_columns);
end
end
Cf_Pole_RV=normrnd(0.9,0.9*0.12,n_rows,n_columns);
Cf_Wire_RV=normrnd(1,1*0.12,n_rows,n_columns);
Q_AirDensity=0.00256;
Kzt=1;
if Hazard_Type=="Tornado"
Tornado_Wire_f_RV=((rand(n_rows,n_columns)*0.36+1).^2+(rand(n_rows,n_columns)*0.17+0.47).^2);
else if Hazard_Type=="Hurricane"
Tornado_Wire_f_RV=1;
end
```

```
end


f_Pole_RV=Q_AirDensity.*Kz_Pole_RV.*Kzt.*Gust_Pole_RV.*Cf_Pole_RV;
V_Tornado_Pole=EF_Velocity(EF_Tornado,Angle_Tornado,X_Center_Tornado,Y_Center_Tornado,X_Ce
nter_Pole,Y_Center_Pole);
F_Pole_RV=f_Pole_RV.*Pole_Area_RV.*V_Tornado_Pole.^2;
M_Pole_RV=F_Pole_RV.*Pole_Centriod_RV;

%
if EF_Tornado==0
Width_Tornado=132;
else if EF_Tornado==1
Width_Tornado=315;
else if EF_Tornado==2
Width_Tornado=650;
else if EF_Tornado==3
Width_Tornado=1375;
else if EF_Tornado==4
Width_Tornado=2195;
else if EF_Tornado==5
Width_Tornado=2750;
end
end
end
end
end
end
%
if Width_Tornado/4<L_wire1 && Width_Tornado/4<L_wire2
L_Segment_max=Width_Tornado/4;
else
L_Segment_max=Width_Tornado/2-min(L_wire1,L_wire2);
end

f_Wire_RV=Tornado_Wire_f_RV.*Q_AirDensity.*Kz_Wire_RV.*Kzt.*Gust_Wire_RV.*Cf_Wire_RV;
%F_Wire_RV=f_Wire_RV.*(Wire_Area1_RV+Wire_Area2_RV)./2.*V_Tornado_Pole.^2;
%F_Wire_RV:
Wire_Segments=10;
F_Wire_RV=0;
for iii=1:Wire_Segments
Wire_Area1_Segment_RV=Wire_Area1_RV/Wire_Segments;
X_Center_Segment_Before=iii*(X_Center_Pole-X_Center_Pole_Before)/10-(X_Center_Pole-
X_Center_Pole_Before)/20+X_Center_Pole;
Y_Center_Segment_Before=iii*(Y_Center_Pole-Y_Center_Pole_Before)/10-(Y_Center_Pole-
Y_Center_Pole_Before)/20+Y_Center_Pole;
L_Segment_Before=5280*sqrt((X_Center_Pole-X_Center_Segment_Before)^2+(Y_Center_Pole-
Y_Center_Segment_Before)^2);
if L_Segment_Before<=L_Segment_max
V_Tornado_Segment_Before=EF_Velocity(EF_Tornado,Angle_Tornado,X_Center_Tornado,Y_Center_T
ornado,X_Center_Segment_Before,Y_Center_Segment_Before);
F_Wire_Segment_Before_RV=f_Wire_RV.*Wire_Area1_Segment_RV.*V_Tornado_Segment_Before.^2.
*((L_wire1-L_Segment_Before)/L_wire1);
else
F_Wire_Segment_Before_RV=0;
end
```

```
Wire_Area2_Segment_RV=Wire_Area2_RV/Wire_Segments;
X_Center_Segment_After=iii*(X_Center_Pole-X_Center_Pole_After)/10-(X_Center_Pole-
X_Center_Pole_After)/20+X_Center_Pole;
Y_Center_Segment_After=iii*(Y_Center_Pole-Y_Center_Pole_After)/10-(Y_Center_Pole-
Y_Center_Pole_After)/20+Y_Center_Pole;
L_Segment_After=5280*sqrt((X_Center_Pole-X_Center_Segment_After)^2+(Y_Center_Pole-
Y_Center_Segment_After)^2);
if L_Segment_After<=L_Segment_max
V_Tornado_Segment_After=EF_Velocity(EF_Tornado,Angle_Tornado,X_Center_Tornado,Y_Center_Tor
nado,X_Center_Segment_After,Y_Center_Segment_After);
F_Wire_Segment_After_RV=f_Wire_RV.*Wire_Area2_Segment_RV.*V_Tornado_Segment_After.^2.*((
L_wire1-L_Segment_After)/L_wire1);
else
F_Wire_Segment_After_RV=0;
end
F_Wire_RV=F_Wire_RV+F_Wire_Segment_Before_RV+F_Wire_Segment_After_RV;
end
%
M_Wire_RV=F_Wire_RV.*Wire_Centriod_RV;
M_Demand_RV=M_Pole_RV+M_Wire_RV;
%

end

function [PF_Pole] =
PF__Pole(Tornado_Properties,X_Center_Pole,Y_Center_Pole,Angle_Pole_Before,Angle_Pole_After,Pole
_Material,Pole_Length,Pole_Class,N_wire1,D_wire1,L_wire1,N_wire2,D_wire2,L_wire2,height_Wire_to
p)

Constants;
t_M=Tornado_Properties(1,1);
t_Sd=Tornado_Properties(2,1);
EF_Tornado=Tornado_Properties(3,1);
Angle_Tornado=Tornado_Properties(4,1);
X_Center_Tornado=Tornado_Properties(5,1);
Y_Center_Tornado=Tornado_Properties(6,1);


X_Center_Pole_Before=X_Center_Pole-cosd(Angle_Pole_Before)*L_wire1*0.000189394;
Y_Center_Pole_Before=Y_Center_Pole-sind(Angle_Pole_Before)*L_wire1*0.000189394;
X_Center_Pole_After=X_Center_Pole+cosd(Angle_Pole_After)*L_wire2*0.000189394;
Y_Center_Pole_After=Y_Center_Pole+sind(Angle_Pole_After)*L_wire2*0.000189394;


V_Tornado_Pole=EF_Velocity(EF_Tornado,Angle_Tornado,X_Center_Tornado,Y_Center_Tornado,X_Ce
nter_Pole,Y_Center_Pole);
V_Tornado_Pole_Before=EF_Velocity(EF_Tornado,Angle_Tornado,X_Center_Tornado,Y_Center_Torna
do,X_Center_Pole_Before,Y_Center_Pole_Before);
V_Tornado_Pole_After=EF_Velocity(EF_Tornado,Angle_Tornado,X_Center_Tornado,Y_Center_Tornado
,X_Center_Pole_After,Y_Center_Pole_After);

if EF_Tornado==1
t=rand(n_rows,n_columns)*20+(t_M-10);
else
if t_M==0
   t_Cov=0;
```

```
else
   t_Cov=t_Sd/t_M;
end
t_z=sqrt(log(1+t_Cov^2));
t_L=log(t_M)-0.5*t_z^2;
t=lognrnd(t_L,t_z,n_rows,n_columns);
end


if V_Tornado_Pole>0 || V_Tornado_Pole_Before>0 || V_Tornado_Pole_After>0
M_Capacity_RV=M__Capacity(t,Pole_Material,Pole_Length,Pole_Class);
M_Demand_RV=M__Demand(Tornado_Properties,X_Center_Pole,Y_Center_Pole,X_Center_Pole_Befor
e,Y_Center_Pole_Before,X_Center_Pole_After,Y_Center_Pole_After,Pole_Material,Pole_Length,Pole_Cl
ass,N_wire1,D_wire1,L_wire1,N_wire2,D_wire2,L_wire2,height_Wire_top);
G_PF_RV=M_Capacity_RV-M_Demand_RV;
Z_PF=sum(G_PF_RV<0);
PF_Pole=Z_PF/n_rows;
else
PF_Pole=0;
end

end

function [Line_PF_Pole,Line_PF_L,Line_PF_U]=Line_PF(
Tornado_Properties,Line_Poles_Properties__Modified )

Constants;
t_M=Tornado_Properties(1,1);
t_Sd=Tornado_Properties(2,1);
EF_Tornado=Tornado_Properties(3,1);
Angle_Tornado=Tornado_Properties(4,1);
X_Center_Tornado=Tornado_Properties(5,1);
Y_Center_Tornado=Tornado_Properties(6,1);

Number_Poles=size(Line_Poles_Properties__Modified,1);

if t_M==0
   t_Cov=0;
else
   t_Cov=t_Sd/t_M;
end
t_z=sqrt(log(1+t_Cov^2));
t_L=log(t_M)-0.5*t_z^2;
t=lognrnd(t_L,t_z,n_rows,n_columns);

Line_PF_U_Complement=1;

for i=1:1:Number_Poles
for j=-1:1:1
k=i+j;
if k<=0|k>Number_Poles
   P_Failure=0;
else
   if Line_Poles_Properties__Modified(k,2)==1
      Pole_Material="Wood";
   else if Line_Poles_Properties__Modified(k,2)==2
```

```
        Pole_Material="Steel";
        end
    end
    Pole_Length=Line_Poles_Properties__Modified(k,3);
    Pole_Class=Line_Poles_Properties__Modified(k,4);
    N_wire1=Line_Poles_Properties__Modified(k,5);
    N_wire2=Line_Poles_Properties__Modified(k,6);
    if j==-1
        L_wire1=Line_Poles_Properties__Modified(k,7)+Line_Poles_Properties__Modified(k+1,7);
        L_wire2=Line_Poles_Properties__Modified(k,8);
    else if j==0
        L_wire1=Line_Poles_Properties__Modified(k,7);
        L_wire2=Line_Poles_Properties__Modified(k,8);
    else if j==1
        L_wire1=Line_Poles_Properties__Modified(k,7);
        L_wire2=Line_Poles_Properties__Modified(k,8)+Line_Poles_Properties__Modified(k-1,8);
        end
        end
    end
    D_wire1=Line_Poles_Properties__Modified(k,9);
    D_wire2=Line_Poles_Properties__Modified(k,10);
    h_crossarm=Line_Poles_Properties__Modified(k,11);
    t_crossarm=Line_Poles_Properties__Modified(k,12);
    height_Wire_top=Line_Poles_Properties__Modified(k,13);
    X_Center_Pole=Line_Poles_Properties__Modified(k,14);
    Y_Center_Pole=Line_Poles_Properties__Modified(k,15);
    Angle_Pole_Before=Line_Poles_Properties__Modified(k,16);
    Angle_Pole_After=Line_Poles_Properties__Modified(k,17);


P_Failure=PF__Pole(Tornado_Properties,X_Center_Pole,Y_Center_Pole,Angle_Pole_Before,Angle_Pole_
After,Pole_Material,Pole_Length,Pole_Class,N_wire1,D_wire1,L_wire1,N_wire2,D_wire2,L_wire2,height
_Wire_top);
    Poles_PF(i,j+2)=P_Failure;
end
end
Line_PF_Pole(i,1)=Poles_PF(i,2)*(Poles_PF(i,1)+Poles_PF(i,3)-Poles_PF(i,1)*Poles_PF(i,3));
Line_PF_U_Complement=(1-Line_PF_Pole(i,1))*Line_PF_U_Complement;
end

Line_PF_U=1-Line_PF_U_Complement;
Line_PF_L=max(Line_PF_Pole(:,1));


end

function [Burried_Depth,Diameter_G,Diameter_Top,t_Pole_S]=ANSI(Pole_Length,Pole_Class)

Constants;
Burried_Depth_Table=[20 4;25 5;30 5.5;35 6;40 6;45 6.5;50 7;55 7.5;60 8];
Min_Cir_Top_Table=[1 2 3 4 5 6 7 9 10;27,25,23,21,19,17,15,15,12];
Min_Cir_6ft_Table=[0 1 2 3 4 5 6 7 9 10;20 31 29 27 25 23 21 19.5 17.5 14;25 33.5 31.5 29.5 27.5 25.5 23
21.5 19.5 15;30 36.5 34 32 29.5 27.5 25 23.5 20.5 10^5;35 39 36.5 34 31.5 29 27 25 10^5 10^5;40 41 38.5
36 33.5 31 28.5 10^5 10^5 10^5;45 43 40.5 37.5 35 32.5 30 10^5 10^5 10^5;50 45 42 39 36.5 34 10^5
```

```
10^5 10^5 10^5;55 46.5 43.5 40.5 38 10^5 10^5 10^5 10^5 10^5;60 48 45 42 39 10^5 10^5 10^5 10^5
10^5];

for i=1:1:9
   if Pole_Length==Burried_Depth_Table(i,1)
      Burried_Depth=Burried_Depth_Table(i,2);
   end
end

for i=1:1:9
   if Pole_Class==Min_Cir_Top_Table(1,i)
      Min_Cir_Top=Min_Cir_Top_Table(2,i);
   end
end
Diameter_Top=Min_Cir_Top/pi();

for i=1:1:10
   for j=1:1:10
   if Pole_Class==Min_Cir_6ft_Table(1,j)&Pole_Length==Min_Cir_6ft_Table(i,1)
      Min_Cir_6ft=Min_Cir_6ft_Table(i,j);
   end
   end
end
Diameter_G=((Min_Cir_6ft-Min_Cir_Top)/(Pole_Length-6)*(Pole_Length-
Burried_Depth)+Min_Cir_Top)/pi();

t_Pole_S=Diameter_G/2-(-
(Strength_Pole_W*pi()*Diameter_G^3/32)*32*Diameter_G/pi()/Strength_Pole_S+Diameter_G^4)^0.25/2;

end

function [ d_age ] = Decay( t,Pole_Materail )

Constants;

f_rain_o=10*(1-exp(-0.001*max(rain-250,0)));
f_rain=max(f_rain_o*(1-N_dry_months/6),0);
if temperature<5
   g_temperature=0;
else if temperature<20
   g_temperature=-1+0.2*temperature;
else
   g_temperature=-25+1.4*temperature;
   end
end
k_climate=f_rain^0.3*g_temperature^0.2;
k_wood=5.44;
r_untreated=k_climate*k_wood;
B_treat=45;
D_treat=617;
C_creosote=D_treat/100;
C_CCA_eq=0.07*C_creosote;
r_treated=r_untreated/(1+B_treat*C_CCA_eq);
t_lag=5.5*r_treated^-0.95;
d_age_W=r_treated/25.4*max(t-t_lag,0);
```

```
t_steel_min=((rand(n_rows,n_columns)*10+20));
t_steel_effective=max(t-t_steel_min,0);
d_age_S=k_steel_corr.*t_steel_effective.^alpha_steel_corr./25.4;

if Pole_Materail=="Wood"
   d_age=d_age_W;
else if Pole_Materail=="Steel"
   d_age=d_age_S;
   end
end

end

% System__Properties script:(This is for EF2 scenario. For EF1, change the first value to 1)
System_Properties=[2
45
0.1
0.15
0
0
-0.0284091
-0.01420455
0
0
];


%Lines__Properties script: (This is for unhardened systems. Pole classes and ages must be changed for hardened systems)

Lines_Properties=[1 0.1 1   1   45  4   3   0.724   0   0   2   31.2    14.6    6   180 120 8   90  93.75   0   0   0
0   0   0   0   0   0   0   0   0.00    0   5   1.53    0   0   2.7 0
2   1   1   1   45  4   3   0.724   0   0   2   31.2    14.6    12  0   150 0   0   0   0   0   0   0   0   0   0   0   0   0   0
0.00    1   10  1.53    0   0   2.7 0
3   2   1   1   45  4   3   0.724   0   0   2   31.2    14.6    5   270 150 0   0   0   0   0   0   0   0   0   0   0   0   0   0
0.42    1   10  1.53    0   0   2.7 0
4   1   1   1   45  4   3   0.724   0   0   2   31.2    14.6    16  0   150 0   0   0   0   0   0   0   0   0   0   0   0   0   0
0.25    2   23  1.53    0   0   2.7 0
5   1   1   1   45  4   3   0.724   0   0   2   31.2    14.6    16  0   150 0   0   0   0   0   0   0   0   0   0   0   0   0   0
0.50    2   23  1.53    0   0   2.7 0
6   1   1   1   45  4   3   0.724   0   0   2   31.2    14.6    16  0   150 0   0   0   0   0   0   0   0   0   0   0   0   0   0
0.75    2   23  1.53    0   0   2.7 0
7   1   1   1   45  4   3   0.724   0   0   2   31.2    14.6    20  0   120 0   0   0   0   0   0   0   0   0   0   0   0   0   0
1.00    2   0   1.53    15  110.21  2.7 3253
8   1   1   1   45  4   3   0.724   0   0   2   31.2    14.6    5   90  150 0   0   0   0   0   0   0   0   0   0   0   0   0   0
1.00    2   0   1.53    0   0   2.7 0
9   8   1   1   45  4   3   0.724   0   0   2   31.2    14.6    4   180 187.5   0   0   0   0   0   0   0   0   0   0   0   0   0
0   1.00    1   4   1.53    0   0   2.7 0
10  9   1   1   45  4   3   0.724   0   0   2   31.2    14.6    5   90  150 0   0   0   0   0   0   0   0   0   0   0   0   0   0
0.50    1   17  1.53    0   0   2.7 0
11  9   1   1   45  4   3   0.724   0   0   2   31.2    14.6    5   90  150 0   0   0   0   0   0   0   0   0   0   0   0   0   0
1.00    1   9   1.53    0   0   2.7 0
12  8   1   1   45  4   3   0.724   0   0   2   31.2    14.6    5   90  150 0   0   0   0   0   0   0   0   0   0   0   0   0   0
1.00    1   13  1.53    0   0   2.7 0
```

```
13  8   1   1   45  4   3   0.724   0   0   2   31.2    14.6    4   0   187.5   0   0   0   0   0   0   0   0   0   0   0   0   0
0   1.00    1   6   1.53    0   0   2.7 0
14  13  1   1   45  4   3   0.724   0   0   2   31.2    14.6    5   90  150 0   0   0   0   0   0   0   0   0   0   0   0   0   0
0.50    1   12  1.53    0   0   2.7 0
15  13  1   1   45  4   3   0.724   0   0   2   31.2    14.6    6   90  135 0   0   0   0   0   0   0   0   0   0   0   0   0   0
1.00    1   3   1.53    0   0   2.7 0
16  13  1   1   45  4   3   0.724   0   0   2   31.2    14.6    11  0   150 0   0   0   0   0   0   0   0   0   0   0   0   0   0
1.00    1   16  1.53    0   0   2.7 0
17  15  1   1   45  4   3   0.724   0   0   2   31.2    14.6    11  0   150 0   0   0   0   0   0   0   0   0   0   0   0   0   0
0.17    1   16  1.53    0   0   2.7 0
18  15  1   1   45  4   3   0.724   0   0   2   31.2    14.6    11  0   150 0   0   0   0   0   0   0   0   0   0   0   0   0   0
0.33    1   16  1.53    0   0   2.7 0
19  15  1   1   45  4   3   0.724   0   0   2   31.2    14.6    11  0   150 0   0   0   0   0   0   0   0   0   0   0   0   0   0
0.50    1   16  1.53    0   0   2.7 0
20  15  1   1   45  4   3   0.724   0   0   2   31.2    14.6    11  0   150 0   0   0   0   0   0   0   0   0   0   0   0   0   0
0.67    1   16  1.53    0   0   2.7 0
21  15  1   1   45  4   3   0.724   0   0   2   31.2    14.6    11  0   150 0   0   0   0   0   0   0   0   0   0   0   0   0   0
0.83    1   16  1.53    0   0   2.7 0
22  15  1   1   45  4   3   0.724   0   0   2   31.2    14.6    11  0   150 0   0   0   0   0   0   0   0   0   0   0   0   0   0
1.00    1   16  1.53    0   0   2.7 0
23  13  1   1   45  4   3   0.724   0   0   2   31.2    14.6    3   270 187.5   0   0   0   0   0   0   0   0   0   0   0   0
0   0   1.00    1   0   1.53    0   0   2.7 0
24  23  1   1   45  4   3   0.724   0   0   2   31.2    14.6    11  0   150 0   0   0   0   0   0   0   0   0   0   0   0   0   0
0.33    1   16  1.53    0   0   2.7 0
25  23  1   1   45  4   3   0.724   0   0   2   31.2    14.6    11  0   150 0   0   0   0   0   0   0   0   0   0   0   0   0   0
0.67    1   16  1.53    0   0   2.7 0
26  23  1   1   45  4   3   0.724   0   0   2   31.2    14.6    4   180 150 0   0   0   0   0   0   0   0   0   0   0   0   0
0   0.67    1   14  1.53    0   0   2.7 0
27  23  1   1   45  4   3   0.724   0   0   2   31.2    14.6    11  0   150 0   0   0   0   0   0   0   0   0   0   0   0   0   0
1.00    1   11  1.53    0   0   2.7 0
28  0.2 1   1   45  4   3   0.724   0   0   2   31.2    14.6    5   180 150 3   90  150 7   180 150 0   0   0   0   0   0
0   0   0.00    0   10  1.53    1   8.51    2.7 886
29  28  2   0   0   0   0   0   0   0   0   0   1   180 2550    0   0   0   0   0   0   0   0   0   0   0   0   0   0   1.00
1   12  1.53    0   0   2.7 0
30  28  2   0   0   0   0   0   0   0   0   0   1   180 1950    0   0   0   0   0   0   0   0   0   0   0   0   0   0   1.00
1   14  1.53    2   8.51    2.7 886
31  28  1   1   45  4   3   0.724   0   0   2   31.2    14.6    6   90  187.5   0   0   0   0   0   0   0   0   0   0   0   0   0
0   1.00    3   0   1.53    0   0   2.7 0
32  31  2   0   0   0   0   0   0   0   0   0   1   0   1050    0   0   0   0   0   0   0   0   0   0   0   0   0   0   0.33    1
4   1.53    5   8.51    2.7 886
33  31  2   0   0   0   0   0   0   0   0   0   1   180 1950    0   0   0   0   0   0   0   0   0   0   0   0   0   0   0.33
1   12  1.53    1   8.51    2.7 0
34  31  2   0   0   0   0   0   0   0   0   0   1   0   1050    0   0   0   0   0   0   0   0   0   0   0   0   0   0   0.67    1
8   1.53    4   8.51    2.7 886
35  31  2   0   0   0   0   0   0   0   0   0   1   180 1950    0   0   0   0   0   0   0   0   0   0   0   0   0   0   0.67
1   13  1.53    0   0   2.7 0
36  31  1   1   45  4   3   0.724   0   0   2   31.2    14.6    2   0   150 0   0   0   0   0   0   0   0   0   0   0   0   0   0
1.00    1   3   1.53    0   0   2.7 0
37  31  2   0   0   0   0   0   0   0   0   0   1   180 1950    0   0   0   0   0   0   0   0   0   0   0   0   0   0   1.00
1   19  1.53    0   0   2.7 0
38  31  1   1   45  4   3   0.724   0   0   2   31.2    14.6    6   90  150 0   0   0   0   0   0   0   0   0   0   0   0   0   0
1.00    1   12  1.53    0   0   2.7 0
];

% Constants script:
```

```
%Number of MCS values:
n_rows=10^5;
n_columns=1;
%

%Hazard: (Tornado,Hurricane)
Hazard_Type="Tornado";


%Material Strenghts:
Strength_Pole_W=8000;
Strength_Pole_S=65000;
%

%City:
%Cities: (Norman,Xenia,Tampa,Others)
City="Norman";
%

%COV:
Cov_dim_W=0.04;
Cov_dim_S=0.025;
Cov_crossarm=0.025;
Cov_D_wire=0.03;
Cov_L_wire=0.06;
Cov_Strength_S=0.15;
%

%Wood Decay Parameters:
if City=="Norman"
rain=987;
temperature=15.58;
N_dry_months=0;
elseif City=="Xenia"
rain=1065;
temperature=11.86;
N_dry_months=0;
elseif City=="Tampa"
rain=1176;
temperature=22.97;
N_dry_months=0;
else
rain=987;
temperature=15.58;
N_dry_months=0;
end
%

%Steel Decay Parameters:
if City=="Norman"
   k_steel_corr=0.144;
   alpha_steel_corr=0.734;
elseif City=="Xenia"
   k_steel_corr=0.163;
   alpha_steel_corr=0.793;
```

```
elseif City=="Tampa"
   k_steel_corr=0.144;
   alpha_steel_corr=0.734;
else
   k_steel_corr=0.163;
   alpha_steel_corr=0.793;
   t_steel_corr=3.06;
end
%

%EF Range:
Velocity_Tornado_EF0_L=65;
Velocity_Tornado_EF01=86;
Velocity_Tornado_EF12=111;
Velocity_Tornado_EF23=136;
Velocity_Tornado_EF34=166;
Velocity_Tornado_EF45=200;
Velocity_Tornado_EF5_U=250;
%

%Costs:
C_repair_Pole=4000;
C_harden_Pole_4=2998;
C_harden_Pole_3=3064;
C_harden_Pole_2=3119;
C_harden_Pole_1=3223;
t_restoration=25.5;
%
```

List of References

AGA. (2011a). “Service Life of Galvanized Steel Articles in Soil Applications”. Retrieved March 30, 2018, from: https://www.galvanizeit.org/uploads/publications/Galvanized_Steel_Performance_in_Soil.pdf

AGA. (2011b). “Zinc coating: A Comparative Analysis of Process and Performance Characteristics”. Retrieved March 30, 2018, from: https://www.galvanizeit.org/uploads/publications/Zinc_Coatings.pdf

Ahmed, S., & Munudhada, A. (2013). “Comparative Study of pre-tensioned prestressed Concrete electric poles of type I, II & III”. International Journal of Emerging Technology and Advanced Engineering, 3(12), 594-598.

Alrasheedi, N. H., & Selvam, R. P. (2011). “Tornado forces on different building sizes using computer modeling”. In ASME Early Career Technical Conference.

Amini, M. O., & van de Lindt, J. W. (2013). “Quantitative insight into rational tornado design wind speeds for residential wood-frame structures using fragility approach”. Journal of Structural Engineering, 140(7), 04014033.

ANSI-O5.1. (2002). “Wood poles specifications and dimensions”. Birmingham, AL: American Wood Protection Association.

ASCE7-16 (2016). ‘‘Minimum design loads for buildings and other structures’’.

ASCE-72. (1990). “Design of steel transmission pole structures”. New York, NY: American Society of Civil Engineers.

ASTM. (2005). “Standard specification for steel strand, uncoated seven-wire for prestressed concrete.” ASTM A416-05, West Conshohocken, Pa.

ASTM. (2007). “Standard specification for high-strength low-alloy columbium-vanadium structural steel.” ASTM A572/A572M-07, West Conshohocken, PA.

ASTM. (2013). “Standard specification for zinc (hot-dip galvanized) coatings on iron and steel products.” ASTM A123, West Conshohocken, PA.

ATS. (2018). “Products and pricing”. Retrieved June 14, 2018, from:

http://www.americantimberandsteel.com/poles-pilings-utility-poles-unframed-cca.html

Bagchi, A., Sprintson, A., & Singh, C. (2009, October). “Modeling the impact of fire spread on the electrical distribution network of a virtual city”. In North American Power Symposium (NAPS), 2009 (pp. 1-6). IEEE.

Bentz, D. P., Guthrie, W. S., Jones, S. Z., & Martys, N. S. (2014). “Predicting service life of steel-reinforced concrete exposed to chlorides”. Concrete international, 36(9), 55-64.

Bolin, C. A., & Smith, S. T. (2011). “Life cycle assessment of pentachlorophenol-treated wooden utility poles with comparisons to steel and concrete utility poles”. Renewable and Sustainable Energy Reviews, 15(5), 2475-2486.

Brown, R. E. (2008). “Electric power distribution reliability”. CRC press.

Brown, R. E. (2009). “Cost-benefit analysis of the deployment of utility infrastructure upgrades and storm hardening programs”. *Quanta Technology, Raleigh*.

Brumbelow K, Torres J, Guikema S, Bristow E, & Kanta L. (2007). “Virtual cities for water distribution and infrastructure system research”. Paper presented at the World Environmental and Water Resources Congress.

Caleyo, F., Velázquez, J. C., Valor, A., & Hallen, J. M. (2009). “Probability distribution of pitting corrosion depth and rate in underground pipelines: A Monte Carlo study”. Corrosion Science, 51(9), 1925-1934.

Campbell, R. J. (2012, August). “Weather-related power outages and electric system resiliency”. Washington, DC: Congressional Research Service, Library of Congress.

Chowdhury, A., & Koval, D. (2011). “Power distribution system reliability: practical methods and applications”. John Wiley & Sons.

Church, C., Snow, J. T., Baker, G. L., & Agee, E. M. (1979). “Characteristics of tornado-like vortices as a function of swirl ratio: A laboratory investigation”. Journal of the Atmospheric Sciences, 36(9), 1755-1776.

Dagher, H. J. (Ed.). (2006, August). “Reliability-based design of utility pole structures”. American Society of Civil Engineers.

Darestani, Y. M., Shafieezadeh, A., & DesRoches, R. (2016). “An equivalent boundary model for effects of adjacent spans on wind reliability of wood utility poles in overhead distribution lines”. Engineering Structures, 128, 441-452.

Darestani, Y. M., Shafieezadeh, A., & DesRoches, R. (2017). “Effects of Adjacent Spans and Correlated Failure Events on System-Level Hurricane Reliability of Power Distribution Lines” IEEE Transactions on Power Delivery.

Darmawan, M. S., & Stewart, M. G. (2007a). “Effect of pitting corrosion on capacity of prestressing wires”. Magazine of Concrete Research, 59(2), 131-139.

Darmawan, M. S., & Stewart, M. G. (2007b). “Spatial time-dependent reliability analysis of corroding pretensioned prestressed concrete bridge girders”. Structural Safety, 29(1), 16-31.

Davidson, R. A., Liu, H., Sarpong, I. K., Sparks, P., & Rosowsky, D. V. (2003). “Electric power distribution system performance in Carolina hurricanes”. Natural Hazards Review, 4(1), 36-45.

Doan, P. L. (1970). “Tornado considerations for nuclear power-plant structures”. United Engineers and Constructors, Inc., Philadelphia.

Edwards, R., LaDue, J. G., Ferree, J. T., Scharfenberg, K., Maier, C., & Coulbourne, W. L. (2013). “Tornado intensity estimation: Past, present, and future”. Bulletin of the American Meteorological Society, 94(5), 641-653.

EIA. (2018a). “Energy information administration.” Retrieved June 14, 2018, from:
https://www.eia.gov/electricity/data.php#traderel

EIA. (2018b). “Energy information administration.” Retrieved October 08, 2018, from:
https://www.eia.gov/electricity/data.php

Ellingwood, B. R., & Tekie, P. B. (1999). “Wind load statistics for probability-based structural design”. Journal of Structural Engineering, 125(4), 453-463.

Ellingwood, B. R., Rosowsky, D. V., Li, Y., & Kim, J. H. (2004). “Fragility assessment of light-frame wood construction subjected to wind and earthquake hazards”. Journal of Structural Engineering, 130(12), 1921-1930.

Elsner, J. B., Jagger, T. H., & Elsner, I. J. (2014). “Tornado intensity estimated from damage path dimensions”. PloS one, 9(9), e107571.

FEMA (1992). “A benefit-cost model for the seismic rehabilitation of buildings”. Washington, DC: Federal Emergency Management Agency

Foedinger, R., Boozer, J., Bronstad, M., & Davidson, J. (2003). “Development of energy-absorbing composite utility pole”. Transportation Research Record: Journal of the Transportation Research Board, (1851), 149-157.

Fouts, J. L. (2002). “Pressure distribution on cubical model in tornado-like flow”. In Proceedings for the 12th International Conference on Wind Engineering, Lubbock, Texas, 2002.

Francis, R. A., Falconi, S. M., Nateghi, R., & Guikema, S. D. (2011). “Probabilistic life cycle analysis model for evaluating electric power infrastructure risk mitigation investments”. *Climatic change*, *106*(1), 31-55.

Fujita, T. T. (1987). “US tornadoes. Part 1: 70-year statistics”.

Goliger, A. M., & Milford, R. V. (1998). “A review of worldwide occurrence of tornadoes”. Journal of Wind Engineering and Industrial Aerodynamics, 74, 111-121.

Gonzalez, J. A., Andrade, C., Alonso, C., & Feliu, S. (1995). “Comparison of rates of general corrosion and maximum pitting penetration on concrete embedded steel reinforcement". Cement and concrete research, 25(2), 257-264.

Haan Jr, F. L., Balaramudu, V. K., & Sarkar, P. P. (2009). "Tornado-induced wind loads on a low-rise building". Journal of Structural Engineering, 136(1), 106-116.

Haan Jr, F. L. (2017). "An examination of static Pressure and Duration effects on Tornado-induced Peak Pressures on a low-rise Building". Frontiers in Built Environment, 3, 20.

Hamada, A., El Damatty, A. A., Hangan, H., & Shehata, A. Y. (2010). "Finite element modelling of transmission line structures under tornado wind loading". Wind and Structures, 13(5), 451.

Hamada, A., & El Damatty, A. A. (2011). "Behavior of guyed transmission line structures under tornado wind loading". Computers & Structures, 89(11-12), 986-1003.

Hamada, A., & El Damatty, A. A. (2014, August). "Nonlinear formulation of four-noded cable element and application to transmission lines under tornadoes". In 2014 International conference on advances in wind and structures (AWAS14)–ACEM14. Busan, Korea.

Hamada, A., & El Damatty, A. A. (2015). "Failure analysis of guyed transmission lines during F2 tornado event". Engineering Structures, 85, 11-25.

Hangan, H., & Kim, J. D. (2008). "Swirl ratio effects on tornado vortices in relation to the Fujita scale". Wind and Structures, 11(4), 291-302.

Harlow, F. H., & Stein, L. R. (1974). Structural analysis of tornado-like vortices. Journal of the Atmospheric Sciences, 31(8), 2081-2098.

Hart, G. C. (1985). "The Los Angeles, California, Tornado of March 1, 1983". National Academies.

Hines, P., Apt, J., & Talukdar, S. (2008, July). "Trends in the history of large blackouts in the United States". In Power and Energy Society General

Meeting-Conversion and Delivery of Electrical Energy in the 21st Century, 2008 IEEE (pp. 1-8). IEEE.

Hoekstra, S., Klockow, K., Riley, R., Brotzge, J., Brooks, H., & Erickson, S. (2011). “A preliminary look at the social perspective of warn-on-forecast: Preferred tornado warning lead time and the general public’s perceptions of weather risks”. Weather, Climate, and Society, 3(2), 128-140.

Hope, B & Nmai, C (2001). “Corrosion of prestressing steels”. American Society of Civil Engineers.

Hu, H., Yang, Z., Sarkar, P., & Haan, F. (2011). “Characterization of the wind loads and flow fields around a gable-roof building model in tornado-like winds”. Experiments in fluids, 51(3), 835.

Ibrahim, A. M., El Damatty, A. A., & El Ansary, A. M. (2017). “Finite element modelling of pre-stressed concrete poles under downbursts and tornadoes”. Engineering Structures, 153, 370-382.

Ishac, M. F., & White, H. B. (1994, April). “Effect of tornado loads on transmission lines”. In Transmission and Distribution Conference, 1994., Proceedings of the 1994 IEEE Power Engineering Society (pp. 521-527). IEEE.

Jischke, M. C., & Light, B. D. (1984). “Laboratory simulation of tornadic wind loads on a rectangular model structure”. In Wind Engineering 1983, Part 3A (pp. 371-382).

Kashani, A. G., Graettinger, A. J., & Dao, T. (2016). “Lidar-Based Methodology to Evaluate Fragility Models for Tornado-Induced Roof Damage”. Natural Hazards Review, 17(3), 04016006.

LaCommare, K. H., & Eto, J. H. (2006). “Cost of power interruptions to electricity consumers in the United States (US)”. Energy, 31(12), 1845-1855.

Lacoursiere, B. (1999). “Steel utility poles: advantages and applications”. In Rural Electric Power Conference, 1999 (pp. B2-1). IEEE.

Lewellen, W. S., Lewellen, D. C., & Sykes, R. I. (1997). “Large-eddy simulation of a tornado’s interaction with the surface”. Journal of the Atmospheric Sciences, 54(5), 581-605.

Lewellen, D. C., Lewellen, W. S., & Xia, J. (2000). “The influence of a local swirl ratio on tornado intensification near the surface”. Journal of the atmospheric sciences, 57(4), 527-544.

Li, Y., Yeddanapudi, S., McCalley, J. D., Chowdhury, A. A., & Moorehead, M. (2005). “Degradation-path model for wood pole asset management”. In Power Symposium, 2005. Proceedings of the 37th Annual North American (pp. 275-280). IEEE.

Li, Y., & Ellingwood, B. R. (2006). “Hurricane damage to residential construction in the US: Importance of uncertainty modeling in risk assessment”. Engineering structures, 28(7), 1009-1018.

Li, W. (2014). “Risk assessment of power systems: models, methods, and applications”. John Wiley & Sons.

Lineweber, D., & McNulty, S. (2001). “The cost of power disturbances to industrial & digital economy companies”. Prepared for the Electric Power Research Institute, 98pp. www. onpower. com/pdf/EPRICostOfPowerProblems. pdf [accessed October 10, 2014].

Lu, H. R., & El Hanandeh, A. (2017). “Environmental and economic assessment of utility poles using life cycle approach”. Clean Technologies and Environmental Policy, 19(4), 1047-1066.

Malaeb, D. A. (1980). “Simulation of tornado-generated missiles” (Doctoral dissertation).

Mangual, J., ElBatanouny, M., Ziehl, P., & Matta, F. (2012). “Corrosion damage quantification of prestressing strands using acoustic emission”. Journal of Materials in Civil Engineering, 25(9), 1326-1334.

Mankowski, M., Hansen, E., & Morrell, J. (2002). “Wood pole purchasing, inspection, and maintenance: A survey of utility practices”. Forest products journal, 52(11/12), 43.

Masoomi, H., & van de Lindt, J. W. (2016). “Tornado fragility and risk assessment of an archetype masonry school building”. Engineering Structures, 128, 26-43.

Masoomi, H., & van de Lindt, J. W. (2018). “Restoration and functionality assessment of a community subjected to tornado hazard”. Structure and Infrastructure Engineering, 14(3), 275-291.

McDonald, J. R., Mehta, K. C., & Minor, J. E. (1974). “Tornado-resistant design of nuclear power-plant structures”. Texas Tech. Univ., Austin.

McDonald, J. R., & Murray, R. (1999). “Rationale for wind-borne missile criteria for DOE facilities” (No. UCRL-CR-135687; DP0514030). Lawrence Livermore National Lab., CA (US).

McDonald, J. R., & Mehta, K. C. (2006). “A recommendation for an enhanced Fujita scale (EF-scale)”. Wind Science and Engineering Center, Texas Tech University.

Meaden, G. T., Kochev, S., Kolendowicz, L., Kosa-Kiss, A., Marcinoniene, I., Sioutas, M., ... & Tyrrell, J. (2007). “Comparing the theoretical versions of the Beaufort scale, the T-Scale and the Fujita scale”. Atmospheric research, 83(2-4), 446-449.

Mehta, K. C., & National Research Council. (1975). “Engineering Aspects of the Tornadoes of April 3-4, 1974”. National Academies.

Memari, M., Attary, N., Masoomi, H., Mahmoud, H., van de Lindt, J. W., Pilkington, S. F., & Ameri, M. R. (2018). “Minimal building fragility portfolio for damage assessment of communities subjected to tornadoes”. Journal of Structural Engineering, 144(7), 04018072.

Miles, S. B., Gallagher, H., & Huxford, C. J. (2013). “Restoration and impacts from the September 8, 2011, San Diego power outage”. Journal of Infrastructure Systems, 20(2), 05014002.

Mishra, A. R., James, D. L., & Letchford, C. W. (2008). “Physical simulation of a single-celled tornado-like vortex, part A: flow field characterization”. Journal of Wind Engineering and Industrial Aerodynamics, 96(8-9), 1243-1257.

Morrell, J. J. (2008). “Estimated service life of wood poles”. Technical Bulletin, North American Wood Pole Council.

Morrell, J. J. (2012). “Wood Pole Maintenance Manual: 2012 Edition”. Oregon State University. Forest Research Laboratory.

Mughabghab, S. F., & Sullivan, T. M. (1989). “Evaluation of the pitting corrosion of carbon steels and other ferrous metals in soil systems”. Waste management, 9(4), 239-251.

NIST. (2014). “Technical invistigation of the May 22, 2011, Tornado in Joplin Missouri”. Retrieved May 30, 2018, from: https://nvlpubs.nist.gov/nistpubs/NCSTAR/NIST.NCSTAR.3.pdf

NOAA. (2012). “US tornado climatology/ tornado alley”. Retrieved April 07, 2018, from:
https://www.ncdc.noaa.gov/climate-information/extreme-events/us-tornado-climatology/tornado-alley

NOAA. (2013). “The May 19, 2013 Lake Thunderbird-Shawnee EF-4 Tornado”. Retrieved June 13, 2018, from:
https://www.weather.gov/oun/events-20130519-ef4tornado

NWS. (2018). “Moore, Oklahoma Tornadoes (1890-present)”. Retrieved October 09, 2018, from: https://www.weather.gov/oun/tornadodata-city-ok-moore

Oliphant, W. J., & Sherman, D. C. (Eds.). (2012, August). “Prestressed Concrete Transmission Pole Structures: Recommended Practice for Design and Installation”. American Society of Civil Engineers.

Pope, T. (2004). “Wood Pole Survivor Rates by Decay Hazard Zone: Initial Inspection vs. Recycle Inspection”. Proceedings of the American Wood Protection Association, 100, 255-262.

Rausand, M., & Arnljot, H. Ã. (2004). “System reliability theory: models, statistical methods, and applications”. John Wiley & Sons.

Revie, W. & Uhlig, H. (2008). “Corrosion and corrosion control: An introduction to corrosion science and engineering”. John Wiley & Sons, Inc.

Robinson, J. (2005). “Predicting the in-ground performance of galvanized steel”. Mount Townsend Solutions Pty Ltd.

Rodgers, T.E. (1984). “Prestressed Concrete Poles – State of the Art”. PCI Journal, Vol. 29, No. 4, 53 pp.

Romanoff, M. (1957). “Underground corrosion”. Washington (DC: US Government Printing Office.

Roueche, D. B., Prevatt, D. O., Haan, F. L., & Datin, P. L. (2015). “An estimate of tornado loads on a wood-frame building using database-assisted design methodology”. Journal of Wind Engineering and Industrial Aerodynamics, 138, 27-35.

Ryan, P. C., Stewart, M. G., Spencer, N., & Li, Y. (2014). “Reliability assessment of power pole infrastructure incorporating deterioration and network maintenance”. Reliability Engineering & System Safety, 132, 261-273.

Sarkar, P. P., Haan, Jr, F. L., Balaramudu, V., & Sengupta, A. (2006). “Laboratory simulation of tornado and microburst to assess wind loads on buildings”. In Structures Congress 2006: Structural Engineering and Public Safety (pp. 1-10).

Salman, A. M., Li, Y., & Stewart, M. G. (2015). “Evaluating system reliability and targeted hardening strategies of power distribution systems subjected to hurricanes”. Reliability Engineering & System Safety, 144, 319-333.

Salman, A. M., & Li, Y. (2016). “Age-dependent fragility and life-cycle cost analysis of wood and steel power distribution poles subjected to hurricanes”. Structure and Infrastructure Engineering, 12(8), 890-903.

Sarkar, P., Haan, F., Gallus Jr, W., Le, K., & Wurman, J. (2005, May). “Velocity measurements in a laboratory tornado simulator and their comparison with numerical and full-scale data”. In 37th joint meeting panel on wind and seismic effects.

Savory, E., Parke, G. A., Zeinoddini, M., Toy, N., & Disney, P. (2001). “Modelling of tornado and microburst-induced wind loading and failure of a lattice transmission tower”. Engineering Structures, 23(4), 365-375.

Selvam, R. P., & Millett, P. C. (2003). “Computer modeling of tornado forces on a cubic building using large eddy simulation”. Journal of the Arkansas Academy of Science, 57(1), 140-146.

Sengupta, A., Haan, F. L., Sarkar, P. P., & Balaramudu, V. (2008). “Transient loads on buildings in microburst and tornado winds”. Journal of Wind Engineering and Industrial Aerodynamics, 96(10-11), 2173-2187.

Shafieezadeh, A., Onyewuchi, U. P., Begovic, M. M., & DesRoches, R. (2014). “Age-dependent fragility models of utility wood poles in power distribution networks against extreme wind hazards”. IEEE Transactions on Power Delivery, 29(1), 131-139.

Shehata, A. Y., & El Damatty, A. A. (2007). “Behaviour of guyed transmission line structures under downburst wind loading”. Wind and Structures, 10(3), 249-268.

Short, T. A. (2014). “Electric power distribution handbook”. CRC press.

Smith, D. J., & Sutter, D. (2013). “Response and recovery after the Joplin tornado: Lessons applied and lessons learned”. The Independent Review, 18(2), 165-188.

Standohar-Alfano, C. D., & van de Lindt, J. W. (2014). “Empirically based probabilistic tornado hazard analysis of the United tates using 1973–2011 data”. Natural Hazards Review, 16(1), 04014013.

Stewart, A. J. (1996). “Utility poles: how long do they last”. In Proceeding of the Conference on Poles and Piles, Fort Collins, CO.

Stewart, M. G., & Rosowsky, D. V. (1998). “Structural safety and serviceability of concrete bridges subject to corrosion”. Journal of Infrastructure systems, 4(4), 146-155.

Stewart, M. G., & Mullard, J. A. (2007). “Spatial time-dependent reliability analysis of corrosion damage and the timing of first repair for RC structures”. Engineering Structures, 29(7), 1457-1464.

Taras, A., Ratel, G., & Chouinard, L. (2004). “A life-cycle cost approach to the maintenance of overhead line supports”. In Reliability and Optimization of Structural Systems: Proceedings of the 11th IFIP WG7. 5 Working Conference, Banff, Canada, 2-5 November 2003 (p. 241). CRC Press.

Thoft-Christensen, P., & Middleton, C. R. (1996). “Reliability assessment of concrete bridges”. In Proc. Symposium on “The Safety of Bridges”, London.

Unnikrishnan, V. U., & van de Lindt, J. W. (2016). “Probabilistic framework for performance assessment of electrical power networks to tornadoes”. Sustainable and Resilient Infrastructure, 1(3-4), 137-152.

U.S. Climate Data (2018). Retrieved September 24, 2018, from: https://www.usclimatedata.com/

Val, D. V., & Melchers, R. E. (1997). “Reliability of deteriorating RC slab bridges”. Journal of structural engineering, 123(12), 1638-1644.

van de Lindt, J. W., Pei, S., Dao, T., Graettinger, A., Prevatt, D. O., Gupta, R., & Coulbourne, W. (2012a). “Dual-objective-based tornado design philosophy”. Journal of Structural Engineering, 139(2), 251-263.

van de Lindt, J., Amini, M. O., Standohar-Alfano, C., & Dao, T. (2012b). “Systematic study of the failure of a light-frame wood roof in a tornado”. Buildings, 2(4), 519-533.

Velázquez, J. C., Caleyo, F., Valor, A., & Hallen, J. M. (2009). “Predictive model for pitting corrosion in buried oil and gas pipelines”. Corrosion, 65(5), 332-342.

Volkanovski, A., Čepin, M., & Mavko, B. (2009). “Application of the fault tree analysis for assessment of power system reliability”. Reliability Engineering & System Safety, 94(6), 1116-1127.

Vu, K. A. T., & Stewart, M. G. (2000). “Structural reliability of concrete bridges including improved chloride-induced corrosion models”. Structural safety, 22(4), 313-333.

Wan, C. A., & Chang, C. C. (1972). “Measurement of the velocity field in a simulated tornado-like vortex using a three-dimensional velocity probe”. Journal of the Atmospheric Sciences, 29(1), 116-127.

Wang C-H , Leicester RH , Nguyen MN (2008). “Manual 3 - Decay in ground contact”. Mel- bourne, Australia: Forest & Wood Products Australia.

Ward, N. B. (1972). “The exploration of certain features of tornado dynamics using a laboratory model”. Journal of the Atmospheric Sciences, 29(6), 1194-1204.

Wen, Y. K., & Kang, Y. J. (2001). “Minimum building life-cycle cost design criteria. I: Methodology”. Journal of Structural Engineering, 127(3), 330-337.

Wolfe, R., & Moody, R. (1997, November). “Standard specifications for wood poles”. In Proceedings of the 1997 Utility Pole Structures Conference and Trade Show, JJ Morrel

Wong, C. Jerry Miller, Michael D.. (2010). “Guidelines for Electrical Transmission Line Structural Loading (3rd Edition)”. American Society of Civil Engineers (ASCE).

WSEC. (2006). “A recommendation for an enhanced Fujita scale (EF-scale)”.

Wurman, J., Kosiba, K., & Mughabghab, P. (2013). “In situ, Doppler radar, and video observations of the interior structure of a tornado and the wind–damage relationship”. Bulletin of the American Meteorological Society, 94(6), 835-846.

Xu, L., & Brown, R. E. (2008). “Undergrounding assessment phase 3 report: Ex ante cost and benefit modeling”. Quanta Technology, Raleigh.

Yang, Z., Sarkar, P., & Hu, H. (2011). “An experimental study of a high-rise building model in tornado-like winds”. Journal of Fluids and Structures, 27(4), 471-486.

Zamanzadeh, M., Kempkes, C. D., Aichinger, D., & Riley, D. (2007). “Laboratory and field corrosion investigation of galvanized utility poles”. In Electrical Transmission Line and Substation Structures: Structural Reliability in a Changing World (pp. 235-249).

Zimmerman, R., Zhu, Q., de Leon, F., & Guo, Z. (2017). “Conceptual modeling framework to integrate resilient and interdependent infrastructure in extreme weather”. Journal of Infrastructure Systems, 23(4), 04017034.